CHARLES UNIVERSITY IN PRAGUE

Faculty of Science

Department of Physical and
Macromolecular Chemistry

**INSTITUTE OF
MACROMOLECULAR CHEMISTRY
AS CR, V.V.I.**

Department of Supramolecular
Polymer Systems

SELF-ASSEMBLY IN MIXTURES OF SURFACTANTS AND STIMULI-RESPONSIVE POLYMERS WITH COMPLEX ARCHITECTURE

Doctoral Thesis

Anna Bogomolova

Supervisor: PhD. Sergey K. Filippov

Prague 2015

UNIVERSITA KARLOVA V PRAYE

Přírodovědecká fakulta

Katedra fyzikální a
macromolekulární chemie

ÚSTAV MAKROMOLEKULÁRNÍ CHEMIE, AV ČR, V.V.I.

Oddělení nadmolekulárních
polymerních systémů

SAMOORGANIZACE VE SMĚSÍCH SURFAKTANTŮ A POLYMERŮ S KOMPLEXNÍ STRUKTUROU CITLIVÝCH KE ZMĚNĚ VNĚJŠÍHO PROSTŘEDÍ

Disertační Práce

Anna Bogomolova

Školitel: Mgr. Sergey K. Filippov, PhD.

Praha 2015

Hereby I declare that I have worked out this doctoral thesis independently, under the guidance of PhD. Sergey K. Filippov, and I have duly cited all the sources used. This work has not been used in order to earn any other academic degree.

PRAGUE 04.02.2015 ANNA BOGOMOLOVA

If you can't explain it simple, you don't understand it well enough.

- *Albert Einstein*

ACKNOWLEDGEMENTS

First of all, I would like to thank my supervisor, Sergey Filippov, for teaching me most of what I know about the scattering technics. I am grateful for the numerous opportunities he has offered me, for all the help he has provided me during the course of my thesis and for the supporting me in all of my initiatives. I believe, his well-wishing guidance helped me to realize the way of my future career.

Special thanks go to Petr Stepanek, Head of Department, who gave me the opportunity to work in incredibly friendly Department of Supramolecular Polymer Systems. I appreciate all advices, suggestions and encouragement he has provided me during my work.

I would also like to thank Larysa Starovoytova not only for her help and assistance on NMR measurements but more for our funny discussions and sometimes venting my sadness.

Most of all I have to thank whole our Department for being such cheerful and friendly during the time of my thesis. A big thank you goes to all my coworkers who helped me to manage with all technical and administrative problems which arose sometimes. For all the time spent in our "group activities" either in the institute or outside, which made all the difference. So in no particular order: Eva Miskovska Ml., Eva Miskovska St., Zulfiya Cernochova, Peter Cernoch, Martin Hruby, Mariia Rabyk, Jiri Panek, Borislav Angelov, Alexander Zhigunov and many more…..

My thanks as well belong to all my colleagues from Institute of Macromolecular Chemistry, who always create a positive working atmosphere.

SUMMARY

The issue of construction of complex multi-block copolymers is currently one of the most researched areas. It became a logic consequence of the continuous development in polymer chemistry. Nowadays, a great interest is attracted to multi-responsive block copolymers. As a rule, they consist of hydrophilic, hydrophobic and responsive blocks. That responsive block can be thermo-sensitive or pH-sensitive as well as sensitive to some other external stimulus. Current achievements regarding stimuli-responsive polymers are briefly reviewed in the part 1.1, Introduction. That part overviews only homopolymers but it is considering the impact of various stimuli. In the present work, we will try to cover the topic of stimuli-responsive block copolymers and their interactions with different types of surfactants. We believe in the importance of understanding polymer/surfactant interactions. It can be a crucial step for future modeling of drug/polymer or protein(DNA)/surfactant interactions. The part 1.2, chapter Introduction, reviews general features of different surfactants and process of micelle formation, while the part 1.3 characterizes some mechanisms in polymer/surfactant interactions.

Within this work we analyze two principal systems, thermo-sensitive block copolymers on the base of poly(2-alkyl-2-oxazolines) in the order of increase the structure complexity of polymers and their behavior in the presence of ionic and polymeric surfactants, and pH-sensitive polymers on the basis of amino acids in the presence of nonionic surfactant. Three articles devoted to the former topic and one article devoted to the latter one topic have been published and included (chapter Results) in the current doctoral thesis.

We also pay a great attention to the careful analysis and interpretation of isothermal titration calorimetry data that is an important aspect of the present work. We took an attempt not only to qualitatively characterize the experimental results, but also to provide the quantitative analysis by using the modern regular solution theory. Achievements in this field together with other results are summarized in chapter Discussion.

We believe that the findings obtained in the present work can lift a veil in understanding the interaction mechanisms between polymers of the complex structure and different surfactants and also shed light on the methods of their characterization.

TABLE OF CONTENTS

ABBREVIATIONS

cac	critical aggregation concentration
cmc	critical micellar concentration
cmt	critical micellar temperature
cpt	cloud point temperature
$C_{12}E_8$	octaethylene glycol monododecyl ether
CTAB	cetyltrimethylammonium bromide
DTAB	decyltrimethylammonium bromide
DLS	dynamic light scattering
fm	femtometer
LCST	lower critical solution temperature
LiDS	lithium dodecylsulfate
PAA	poly(acrylic acid)
PBuOZ	poly(2-butyl-2-oxazoline)
PDMAEMA	poly(dimethylaminoethyl methacrylate)
PDEAEMA	poly(diethylaminoethyl methacrylate)
PEO	poly(ethylene oxide)
PEtOZ	poly(2-ethylene oxazoline)
PiPrOz	poly(2-i-propyl-2-oxazoline)
PMAA	poly(methacrylic acid)
PMeOZ	poly(2-methyl-2-oxazoline)
PNIPAM	poly(N-isopropylacrylamide)
PNonOZ	poly(2-nonyl-2-oxazoline)
POEGMA	poly(oligo(ethylene glycol)methacrylate)
PPhOZ	poly(2-phenyl-2-oxazoline)
PPO	poly(propylene oxide)
PSS	poly(styrenesulfonate)
PVME	poly(vinyl methyl ether)
P2VP	poly(2-vinylpyridine)
P4VP	poly(4-vinylpyridine)
SANS	small-angle neutron scattering
SAXS	small-angle X-ray scattering
SDS	sodium dodecylsulfate
SLS	static light scattering
TTAB	tetradecyltrimethylammonium bromide
UCST	upper critical solution temperature

SYMBOLS

A_2	second virial coefficient of the osmotic pressure
C_2	saturation concentration of surfactant
D_o	translational diffusion coefficient
$g^{(1)}(t)$	normalized time correlation function of the electric field
$G^{(1)}(t)$	correlation function of the electric field
$G^{(2)}(t)$	intensity correlation function
I_S	scattering intensity
M_W	mass-averaged molar mass
M_N	number-averaged molar mass
$P(\theta)$	form factor
q	amplitude of the scattering vector
R_h	hydrodynamic radius
R_G	radius of gyration
Γ	relaxation (decay) rate
τ	relaxation time
θ	scattering angle
χ	Flory-Huggins interaction parameter

1. INTRODUCTION

1.1. Stimuli-Responsive Polymers

Stimuli-responsive polymers or smart polymers are polymers that change their conformation according to environment. Such materials can be sensitive to a number of factors, such as temperature, humidity, pH, ionic strength, solvent conditions, the intensity of incident light or strength of electrical or magnetic field and can respond in various ways, like altering color or transparency, becoming conductive or permeable to water or changing shape (shape memory polymers). Usually, minor changes in the environment are sufficient to induce greater change in the polymer's properties.

The nonlinear response in stimuli-responsive polymers makes them unique and effective. A significant change in structure and properties can be induced by a very small stimulus. Once that change occurs, there is no further change, meaning a predictable all-or-nothing response occurs, with complete uniformity throughout the polymer. The responses can also be manifold: dissolution/precipitation, degradation, change in hydration state, swelling/collapsing, hydrophilic/hydrophobic surface, change in shape, conformational change and micellization.

Another factor in the effectiveness of smart polymers lies in the inherent nature of polymers in general. The strength of each molecule's response to changes in stimuli is a combination of changes of individual monomer units which, alone, would be weak. However, these weak responses, repeated hundreds or thousands of times, create a considerable force for driving processes.

The chemical structures of the most common stimuli-sensitive polymers are shown in Figure 1.1. In the following only the most frequently employed stimuli will be discussed further. These stimuli are temperature and pH. Other stimuli will be briefly reviewed during this work as well.

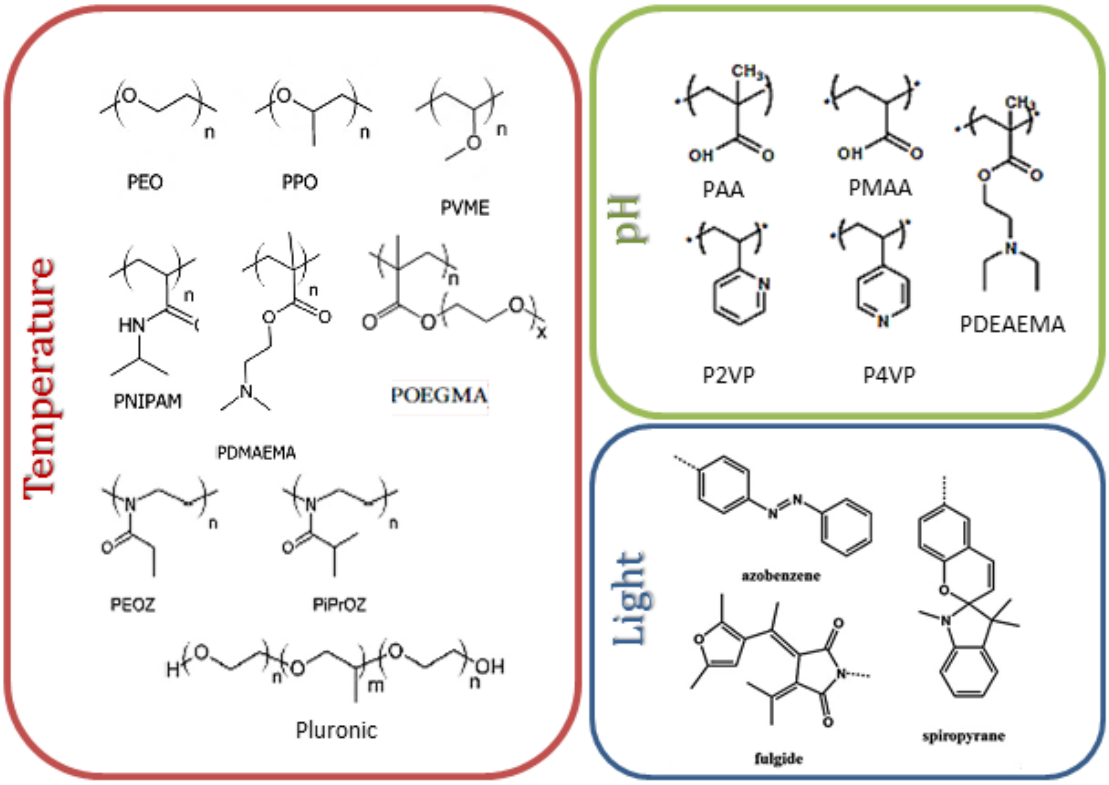

Figure 1.1 Chemical structures of the most common stimuli-responsive polymers, divided by type of stimuli.

1.1.1. Temperature-Responsive Polymers

Polymers that respond to temperature are one of the widely used classes of polymer materials. Temperature-sensitive polymers in diluted solutions undergo a coil-to-globule transition upon a change in the solution temperature. The coil-to-globule transition is generally characterized by a change of the solvent quality from good to poor. There are two typical phenomena characterized by upper critical solution temperature (UCST), when the transition occurs upon cooling, and lower critical transition temperature (LCST), when the transition appears with increasing temperature. The second one is of the greatest interest over the last decade due to numerous possible applications: tissue engineering, drug delivery, surface engineering.[1-6] Figure 1.2 shows the idealized phase diagrams for the UCST and LCST type transitions in dependence of polymer concentration (ϕ) and temperature.

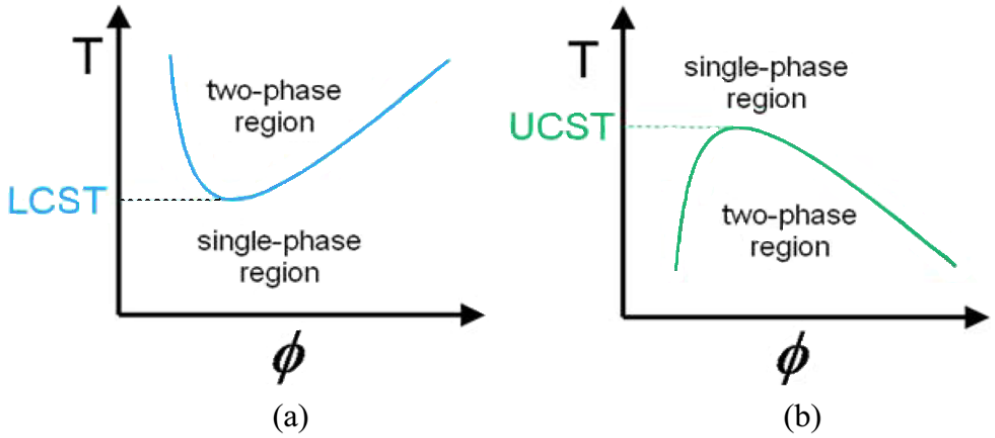

Figure 1.2 Idealized phase diagram for the (a) LCST-; and (b) UCST-transition.

The UCST and LCST temperatures are defined as the highest and lowest points on the binodal, respectively. At all points of the binodal, a sharp transition from a stable single phase to two phases can be observed while increasing the temperature of the system (LCST). However, this phenomenon of a temperature-triggered hydrophobic-to-hydrophilic transition is fully reversible and cooling down the polymer solution can regenerate the initial state. This phenomenon is generally governed by the ratio of hydrophilic to lipophilic moieties on the polymer chain and is an energy-driven phenomenon which depends on the free energy of mixing or the enthalpy or entropy of the system. While the LCST (UCST) characterizes the lowest (highest) temperature at which phase separation can be observed on the phase diagram, the cloud point temperature (*cpt*) defines the onset of separation at each particular concentration. Polymer starts to phase separate from solution due to a molecular transition from a coiled, enthalpic favored structure to a dense globular, entropically favored structure. This process will minimize the free energy of the system considerably. The value of LCST might be dependent on such parameters as molecular weight, tacticity, incorporation of co-monomers and chemical nature.[6-8]

The class of thermo-responsive polymers includes various polyacrylamides, polyvinylethers, polyoxazolines, as well as poly(oligoethyleneoxide)methacrylates (Figure 1.1). Poly(N-isopropylacrylamide) (PNiPAAm) is probably most investigated thermo-responsive polymer in aqueous solution, what might be explained by the value of LCST of about 32 ºC, very close to body temperature.[6,9-11] Phase transition here is caused by the formation of hydrogen bonds in system. Initially formed hydrogen bonds between the amide groups of the polymer and water molecules are partly replaced by polymer/polymer inter- and intramolecular hydrogen bonds with increasing temperature and phase separation occurrs. The LCST phenomenon itself is quite widespread for polymers containing H-bonding sites for water.[7,12] One practical phenomenon

has to be noted, PNiPAAm shows a hysteresis in the heating/cooling process. That phenomenon is explained by the mentioned inter-, intra-molecular hydrogen bonds, which hinder rehydration process with decreasing temperature. Moreover, changes in hydrophilic/hydrophobic balance also contribute to the separation process. The LCST of PNiPAAm is almost independent of the molecular weight, but it can be changed upon shifting the hydrophilic/hydrophobic balance. Copolymerization with a second monomer could be used for that purpose. Hydrophobic comonomers favorable to segment-segment interactions in polymer tend to decrease the LCST, whereas hydrophilic comonomers favorable to segment-solvent interactions have the opposite effect.[6,8]

Another interesting class of thermo-responsive polymers is poly(2-alkyl-2-oxazolines). Their properties vary from high hydrophilicity in (poly(2-metyl-2-oxazoline) (PMeOZ)[11] through thermal sensitivity in poly-(2-ethyl-2-oxazolne (PEtOZ), poly(2-*n*-propyl-2-oxazoline) and poly(2-isopropyl-2-oxazoline)(PiPrOZ))[2,13] with LCST transitions at 65 ºC, 36 ºC, and 24 ºC, respectively, to hydrophobicity typical for hydrophobic aromatic or aliphatic polymers (poly(2-phenyl, butyl, nonyl etc.-2-oxzolines) (PPhOZ, PBuOZ, PNonOZ).[6,14] In contrast to PNiPAAm, poly(alkyl oxazoline)s show a solubility transition at LCST without hysteresis, which makes them more suitable for all applications involving a reversible assembly/disassembly event (e.g. smart surfaces, thermoresponsive micelles). It is interesting to note that poly(2-isopropyl-2-oxazoline) (PiPrOZ) is a structural isomer of PNiPAAm and of poly(L-leucine). However, conversely to PNiPAAm and polypeptides, poly(alkyl oxazoline)s' molecular structure lacks H-bond donors. Therefore, no stabilization of the dehydrated molecules by additional interactions occurs above LCST.[8] Poly(2-alkyl-2-oxazolines) attracted increased attention in biomedical research due to their peptide-like structure and a wide range of adjustable physicochemical and biological properties depending on an alkyl substituent.[6,9,10]

The relationship between molecular weight and transition temperature is more pronounced for all poly(2-oxazoline)s and particularly for the more hydrophilic ones (PEtOZ, PiPrOZ) than with PNIPAM. PiPrOZ samples of molecular weights ranging from 1900 to 5700 g/mol exhibited cloud points from 45–63 ºC.[15,16] Even though the phase transition of PiPrOZ has been reported to be fully reversible, an irreversible formation of coagulate particles was observed when annealing a solution of PiPrOZ for several hours at 60 ºC, which is far above the cloud point temperature. This observed coagulation was found to be a hierarchical self-assembly process based on the directional crystallization of PiPrOZ into nanoribbons, which further assemble into nanofibers.[8,15]

In contrast to the numerous studies on the LCST behavior of poly(2-oxazoline)s in solution, only in a few recent reports has been discussed an upper critical solution temperature (UCST). It was found that PPhOZ exhibited an UCST in ethanol. Interestingly, the solubility of PPhOZ increased on addition of water to the ethanol solution, leading to a solubility maximum in the range 6–25 wt% of water in ethanol. In addition, it was reported that PEtOZ80-*stat*-PPhOZ20 exhibits both LCST and UCST transitions when heated in a water/ethanol mixture with 40 wt% ethanol. Furthermore, copolymers of EtOZ and NonOZ also display UCST behavior in water/ ethanol solvent mixtures. Moreover, the adjustment in LCST and UCST value can be done by copolymerization of several different moieties.

The other class of thermoresponsive polymers, that has to be mentioned, is triblock copolymers of poly(alkylene oxide)s. The most famous poly(alkylene oxide)s are poly(ethylene oxide) (PEO) and poly(propylene oxide) (PPO). The PEO displays the presence of both LCST and UCST behavior, which can be described by a close-loop temperature vs. concentration phase diagram. However the range of PEO solubility is wide enough in regard to temperature and concentration. The LCST of PEO is above 100 ºC for low molecular weight chains, it decreases to 100 ºC with the molecular weight above 10^6 g/mol. The LCST and UCST behavior has been studied both experimentally and theoretically, and been explained by the interaction between EO monomers and water molecules.[8,17]

As should be expected, the solubility of poly(alkylene oxide) decreases with an increasing number of (hydrophobic) carbon atoms per monomer. Poly(propylene oxide) with a molecular weight of 1200 g/mol shows a LCST only at around -5ºC. In order to design water-soluble poly(alkylene oxide) polymers with a tunable LCST, copolymers of ethylene oxide and more hydrophobic monomers were prepared. Ucon® is for instance a random (statistical) copolymer of ethylene oxide (EO) and propylene oxide (PO). Ucon® with 50% of EO and 50% of PO and M_n = 4000 g/mol exhibits a LCST of 55 ºC in water.[8] Nevertheless, the thermoresponsive block copolymers composed of PEO and PPO chains are more exploited. Pluronic® is a family of PEO-b-PPO-b-PEO triblock copolymers. They self-assemble at room temperature into micelles in aqueous solutions and were widely studied for formulation applications. In opposite to the polymers mentioned above, Pluronic®s, besides the LCST, are characterized by critical micelle concentration (*cmc*) and critical micelle temperature (*cmt*). Typical phase diagram for Pluronic® molecules are presented in Figure 1.3.

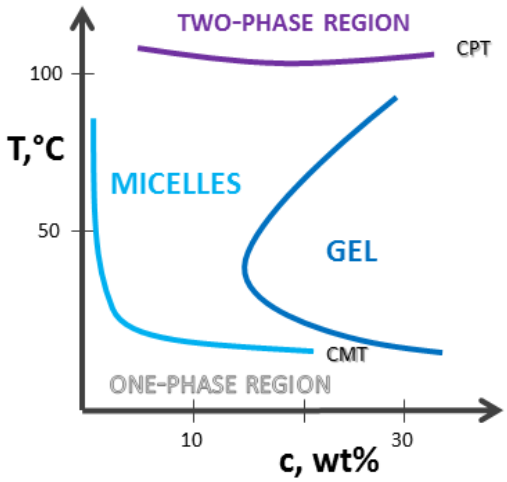

Figure 1.3 Idealized phase diagram for the system of Pluronic molecules dissolved in water.

1.1.2. pH-Responsive Polymers

Another class of stimuli-responsive polymers is polymers with pH sensitivity (Figure 1.1). pH-sensitive polymers have attracted considerable research interest because of the potential usage as drug delivery agents. The pH-sensitive polymers can be classified into three categories: anionic, cationic, and neutral. Ionic polymers contain ionizable groups that can reversibly change solubility through ionization/deionization. pH- sensitive neutral polymers normally contain acid-labile bonds in the main chain or side chains of the polymers. The most frequently used acid-labile bonds include acetal, hydrazone, and benzoic imine bonds.[18] These bonds are usually degraded under mild acidic conditions (pH 5 to 7), resulting in the formation of a new hydrophilic polymer and the destruction of the initial structure of system. An important parameter of a pH-sensitive polymer is pK_a value. Ionizable polymers with a pK_a value between 4 and 8 are candidates for pH-responsive systems.[6,18] Polymers with ionizable groups are usually referred to polyelectrolytes. It is possible to divide polyelectrolytes into two groups, strong and weak types. Strong polyelectrolytes, such as polysulfonates or polyphosphates, in sufficiently dilute solutions completely remove the counterions from the polyion. At the same time, in weak polyelectrolytes even at high charge density the counterion remains in close proximity of the polymer chain.[19] Thus, it creates the ability for a careful adjustment of dissociation process. In highly polar solvents such as water, ionizable groups can dissociate, leaving charges on polymer chains and releasing counterions in solution. Electrostatic interactions between charges lead to the expanded rod-like conformation of the macromolecule. When the polymer is protonated an effective attraction between monomers prevails over monomer-solvent interactions, which causes a neutral polymer chain without charged groups to

collapse into dense spherical globules in order to maximize the number of favorable polymer-polymer contacts and minimize the number of unfavorable polymer-solvent contacts. Thus, a polyelectrolyte chain undergoes an abrupt conformational transition from an extended to a collapsed state with decreasing chain charge.[20] Thus, for polyelectrolytes one can define the pK_a as a pH value where transition from expanded coil to globule conformation can occur. Cationic polymers deionize above their pK_a and ionize below it causing an increase in hydrophilicity and electrostatic repulsions of the polymer molecules, whereas the opposite holds for anionic polymers.[21] The pH-dependent protonation/deprotonation mechanism of the weak base/acid regulates the overall polarity (charge density) of the polymer and, together with Coulombic repulsion of identically charged chains, leads to pH-responsiveness.[22] The electrostatic interactions between charged monomers in polar solvents can be decreased by addition of salt. The presence of high amount of counterions leads to the screening of polymer charges that decreases the electrostatic interaction and results in increase on polymer flexibility.[20] Eventually, the pK_a value of a polymer can be adjusted by controlling the molecular weight of the polymer, changing the chemical environment of the ionizable groups, or copolymerizing monomers with different pK_a values. [23-25]

The most frequently used pH-sensitive anionic polymers are polyacids. Among them, poly(acrylic acid) (PAA) and its derivative poly(methacrylate acid) (PMAA), which have pK_a values of about 4–5, are the most representative. The transition in polymer solubility for PAA and PMAA corresponds to the range of pH fluctuation in human gastro-intestinal tract. PAA and PMAA are hydrophilic at the physiological pH 7.4 and hydrophobic at low pH (pH about 1–2), which makes them prospective for oral drug delivery. [26] [23-25,27,28] Moreover, there is specificity for the behavior of aqueous solution of polyacids in protonated state. They enable the formation of intra- and inter-molecule hydrogen bonds with either water or suitable side compounds or even between each other.[29-35] That feature has a major effect on solution properties of the systems. Even more, the temperature dependence of hydrogen bond's formation can determine the thermo-sensitivity of a whole system.[30,31]

The cationic polymers with ionizable amine groups are prospective in cancer therapy. By controlling the pK_a of the amine groups, these polymers can be made to deprotonate at pH 7.4 and protonate when the pH is slightly reduced to tumor extracellular pH (6.8). The change in conformation state of polymer chain is used as essential mechanism for the release of loaded drug.[23] Cationic polymers have also been used in the task, which they can complex with nucleotides trough electrostatic interaction. Poly(ethylene imine) has been widely used as DNA nanocarrier.[6,18,24,36]

Another interesting object is poly(dialkylaminoethyl methacrylate) (PDMAEMA, PDEAEMA). This polymer displays either pH- or temperature sensitive behavior and may be exploited in dual conditions. At low pH, it is soluble due to the protonation of nitrogen atom. At both basic and neutral pH, PDMAEMA is also water-soluble due to the formation of hydrogen bonds, and the observed lower critical solution temperature of PDMAEMA between 32–52 ºC is dependent on molecular weight. On the other hand, PDEAEMA is more hydrophobic and is water-insoluble at ambient temperature in neutral or basic pH.[24,37,38]

1.1.3. Other Responsive Polymers

Besides the typical triggers (temperature, pH), there are a number of various external physical stimuli, such as light, electric/magnetic field, ultrasound, which also found a certain application.[39] The feature of external triggers is spatial- and temporal impact, which can play sometimes a pivotal role.[40,41]

Here, we also have to mention the special type of responsive polymers – stimuli-responsive block copolymers. These polymers are built up from blocks of different nature. One or two of blocks can possess either pH- or termo-responsivity or even be responsive to other stimuli. Stimuli-responsive block copolymers enable the formation of micelles at certain conditions. Common features of polymeric micelles constructed of such polymers are their high solubility, low toxicity and longtime stability. The thermodynamic and kinetic stability of the micelles is controlled by the mass ratio of hydrophobic and hydrophilic blocks.[6] The hydrophobic domain has a dual assignment. First, hydrophobicity forces the polymer molecules to assemble in aqueous environment and second, the hydrophobic nature can be used for the entrapment of hydrophobic substances into them. Thus, the core, consisting of the hydrophobic domain, acts as a reservoir and protects the load whereas the hydrophilic shell mainly confers aqueous solubility and steric stability to the ensemble. These unique characteristics of amphiphilic block copolymers are responsible for the special advantage of using micelles for various applications. There are considerable numbers of reports on the controlled release of hydrophobic drugs from the block copolymer micelles in aqueous solutions.[23,24,27,28,37,40,42-44]

1.2. Surfactants and Their Applications

Surfactant molecules are molecules that are composed of a polar head that is compatible with water and a nonpolar or hydrophobic part that is compatible with oil. They are generally termed as amphiphilic molecules. This dual nature endows the surfactants with their unique solution and interfacial characteristics. Molecules of surfactant are fully dissolved at low concentration.

However, an increase in surfactant concentration promotes self-assembly and formation of aggregates, where hydrophobic parts of molecules segregate in the internal part of aggregates. Further increase in surfactant concentration leads to a corresponding increase in the amount of aggregates while the monomer concentration stays roughly independent of the total amphiphile concentration. The concentration value, where the pronounced change in the surfactant architecture results in significant change in a large number of solution properties, is named as critical micelle concentration (*cmc*).[45,46]

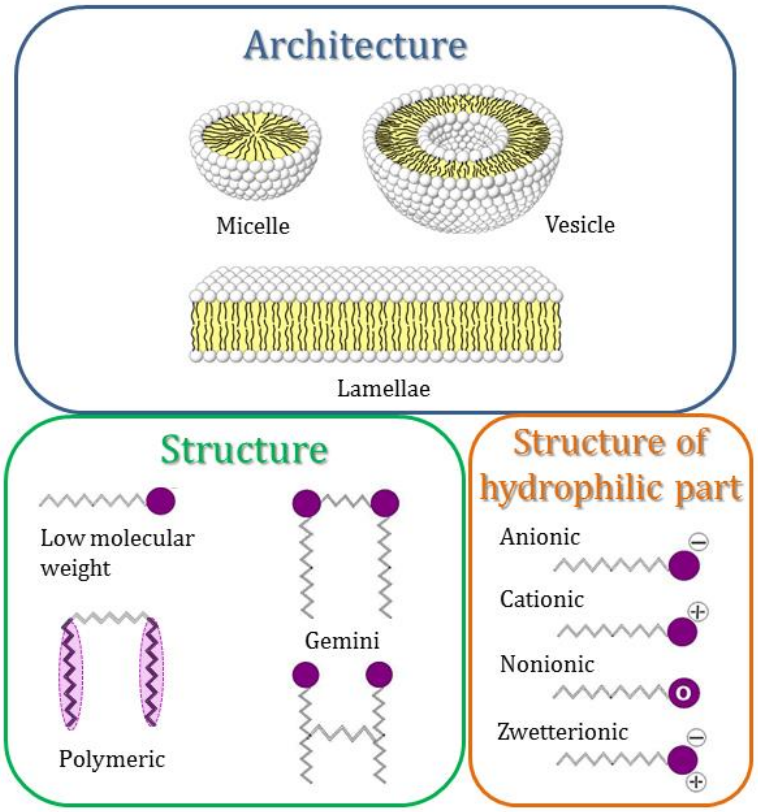

Figure 1.4 Classification of surfactant molecules.

Generally, it is possible to classify surfactants according to several parameters: architecture, nature, structure and chemical structure of hydrophilic part (Figure 1.4). Depending on the solution conditions and the type, surfactants can form the aggregates with spherical, cylidrical, or planar, or even spherical bilayer architecture. The spherical aggregates are usually referred to micelles, the planar aggregates are referred to lamellae and the spherical bilayers containing an encapsulated aqueous phase are called vesicles (Figure 1.4). [45,47,48] The other criteria describe the chemical structure of surfactants on a molecular level. Below we will try to attribute the architecture of surfactant aggregates to their chemical structure.

There are two main classes of surfactants, natural and synthetic surfactants. The term “natural surfactant” is often used in a broad meaning. Most typically it is referred to a surfactant taken directly from a natural source, such as lecithin. However, surfactants synthesized from natural raw materials (fatty acid esters) are also called “natural”, as well as a surfactant with one of the main building blocks obtained from a natural source. The latter class covers a number of compounds such as alkyl glucosides with a ‘natural’ sugar unit polar group or sterol-based surfactant with a ‘natural’ hydrophobic tail.[49] All other surfactants belong to the synthetic compounds and will be described further. Surfactants used in pharmacy and industry are usually called detergents. Detergents typically possess alkylbenzenesulfonate structure.

From the point of spatial structure, surfactants can be divided into three classes: low molecular weight surfactants, polymeric surfactants and Gemini surfactants (Figure 1.4). The polymeric and Gemini surfactants were intensively developed recently. They have certain advantages over low molecular weight surfactants and will be discussed later on. Low molecular weight surfactants that are simple in their spatial structure are usually classified to anionic, cationic, zwitterionic and nonionic ones (Figure 1.5).[50-54]

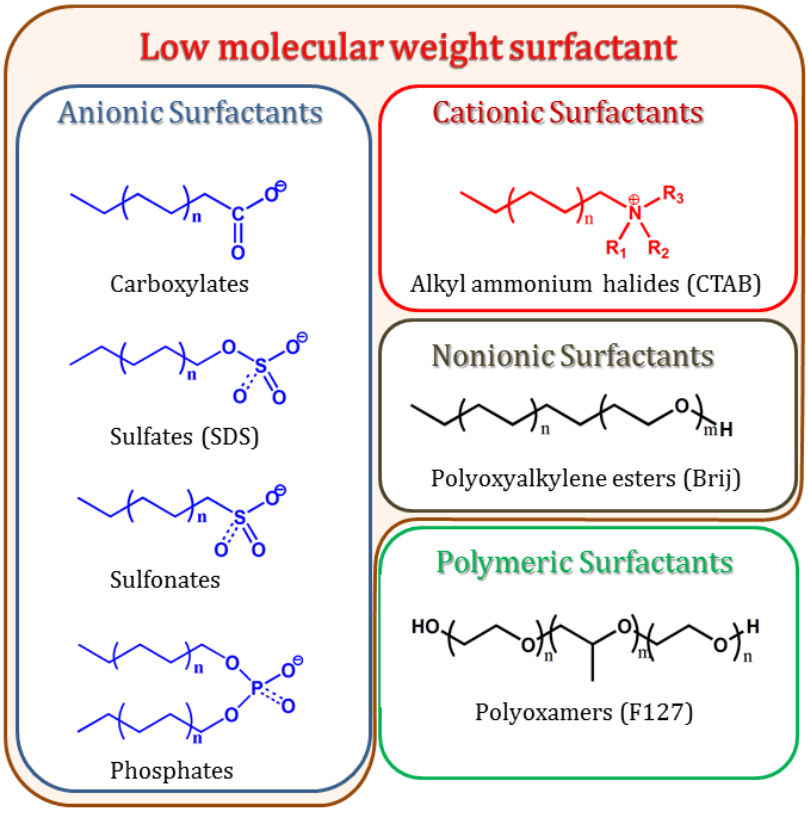

Figure 1.5 Chemical structures of the most typical surfactants, divided by the type of hydrophilic part.

1.2.1. Ionic Surfactants

The term ‘ionic surfactant’ historically defines a big class of either anionic or cationic surfactants. That type of surfactant has a charged group on the hydrophilic head of surfactant molecule. Logically, anionic surfactants carry negative charge while cationic ones are positively charged. The list of most frequently encountered anionic surfactants includes sulfates/sulfonates, carboxylates and phosphates (Figure 1.5).[50] However, the sulfates/sulfonates are mentioned more often. In sulfate the hydrophobe is attached to the hydrophilic group of molecule by a labile C-O-S linkage, this is relatively easily hydrolyzed to the corresponding alcohol and (bi)sulfate ion by dilute aqueous acids. Sulfonates, on the other hand, contain a robust C-S linkage that is much more stable. The sulfonates, therefore, find application in a variety of pH conditions that are too drastic for sulfate esters.[50] Commonly, anionic surfactants find a major application in the fields of detergency and solubilization. The other field of application is destruction the membrane’s lipid bilayers and the following solubilization of involved enzymes, receptors and proteins without their denaturation.[55]

The cationic surfactants are typically the derivatives of alkylammonium or imidazolinium salts with quaternary ammonium substituted (Figure 1.5). The primary usage of cationic surfactants was related to their tendency to absorb at surfaces i.e. metals, minerals, plastics, cell membranes since the majority of surfaces are negatively charged.[53] Cationic surfactants have utility as nucleic acid-binding and cleaning agents, potential pharmacological agents, electron donors/acceptors in intramolecular electron transfer processes, and analytical reagents.[51] Besides that, they have strong bactericidal properties and, thus, are extensively used for cleansing wounds or burns on skin.

Typically, anionic surfactants display the strongest solubilization properties among all surfactant systems and capable to interact with either hydrophilic or hydrophobic polymers. Interestingly, introduction of a cationic surfactant into anionic surfactant mixture and vice versa enhances the solubilization properties of the system. Explanation of that lies in the field of electrostatic interactions. Electrostatic repulsion between the head groups of ionic surfactants with the same charge increases the free energy of micelle formation. If other surfactants with oppositely charged head groups are incorporated into the micelles, the strong attractive interactions between the oppositely charged head groups of the surfactant molecules compensate the repulsive forces between the other ones and stabilize it. [51,52] High sensitivity of ionic surfactants to electrolyte effect can be described by the same process.

1.2.2. Nonionic Surfactants

Nonionic surfactants as opposed to the ionic ones do not have any electrical charges. The hydrophilic part of such surfactants contains either polyether or polyhydroxyl groups. Non-ionic surfactants have long been recognized as compounds with a low irritating effect, and hence are widely used in pharmacy and cosmetics industry. Besides giving physical stability, nonionic surface active agents may have a biological activity as membrane-disrupting permeabilizers or may influence the activity of other molecules. Non-ionic surfactants are known to have effects on the permeability of biological membranes, including the skin. Their comparatively low toxicity and irritation potential have made these compounds good candidates as potential penetration enhancers for use in transdermal drug delivery systems. The nonionic surfactants can be classified as polyol esters, glucoside alkyl esters and poloxamers (block copolymers of polyethylene glycol and polypropylene glycol) (Figure 1.5). The most commonly used non-ionic surfactants are ethers of fatty alcohols.[53]

Non-ionic surfactants are compatible with all other types of surfactants and their physicochemical properties unlike those of ionic surfactants are not markedly affected by electrolytes. The physicochemical properties of ethoxylated compounds are very temperature-dependent and a reverse solubility versus temperature behavior is observed in water. The temperature at which the surfactant becomes insoluble is *cpt*. The cloud point is an important parameter of non-ionic surfactants and several properties, e.g. detergency, relate with *cpt* value.[53]

Zwitterionic (amphoteric) surfactants have both cationic and anionic centers attached to the same molecule. The cationic part is based on primary, secondary, or tertiary amines or quaternary ammonium cations. The anionic part can be variable and usually includes sulfonates or other anionic groups. The zwitterionic surfactants as a group are characterized by excellent dermatological properties. They also exhibit low eye irritation and are frequently used in shampoos and other cosmetic products. They are compatible with all other classes of surfactants, but are the smallest surfactant class, partly due to high price.[53]

1.2.3. Thermodynamics of Association Process in Surfactants

As was mentioned above, the basic reason for micelle formation is the tendency for the alkyl chains to avoid contact with water in combination with the affinity to water of the polar head group. Micellar aggregation is thus due to a delicate balance between these two types of thermodynamic forces. General concept for interpretation of micelle formation mechanism is

based on a partitioning of the free energy in system into a hydrophobic and an electrostatic or solvation part. With reference to monomeric surfactants in solution it is the hydrophobic interaction that promotes aggregation while the electrostatic effects are opposing it. The contribution of hydrophobic interactions can be estimated by considering the aggregate core to be like a liquid hydrocarbon. Then, the magnitude of that contribution is defined by alkyl chain length and is independent of the aggregation number in micelles.[45,56] At the same time, the aggregation number has been found to increase with increasing length of the hydrophobic chain.[46,57] The electrostatic contribution, in the simplest way, was attributed to Coulombic repulsion between the charged head-groups. Moreover, the counterions play a very important role for the stabilization of an overcharged micelle. It was proven experimentally that the energy gain in reducing the water-hydrocarbon contact dominates over the repulsion interactions between the polar headgroups in process of micelles formation.[56] Thus, the micellization process is governed primarily by the entropy gain. This large entropy increase in aqueous medium has been explained in two ways: structuring of the water molecules surrounding the hydrocarbon chains in aqueous medium, resulting in an increase in the entropy of the system when the hydrocarbon chains are removed from the aqueous medium to the interior of the micelle; increased freedom of the hydrophobic chain in the nonpolar interior of the micelle compared to the aqueous environment.[58] Nevertheless, the nature of the hydrophilic group regulates most of the parameters in the aggregation process: *cmc* value, size and shape of structures. The factor of repulsion between polar head-groups of surfactant molecules also exists for nonionic surfactant. This repulsion can be generated by dipolar forces or by the requirement that the polar groups remain solvated by water. It seems that specific solvation effects are of greater importance in the nonionic systems.[56] For a given length of the surfactant tail, the *cmc* value is lower for a nonionic surfactant than for an ionic one.[45]

When the concentration of surfactant exceeds the *cmc* value the formation of aggregates is induced. However, it was noted, the increase in the size of aggregates is limited within the stability region of the isotropic micellar phase, while the change in aggregation number is significant. Nowadays, it is well accepted that micelles exist in dynamic equilibrium with individual surfactant molecules that are constantly being exchanged between the bulk solution and the micelles. Additionally, the micelles themselves are continuously disintegrating and reassembling. There are two relaxation processed involved in micellar solutions. The first is a fast relaxation process with characteristic time in the order of microseconds, which is associated with the quick exchange of monomers between micelles and the surrounding bulk phase. The second relaxation time in the order of milliseconds is attributed to the micelle formation and

dissolution process.[46,56,59] The second process is significantly retarded in nonionic and polymeric surfactants as well as in mixed systems.[46,60-62] Micellar relaxation kinetics shows dependence on temperature, pressure, and concentration, as well as on the addition of other species such as short-chain alcohols.[46] Thus, when the dynamic mechanism of micelle kinetics is taken into account, the behavior in system with increase in surfactant concentration can be easily understood. At concentrations slightly above the *cmc*, micelles are considered to be of spherical shape. A small increase in surfactant concentration above the *cmc* value does not have effect on the shape, size and aggregation number of micelles.[63] The further addition results in the increase an aggregation number of micelles.[58] The size and the shape are kept on the same level by a squeezing the water molecule from the hydration shell. At a certain surfactant concentration, the surface becomes increasingly saturated by surfactant molecules. The aggregation number reaches a second critical value when the spherical shape is no longer the most energetically favorable, then the spherical to rod-like transition takes place. The point of shape transition is strongly dependent on the relative size of the alkyl chains and the polar head group repulsion. For nonionic surfactants the process might be significantly constricted by weak repulsion activity of polar heads. Changes in temperature or additives in the solution may also change the shape and stability of the micelles.

The important molecular characteristics of the surfactant are the alkyl chain length l_o, the volume of the apolar part, v_o, and the polar head cross section area, a_p.[45,56,64] The molecular packing of the surfactant molecules is mainly determined by the area a_p which a surfactant molecule requires at the interface. If the area a_p is larger than the cross section of the hydrocarbon chain in its equilibrium conformation, the interface of the micelle will be curved towards the hydrocarbon core; if they are equal, the interface will be flat on a local scale; and if it is smaller, the interface will be curved the other way. The significant increase in surfactant concentration leads to increase in aggregation number of micelles, as was noted in kinetic determination of aggregation process. The consequence of such behavior would be the change in a_p, which results in curvature change.[46,64] The structure of a micelle, thus, could vary from spherical to rod- or disc-like to lamellar in shape. Additives, such as medium-chain alcohols that are solubilized in the vicinity of the head groups, increase the value of a_p. With ionic surfactants, a_p decreases with increase in the electrolyte content of the solution, due to compression of the electrical double layer, and also with increase in the concentration of the ionic surfactant, since that increases the concentration of counterions in the solution.[58] From simple geometrical considerations it follows that the shape of a micelle can be expressed by the packing parameter $p = v_o / l_o a_p$. The packing parameter varies from 1/3 for spherical micelles to 1 for bilayers (Figure 1.6).[59,64]

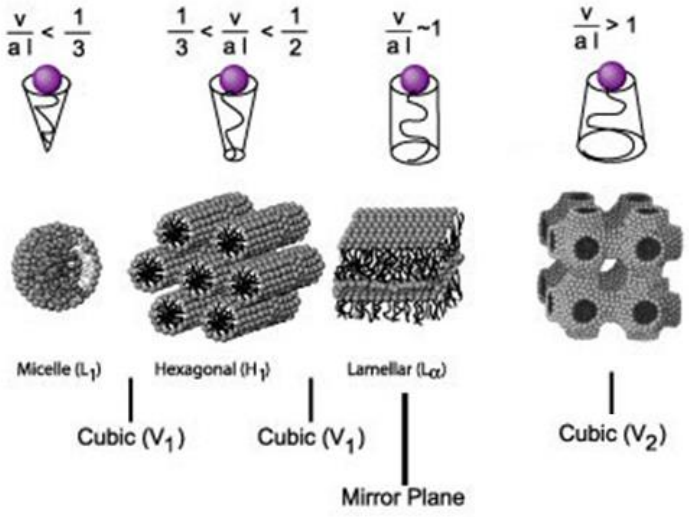

Figure 1.6 Geometric structures of surfactant aggregates in dependence on packing parameter.

The ability of the aqueous surfactant solutions to enhance the solubility of hydrophobic solutes that have poor solubility in water, is one of the distinguishable features of surfactant systems. This solubilization is a consequence of the presence of hydrophobic domains in the surfactant aggregates which act as compatible microenvironment for the location of hydrophobic moieties. The enhanced solubility of a hydrophobic solute has been found to be orders of magnitude higher than its aqueous solubility in the absence of surfactants.[45] If the solubilized molecules are entirely located in the region of the surfactant tails, the shapes of aggregates (micelles) are usually well-preserved. Alternately, if the solubilized molecules form a domain themselves in the interior of the aggregates in addition to being present among the surfactant tails, then the aggregates are referred to as microemulsions.[45] Solubilization is a factor which generally influences the aggregation process. Solubilizates may markedly promote micelle formation, so *cmc* value determined from solubilization studies varies significantly.[47] The presence of electrolyte also decreases the *cmc*, due to the so-called "salting out" effect. The work required to accommodate a nonpolar solute in a specific volume of water is increased in electrolyte solution because of strong water/ion interactions. When surfactant monomers are salted out by the presence of an electrolyte, micellization is favored and the *cmc* is decreased.[46]

1.3. Polymer-Surfactant Interactions

The behavior of polymer-surfactant systems and their interactions observed in mixtures are important for understanding of biochemically and physiologically related issues. They may clarify the behavior and functionality of lung (pulmonary) surfactants, the role of surfactants and lipids in DNA transfection, and the synergistic effects of some natural components. From a

fundamental point of view there is no significant difference in the observed phase behavior of polymer-surfactant systems when proteins or DNA are replaced by a synthetic polymer.[65] Proteins and DNA can be considered as polyelectrolytes in many of their physicochemical properties. Further developments showed that polymer–surfactant mixtures have more appealing applications as gelling agents, stabilizers, thickeners, and regulators of matter exchange. Furthermore, polymer-surfactant systems find more intensive application in field of control drug delivery systems.

Polymers and surfactants are often used together in industrial formulations to combine advantages of their different properties. Polymer-surfactant combinations in aqueous solutions can be broadly classified into four categories, namely uncharged polymer - ionic surfactant, oppositely charged polymer-surfactant, hydrophobe-modified polymer-surfactant and charged polymer – nonionic surfactant systems. While the dominant forces responsible for interactions in the second and third systems are obvious, the reasons for the interaction in the remaining two cases are less clear.[66] Obviously, there are several properties of polymers which influence their interaction with surfactants. In charged polymer-oppositely charged surfactant systems, the interactions are significantly stronger than those in uncharged polymer-charged surfactant systems because of the dominant electrostatic forces. But even here it is quite apparent that it is not only the charge density of the polymer which is important.[66]

1.3.1. Uncharged Polymer – Ionic Surfactant Interactions

According to one theory the driving force for micelle formation and binding of surfactant to the polymer (in the absence of strong ionic interactions) is essentially the same, namely, as the hydrophobic interactions. [67,68] The polymer molecules are considered to be composed of hydrocarbon segments and polar segments. For a given polymer conformation in solution, a definite number of contacts between the polar and the non-polar segments are generated. These contacts between the dissimilar segments resemble on a molecular scale, the macroscopic hydrocarbon-polar medium interface. Therefore, they may be viewed as the probable sites of surfactant binding. Clusters of surfactant molecules bind at these sites to form pseudo-micelles in a such way that the hydrocarbon segments of the polymer as well as the hydrocarbon tail of the surfactant both are effectively shielded from unfavorable contacts with water.[67,68] The model is based on the mass balance equation and on assumed intrinsic equilibrium constant for the binding of surfactant on the polymer and surfactant concentration as essential parameters for the treatment of the binding process. Thus, the equilibrium binding constant is independent of type,

position of binding site on polymer, as well as of surfactant concentration. Even more, the kinetic mechanism of micelle formation was not taken into account.

When surfactant molecules are added to the polymer solution, two possibilities can occur, surfactant can bind to a polymer binding site in the form of a cluster or self-associate to form micellar aggregates in solution. Therefore, at equilibrium, the aqueous solution consists of singly dispersed surfactant molecules and micellar aggregates of all possible sizes in addition to the surfactant-bound polymer molecules with different degrees of saturation. The extent of binding of the surfactant to the polymer depends both on the free surfactant and the free polymer concentrations as well as on the standard free energy difference between the surfactant-bound polymer in solution and the free surfactant plus the free polymer in solution. Because of the similarity of the thermodynamic driving forces and of the end states of the surfactant in the two processes, the standard free energy changes per surfactant molecule associated with the two processes are assumed to be equal. In the case of moderate cooperative binding, the binding of surfactant to polymer occurs only at certain concentration of surfactant. The critical aggregation concentration (*cac*) is a first critical point at which the surfactant binding to polymer is observed. That binding proceeds rapidly as the surfactant concentration is increased. When the free surfactant concentration reaches the critical micelle concentration, a second critical concentration (C_2) is observed corresponding to the onset of micellization which subsequently overtakes the surfactant binding to the polymer. In general case, the *cac* is characteristic of particular surfactant and does not depend on polymer content and molecular weight; on the other hand the C_2 can be considered as the micelle-polymer saturation point and it exhibits strong dependence on the concentration and molecular weight of the polymer. The values of *cac*, *cmc* and C_2 can be deduced from either surface tension technique or isothermal titration calorimetry method (Figure 1.7).[65,69] Experiments show weak dependence of both parameters on temperature and a great one on addition of extra salt. The relation *cac/cmc* is usually used for estimation the interaction strength between compounds.[65,70]

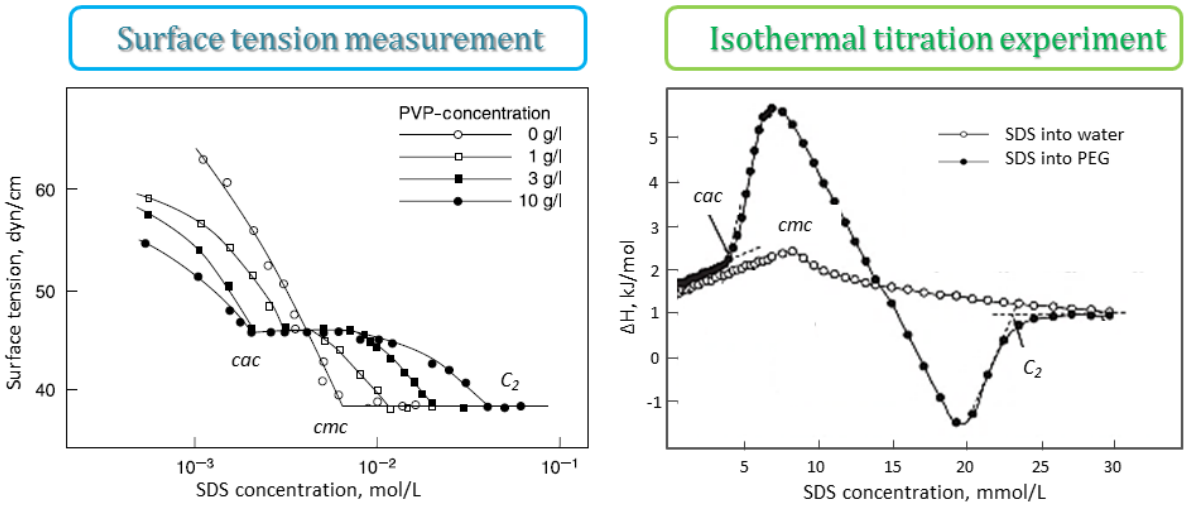

Figure 1.7 Ways of evaluation the characteristic parameters for polymer/surfactant interactions.[65,69]

The model suggests a possible way based on stereochemical rearrangements of the polymer segments for reducing the surfactant binding to the polymer while retaining the polymer characteristics. If the segment lengths of polymer chain are decreased below certain critical values, then due to steric requirements, effective hydrophobic bonding of the hydrocarbon regions of the polymer as well as the surfactant in the pseudomicelles is not realized. That means, that the standard free energy difference associated with surfactant binding to the polymer becomes less favorable than that for micellization. Therefore, the micellization process will overshadow surfactant binding to the polymer, thus reducing, if not eliminating the binding process.[67] Obviously, there is another effect, when the polymer influences the interaction between surfactant head groups making the micellization process weaker or stronger.[66]

Several parameters have effect on the polymer-surfactant interaction process. Among them temperature, salt content, as well as cationic/anionic nature and type of counter ion in surfactant play a predominant role.. As was mentioned above, the type of counter ion plays an important role in the micelle formation process. The counter ion compensates the charge of hydrophilic head group in the surfactant and makes possible the coexistence of surfactant molecules in micelle in spite of the electrostatic repulsion in their head groups. The same effect has the salt addition. The presence of polymer molecule, indeed, results in structure changes in micellar solution that is pronounced in the appearing of *cac*. Thus, the nature of counter ion should have significant effect on the stabilization of polymer-surfactant interactions.

The interactions in uncharged polymer – ionic surfactant system are typically described through the PEO – SDS interactions. Historically, this was the first system under the investigation in polymer-surfactant association process and most of conclusions were done essentially for this system. The counterion of the ionic surfactant is known to be of great importance. Thus, the replacement of Na by Li on SDS molecule increases the strength of polymer-surfactant interaction, while the insertion of Cs has the opposite effect. Moreover, the analysis of surface tension in polymer-surfactant (LiSD) complexes exhibits a slight penetration of the hydrophobic region of surfactant by PEO. Nevertheless, that penetration is not so large to rule out the possibility of complete PEO location in the underside layer of strongly interacting SDS/PEO system.[71] Sodium alkyl phosphates, in comparison with alkyl sulfates (in particular SDS), were seen to interact more weakly than their sulfate analogs. An increase in charge of the alkyl phosphate head group from one to two results in a marked reduction of interaction with PEO.[72] The similar effect was observed for alkyl sulfonate surfactants.[73] The other type of anionic surfactant, carboxylate sodium dodecanoate, exhibits more intensive interactions with PEO than in the case of SDS-PEO system. [74] The analysis shows that the strong surfactant binding is predominantly induced by folding of the polymer molecule around the surfactant aggregates.

In general, nonionic polymers interact strongly with anionic surfactants but weakly with cationic surfactants. This is interpreted as due to the bulkiness of the cationic head group, to a more favorable interaction between anionic surfactants and the hydration shell of polymers, or to an electrostatic repulsion between polymer and the surfactant due to the protonation of polymer.[66,75] The complex formation between cationic surfactants and both poly(vinyl methyl ether) and poly(propylene oxide) was observed, but no interaction has been revealed for PEO or poly(vinyl pyrrolidone). The experiments show that an interaction between PEO and cationic TTAB (tetradecyltrimethylammonium bromide) occurs only at temperatures above 35 ºC. It seems that the strength of polymer-cationic surfactant interactions is a function of polymer hydrophobicity. The more hydrophobic the polymer is, the more pronounced would be interactions in a system. At the same time, the polymer hydrophobicity is defined by solvent quality, surrounding temperature and molecular weight of polymer.[75] By the same factor, the temperature dependence of polymer-surfactant interaction can be described - the increase in temperature reduces the hydration ability of polymer, through the breaking down of stabilized hydrogen bonds, as well as through the solubilization of hydrophobic tails of the surfactant. Therefore, the elevation in temperature speeds up the interaction process.

At the recent time a wide attention was paid to the interaction of block copolymer, type PEO-PPO-PEO, with various surfactants. Water soluble poly(ethylene oxide)–poly(propylene oxide)–poly(ethylene oxide) triblock copolymers are essentially nonionic polymers. They are also surface active and behave like non-ionic surfactants; they form micelles above *cmc*. In polymer–surfactant studies, the most widely used Pluronic®s are the BASF code named F127, EO_{97}–PO_{69}–EO_{97} (M_W 12,500 g/mol) and L64, EO_{13}–PO_{30}–EO_{13} (M_W 2900 g/mol). The Pluronic®s bind strongly to anionic, cationic and non-ionic surfactants.[76-90] We will focus initially on their behavior with SDS because this is the most widely used surfactant. At temperatures below the *cmt* the Pluronic®s exist predominantly as unassociated nonionic polymers and form what is regarded as normal complex with SDS micelles. The Pluronic® monomers have a high affinity for SDS micelles.[80-83] Above the *cmt* the pluronics exist in micellar state and their interaction with SDS is more dramatic. When SDS is first added to micellar F127 or L64 the mixed SDS/pluronic micelles are formed in which the hydrophobic chain of the SDS penetrates to the PPO core of the Pluronic® micelle and the anionic SO_4^{2-} head group together with PEO groups are located on the surface. As SDS content increases, the electrostatic repulsion caused by anionic head groups results in a breakdown of the mixed micelle into smaller mixed aggregates. This gradual decomposition of L64 in the mixed micelles takes place over a broad concentration range of SDS. During this process, SDS binds to Pluronic®, and mixed SDS-rich micelles become to prevail. Eventually the amount of SDS monomers in the mixed micelles reaches a limit and pure SDS micelles are formed.

The Pluronic®s F127 and L64 also interact strongly with the non-ionic surfactant $C_{12}EO_6$ both above and below the *cmt* of the Pluronic®s.[88,89] In all cases mixed Pluronic®–$C_{12}EO_6$ micelles are formed and the mixing of both surfactants is synergistic. The structure of the mixed micelles involves the C_{12} alkyl group incorporated into the PPO core with the EO_6 chains and the EO blocks of the Pluronic®s making out the outer hydrophilic shell of the mixed micelles.

1.3.2. Oppositely Charged Polymer- Ionic Surfactant Interactions

Systems of a polyelectrolyte and an oppositely charged surfactant have been extensively studied in dilute solution.[65,66,91-112] The interactions in such systems start at very low surfactant concentrations, due to the strong attraction between the two species. Often, binding starts at a concentration several orders of magnitude lower than the *cmc* in polymer-free solution. Before going into the details of particular systems, one has to point out some general features for systems of a polyelectrolyte and oppositely charged surfactant. First, it should be noted that,

there is a considerable increase in an uneven radial distribution of ions in a polyelectrolytes solution, due to the electrostatic interactions. The concentration of counterions is highest close to the polyelectrolyte and decays rapidly with increasing distance from it. The uneven distribution of counterions also applies to monomeric surfactant counterions, present in the polyelectrolyte solution. Thus, the Poisson-Boltzmann theory is quite important for a correct interpretation of data, as the electrostatic interactions influence the activity of the surfactant ions. Second, the major reason for cooperative binding of surfactant molecules to an oppositely charged polyelectrolyte is the electrostatic stabilization of the surfactant micelles. In general case, this binding is not related to the amphiphilic nature of the surfactant ions.[66,91] The strong affinity between the components entails ion condensation and phase separation in the system.[65,66,91-93] The process is controlled by the net charge of the macromolecule. An increase in the net charge of a polymer chain modifies the broadness of the interaction region and shifts the charge neutralization line toward high surfactant content.[65]

The current understanding on the interaction between fully ionized polyelectrolyte and oppositely charged surfactant can be exemplified by interaction between polyacrylic acid (PAA) and cationic surfactant, e.g. DTAB. As it will be shown further, the polymer chains induce the formation of bound micelles. The hydrophobic binding ceases as the PAA is progressively ionized and DTAB binds to the charged polymer chains driven by electrostatic attraction. The counterions condensed on the charged polymer chains are released via the ion exchange process. The experiments suggest that the electrostatic binding is a process driven by entropy when the counterions of macromolecules as well as counterions of surfactant are released from the diffusive layer.[94] Continued addition of surfactant results in precipitation. The maximum precipitation yield takes place when the charge ratio between the polyelectrolyte and the surfactant is around 1:1, which implies the formation of precipitate in some kind of stoichiometric manner. Depending on the nature of the polyelectrolyte, further addition of excess surfactant may result in redissolution of the precipitate. Charge sign reversal was also observed in surfactant excess. The point where polyelectrolyte-surfactant complex precipitates was referred to as the point of turbidity.[65,66,92] The efforts for structure characterization in surfactant-polyelectrolyte complexes were based on viscosity measurements on dilute polyelectrolyte solutions. One has observed a dramatic decrease in the viscosity of polyelectrolyte solution on addition of cationic surfactant. That decrease was ascribed to coiling up of the polymer chains accompanying the surfactant binding. A polyelectrolyte chain in water solution is extended due to the repulsive forces in between polymer units. Therefore, the exchange of counterions in polyelectrolyte molecule with the surfactant ions results in coiling up

the polymer chain. The coiling of the chains can be expected both for electrostatic and for topological reasons in order to create a large contact area between the polymer chain and the micelle.[66,95] The polymer wraps around the surfactant micelles.[96] It has to be noted that the present mechanism of complex formation is valid for negatively charged polymer/cationic surfactant (PAA/CTAB [94], poly(sterenesulfonate)/CTAB) [97], poly(vinyl sulfate)/hexadecylbenzyldimethylammonium [98]) as well as vice versa, for positively charged polymer/anionic surfactant (polydiallyldimethylammonium chloride/SDS [92], hedroxyethylcellulose/SDS [99]).

Since, the presence of counterions has a significant effect on screening or reducing the repulsion forces at the micellar surface and makes the micelle formation process essentially possible, then the type of counterion has to be crucial. Therefore, one can consider the interaction process between a charged polymer and ionic surfactant with respect to 1) original counterion in surfactant; 2) type of polyelectrolyte; 3) type of counterion in polyelectrolyte molecule. Added salt and buffer modulate the process, because of the occurrence of some competition in surfactant ions.[65,100]

The experiments on poly(styrenesulfonate) (PSS)/alkyltrimethylammonium surfactant systems show that the type of counterion in surfactant molecule does not affect the interaction process. The halide counterions are effectively expelled from the cluster surface, even at the highest concentrations of added surfactant. All halide counterions are replaced by the polyelectrolyte molecules.[97] In some occasions the strength of polymer-surfactant interactions in polyelectrolyte-oppositely charged surfactant complexes can be tuned by introduction of the nonionic surfactant. The formation of mixed micelles decreases the charge density on micellar surface and attenuates the process of complex formation.[92]

The conformational properties and the dynamic behavior of polyelectrolyte chains are determined by the degree of ionization in polyelectrolyte and by the counterion concentration and distribution. The counterions may be solvated in different ways. The charges on the weak polyacids (PAA) can fluctuate due to the mobility of bound protons, whereas charges on the strong polyanions (PSS) are essentially immutable. Nevertheless, neither PAA nor PSS display any significant dependence on counterion type in interaction with CTAB/$C_{12}E_8$ mixed micelles.[101] While the counterion binding would be expected to diminish the effective charge on polycarboxylic acids, the mobility of bound protons in partially ionized polyacrylic acid can enhance the effective charge density through a polarization effect in which the local degree of ionization of the polyion increases in the vicinity of a positively charged surface.[101] Therefore,

the binding process is insensitive to the degree of ionization, when the value of degree of ionization is high enough. Addition of co-electrolyte such as salt results in sufficient screening of charges on the polymer chain; it makes the macromolecule more flexible.[93] Increase in polymer flexibility makes the polymer-surfactant interactions less favorable. Furthermore, the same effect can prevent the appearance of turbidity point.[93]

One can also try to characterize the interactions between a polyelectrolyte and charged surfactant at low values of degree of polymer ionization (α). The system of PAA and cationic/anionic surfactants has been taken for the analysis. When α is lower than a critical value (α_C), the hydrocarbon chains of dodecyltrimethylammonium bromide (DTAB) cooperatively bind to the apolar segments of PAA driven by hydrophobic interaction in DTAB molecules. The mixture precipitates at sufficiently low concentration of surfactant. It is attributed to the interchain polymer complexation via hydrogen bonding induced by the surfactant binding.[94,102,103] The precipitate is soon resolubilized with further addition of surfactant as more DTAB micelles are bound on the polymer backbones with their ionic head groups extending outwards. Contrary to previous studies on fully ionized polymers, evidence of interaction between anionic SDS and PAA was observed when the degree of neutralization of PAA is lower than 0.2. The process of interaction is the same, as it was mentioned for PAA/DTAB system.[102,103] With increasing α to 0.2 the interaction is significantly weakened and the amount of bound SDS on PAA is reduced considerably due to the enhanced electrostatic repulsion between negatively charged SDS and PAA chains.[94]

Recently, a number of works devoted to the interactions in a new class of block or graft polyelectrolytes with oppositely charged surfactants have been published. The blocked or grafted segments in such polymers could be either hydrophilic (PEO, PVP), hydrophobic (poly(n-alkyl acrylate)) or lipophilic (PNiPAm). Thus, this type of polymer/surfactant complexes represents a special class of lyophilic systems that exhibit combined amphiphilic and polyelectrolyte behavior.[104]

The situation will be somewhat special for the case of so-called hydrophobe-modified polymers. Hydrophobically modified water-soluble polymers consist of long hydrophilic chains to which small amounts of hydrophobic substituents are covalently incorporated as pendant chains, blocks or terminal (end capped) groups.[94] These polymers not only contain hydrophobic “nucleation sites” for micelle formation, but also can self-associate even in absence of surfactant.[105] In case of high persistence length of macromolecule, the elastic constraints do not allow the alkyl chains to segregate into nonpolar domains. The formation of intramolecular micelles is not

possible. Meanwhile, the nucleation of surfactants on the rigid hydrophobically modified chains helps to avoids the exposure of nonpolar moieties in water.[65] In particular, there will be a "mixed micelle" formation between the polymer and the surfactant alkyl chains.[106-108] The mechanism of interaction can be formulated as follows. At low polymer concentration the molecules are fully dissolved in water solution. The increase in polymer concentration results in formation of intermolecular or both intra- and intermolecular clusters of the hydrophobic tails.[105,107-109] As surfactant is added, the surfactant molecules associate with alkyl groups of polymer, often the cross-linking of the alkyl chains via the bound micelles is observed.[66,94,108] Depending on the polymer and surfactant concentrations, this cross-linking can lead to a three dimensional structure showing high viscosity and gel-like behavior.[94,108] As the binding proceeds, more micelles become available for binding and the network structure breaks down. This breakdown and subsequent disintegration of the polymer leads to a dissociated polymer–micellar surfactant complex which is fully saturated with bound micelles. Simplistically, the interaction in hydrophobically modified polymer/surfactant systems can be regarded as interaction between uncharged polymer and ionic surfactants. However, recently it has been reported that hydrophobically modified polymers can be incorporated not only with anionic surfactant, as it is possible for uncharged polymers, but they exhibit a high selectivity to cationic and nonionic surfactant as well.[105,106] There is a clear manifestation of effectiveness of the hydrophobic effect compared to electrostatic forces.[94]

1.3.3. Charged Polymer – Nonionic Surfactant and Uncharged Polymer – Nonionic Surfactant Interactions

There are only few reports on neutral polymer – nonionic surfactant systems.[66] The interactions in these systems are typically weak compared to other classes of polymer/surfactant systems. Ethylene oxide –type nonionic surfactants are, however, known to interact with polycarboxylic acids.[113-116] This interaction is analogous to the interaction between PEO and polycarboxylic acids, and is suggested to proceed by a combination of cooperative hydrogen bonding and hydrophobic interaction. Surface activity is not a requirement for such behavior. It has been found that the addition of polyethoxylated nonionic surfactants to PPO induces a rise in the cloud point temperature (*cpt*), which can be attributed to the interaction process. However, the *cmc* in the presence of polymer is essentially equal to the *cmc* of the pure surfactant, which is an indication of no, or only insignificant, interactions.[66]

1.4. Methods of Characterization

The samples studied in this work are diluted aqueous solutions of polymers or polymer/surfactant mixtures. Several experimental techniques were exploited for samples characterization. Scattering techniques, such as dynamic light scattering (DLS), static light scattering (SLS), small-angle X-ray scattering (SAXS) and small-angle neutron scattering (SANS) have been used for structure characterization of polymer/surfactant complexes in solution and to monitor the evolution of them under the change in the environment.

1.4.1. Dynamic Light Scattering (DLS)

DLS method takes advantage of the fact that the Brownian motion in liquids broadens the spectrum line of the incident laser beam (due to Doppler effect) and changes the dynamics of laser intensity fluctuations.[117] The spectral line widening can be transformed from frequency domain into time domain to analyze the time dependence of the electric field of scattered light represented by autocorrelation function of the electric field $G^{(1)}(t)$:

$$G^{(1)}(t) =< E_s^*(t)E_s(t+\tau) >= \lim_{T\to\infty} \frac{1}{2T}\int_{-T}^{T} E_s^*(t)E_s(t+\tau)dt \quad (1)$$

$$G^{(1)}(t) =< I_s > g^{(1)}(t) \quad (2)$$

where $E_s(t)$ and $E_s(t+\tau)$ are intensities of the electric field at time t and $t+\tau$, resp., τ is the time delay between two observations, $<I_s> =< E_s^*(t)E_s(t)>$ is time-averaged light scattering intensity and $g^{(1)}(t)$ is the normalized time correlation function of the electric field. Experimentally, the intensity correlation function $G^{(2)}(t)$ is measured and it is given by

$$G^{(2)}(t) =< E_s^*(t)E_s(t)E_s^*(t+\tau)E_s(t+\tau) > \quad (3)$$

The relation between $G^{(2)}(t)$ and $g^{(1)}(t)$, allowing calculation of $g^{(1)}(t)$ from experimental data, is given by the Siegert relation

$$G^{(2)}(t) = B\left(1+\beta\left|g^{(1)}(t)\right|^2\right) \quad (4)$$

where B is the "baseline" constant and β is the coherence factor. In the simplest case of dilute dispersions of small ($qR_G < 1$), identical and not interacting spherical particles without any internal structure, the $g^{(1)}(t)$ function can be expressed as

$$g^{(1)}(t) = \exp(-\Gamma t) \quad (5)$$

where

$$\Gamma = \frac{1}{\tau} = D_0 q^2 \qquad q = \frac{4\pi n}{\lambda}\sin(\theta/2) \quad (6,7)$$

Γ is the relaxation (decay) rate, τ is the relaxation time, D_o is the coefficient of translational diffusion of particles, λ is the wavelength of incident light in vacuum, n is the refractive index and θ is the scattering angle. Then, the hydrodynamic radius R_h of the molecules or particles can be calculated from the Stokes-Einstein relation

$$R_h = kT/f = kT/6\pi\eta_0 D_0 \tag{8}$$

where k is the Boltzmann constant, T the absolute temperature, f the friction coefficient and η_o is the viscosity of solvent.

In case of polydispersity, one relaxation time is substituted by a distribution of relaxation times $A(\tau)$ and $g^{(1)}(t)$ is given by its Laplace transformation:

$$g^{(1)}(t) = \int A(\tau) \exp(-t/\tau) d\tau \tag{9}$$

An inverse Laplace transformation is used to obtain the distribution of relaxation times (and corresponding distribution of hydrodynamic radii) from the measured $G^{(2)}(t)$. An illustrative example is given in Figure 1.8, where $g^{(2)}(t) = G^{(2)}(t)/B$ is a normalized intensity correlation function.

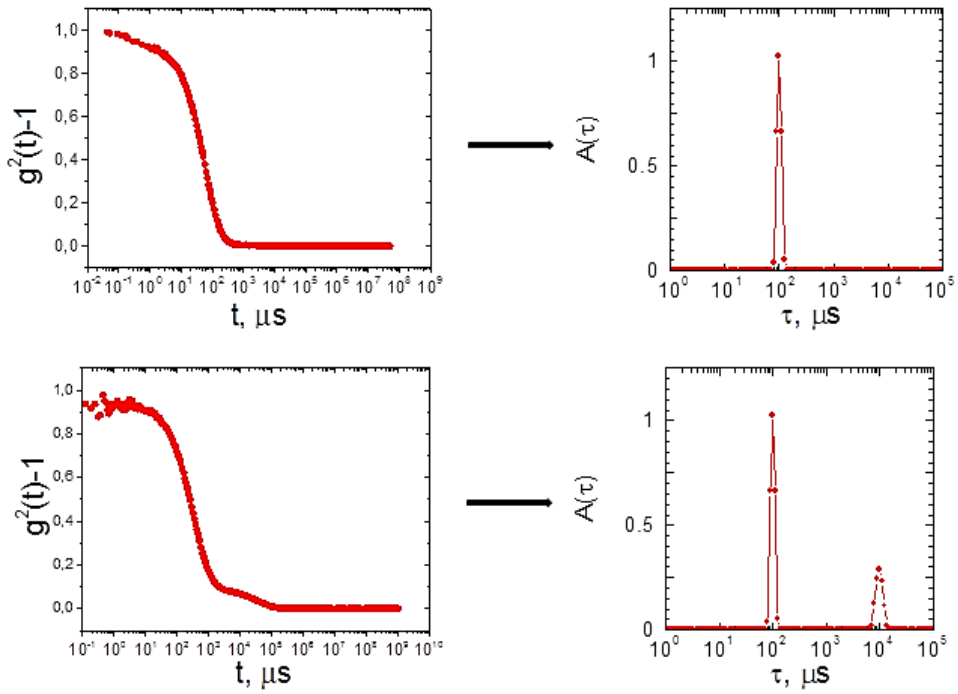

Figure 1.8 Typical correlation function with one and two decays and corresponding distribution functions of relaxation times obtained by inverse Laplace transformation.

1.4.2. Static Light Scattering (SLS)

Using SLS measurement technique, time averaged intensity of the scattered light is measured under assumption of elastic scattering. The light scattering occurs in the presence of fluctuations

of refractive index which have two main sources: density fluctuations and concentration fluctuations.[117] A relation between the changes in refractive index and the thermodynamic quantities (such as osmotic compressibility) was described by Smoluchowski and Einstein in fluctuation theory. Moreover, for particles with characteristic size $d > \lambda/20$ intraparticle interference must be taken into account and the scattered intensity becomes strongly angularly dependent which is described by a form factor $P(\theta)$. It is possible to calculate the form factor for simple geometrical shapes, sphere, rod, Gaussian-coil etc., but generally, the rigorous determination of $P(\theta)$ is very difficult, thus appropriate approximations are used. A useful approximation in respect to angular and concentration dependence is expressed by Zimm equation:

$$\frac{Kc}{R(q)} = \frac{1}{M}\left[1 + \frac{1}{3}R_G^2 q^2\right] + 2A_2 c \qquad (10)$$

This approximation allows to evaluate the molecular mass M_w, second virial coefficient A_2 and radius of gyration R_G independently of the specific form factor, *i.e.* for arbitrary shape of particles (over an interval ca $\lambda/20 < d < \lambda/2$). Typical Zimm plot for a polydisperse system is shown in Figure 1.9.

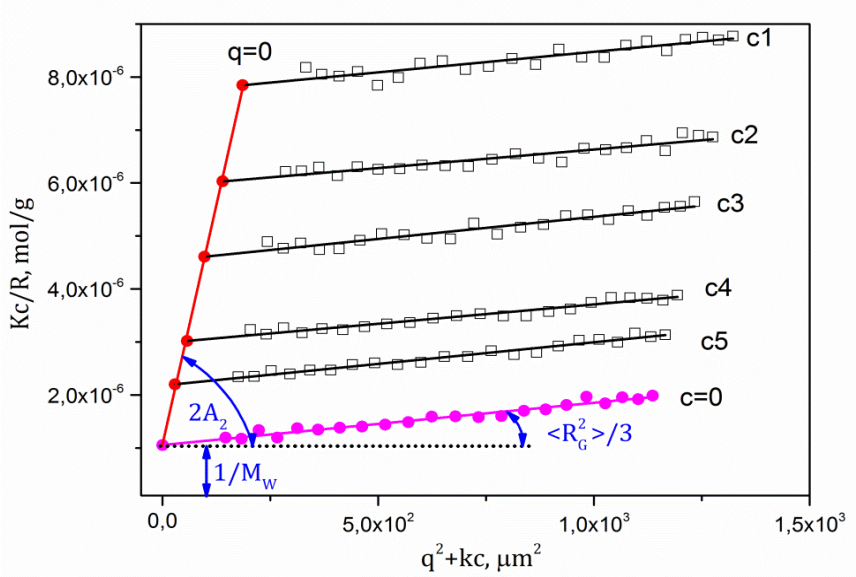

Figure 1.9 Typical Zimm plot obtained for a polydisperse system.

In general, besides the form factor, the structure factor reflecting the possible order of scattering objects in more concentrated systems should be included. Such evaluation can be used both for macromolecules and supramolecular structures.

1.4.3. SAXS and SANS

The small-angle X-ray and neutron scattering can be applied for characterization the nanoparticles with approximately 1-100 nm dimensions. The interference attenuation in such methods arises due to the local variations in scattering density within the sample resulting in a characteristic scattering curve. From that point of view, they are analogs to SLS method. The scattering contrast in X-ray scattering arises from the fluctuations in electron density in the shells of atoms and the interaction of neutrons with atomic nuclei is responsible for the neutron scattering. Nevertheless, the techniques of experimental data interpretation can be built on a common small angle scattering (SAS) theory.[118] Two contributions are also involved here. The form factor brings information about an average particle shape (because of interference from scattering centers within the same particle) and the structure factor gives information about average short or long-range order between the particles (as a result of the interparticle interference). In diluted systems the interparticle interaction decreases and the total intensity is a sum of scattering intensities from the single particles. It has been shown by SAS theory that in diluted systems the form factor can be approximated in accordance with the Guinier law [118]

$$P_0(q) = exp\left(\frac{-q^2 R_G^2}{3}\right) \quad (11)$$

$P_0(q)$ is normalized form factor and R_G is the radius of gyration of the particle. The region of validity of that approximation is usually taken as $qR_G \leq 1$. The behavior of the form factor for $qR_G >> 1$ can be evaluated as the Porod law [119]

$$P_0(q) = 2\pi\left(\frac{S_1}{v_1^2}\right) q^{-4} \quad (12)$$

Here, S_1 and v_1 are the surface and the volume of the particle, respectively. The assumption for validity of the Porod law is the sharpness of the phase boundary. Thus, several parameters can be obtained from the small angle scattering techniques. While the nanoparticle‘s size and shape can be deduced from Guinier regime, their structure can be analyzed by Porod law. Moreover, each of the methods has specific applicability. Synchrotron X-ray radiation offers the opportunity to use high-brilliance beam for collection of scattering patterns over short acquisition times. On the other hand, in SANS, the scattering amplitude can differ considerably between some chemical elements with similar atomic masses and even between isotopes of the same element. The most important pair of such isotopes is hydrogen (scattering amplitude b_i = -3.74 fm) and deuterium (b_i = +6.67 fm). By substituting one for another it is possible to make some moieties “visible” or “invisible” for neutrons, which substantially enhances the use of SANS.

In practice, a number of models can be applied to fit an experimental scattering curve (due to low signal-to-noise ratio or limited *q* interval). Therefore, *apriori* information about structure of nanoparticles is very useful.

1.4.4. Isothermal Titration Calorimetry (ITC)

Isothermal titration calorimetry (ITC) is widely used to study the thermodynamics of interactions in solution. The range of interactions studied by ITC is very general and covers, although not exclusively, protein–protein, protein-peptide or polymer-surfactant interactions. Basically, an ITC instrument, as shown in Figure 1.10, consists of a sample cell containing the analyte solution and a cell containing a reference solution (e.g., buffer solution) within an isothermal enclosure (adiabatic jacket). A syringe is positioned above the sample cell so that small aliquots of a titrant can be titrated into and mixed with the analyte in the sample cell.[120] Injection of titrant into the sample cell produces heat effects that are due to stirring and dilution of the ligand, dilution of the macromolecule and the heat of the interaction. The amount of power that must be applied to actively compensate for the heat produced in the sample cell, after an injection of ligand, is measured directly. The applied thermal power as a function of time that is required to return the calorimeter to its steady state, following an injection, is directly proportional to the absolute heat of reaction.[121]

$$q(i) = N_t \Delta H \tag{13}$$

where *q(i)* is the absolute heat of reaction; ΔH is the enthalpy of the interaction; N_t is the total molar amount of injected titrant. The transfer of power per injection is converted to a transfer of heat by integration of the transfer of power pulse over the time (Figure 1.11). The titration is continued until the transfer of heat reaches a constant minimum value. To obtain the final curves the values of the normalized heat of injection have to be calculated [122]:

$$Q(i) = \frac{q(i)}{\Delta V(i) c^{syr}} + Q_{dil} \tag{14}$$

where $\Delta V(i)$ is the injected volume; c^{syr} is the concentration of the added component (component in the syringe); Q_{dil} is the normalized heat of dilution. Thus, the ITC binding data converted to binding isotherms are the plot of heat per molar amount of injected titrant against the molar concentration of titrant or the ratio of the amounts of titrant and analyte.

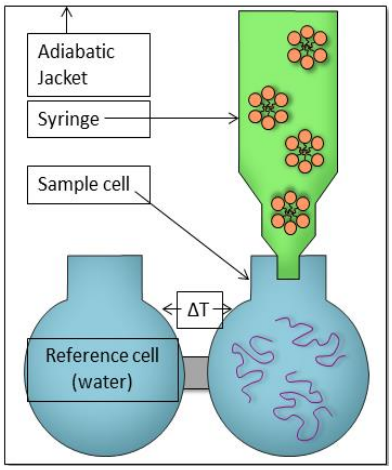

Figure 1.10 Principal scheme of isothermal titration experiment.

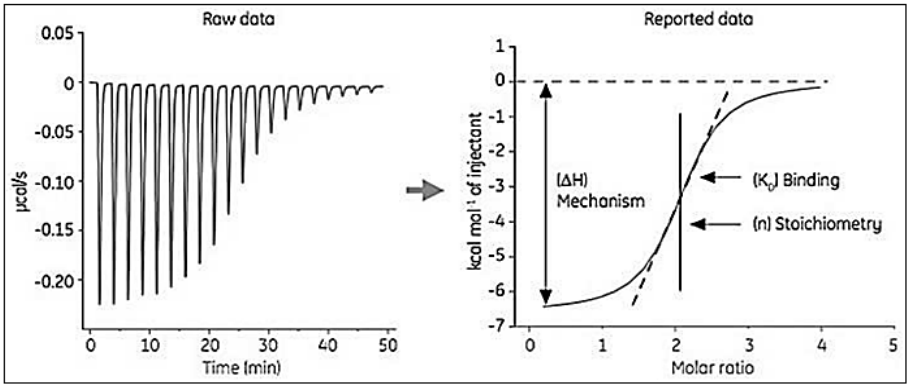

Figure 1.11 The example of data treatment on ITC experiment

Historically, the ITC method has been developed for investigation of interaction in biologically active substances (proteins and peptides). These compounds are, typically, characterized by specific binding sites, that determine the fitting model applied for ITC analysis.[120,121,123,124] The binding process, in general case, can be presented as following:

$$x[Sites] + y[L] \rightarrow y[Sites\ L] + (x - y)[Sites] \quad (15)$$

$$(x - y)[Sites] + y[L] \rightarrow y[Sites\ L] + (x - 2y)[Sites] \quad (16)$$

where, [*Sites*] is molar concentration of specific binding sites; [L] is molar concentration of ligand (titrant). The thermodynamic parameters obtained from such analysis are: the binding constant (K_a), the apparent ratio of the amount of titrant to the amount of analyte, and the reaction enthalpy (ΔH). The binding enthalpy may also include heat contributions from heats of protonation of the buffer if proton transfer occurs in the binding reaction and/or heat contributions from conformational changes occurring in the analyte and/or titrant upon binding. The change in the standard entropy of the reaction or binding entropy can then be determined from the fundamental equation of thermodynamics

$$\Delta G = \Delta H° - T\Delta S° \quad (17)$$

where $$\Delta G = -RTlnK_a \quad (18)$$

That theory seems hardly applied to the case of polymer-surfactant interactions. The main reason to that is high cooperativity of the interaction process. The first added amount of surfactant not only defines the place of binding but also accelerates it (See part Polymer-Surfactant Interactions). Due to that fact, it becomes incorrect to use the former model for the analysis of ITC data in mixed polymer-surfactant systems.

Recently, the regular solution theory has been suggested for the treatment of ITC data.[125-127] This model is based on the assumption of uniform complex formation.

$$[P] + n[S] \rightarrow x[PS_n] \quad (19)$$

$$x[PS_n] + n[S] \rightarrow x_1[PS_j] + x_2[PS_i] \quad (20)$$

where, [P] is concentration of polymer; [S] is concentration of surfactant and [PS_x] is concentration of polymer-surfactant complex in variety of binding ratios . Thus, the addition of one component to the other leads to the formation of one type of complexes irrespective of their mixing ratios. Further addition of a component promotes a rearrangement of the existing complexes. The process takes place until the full exhaustion of the added component. The general equation for the regular solution theory can be written as

$$q(i) = N_s\Delta H = (N_s - N_{mic,s})\Delta H_{mic,s} + \frac{N_p N_s \beta RT}{N_p + N_s} \quad (21)$$

where $q(i)$ is the absolute heat of reaction; ΔH is the enthalpy of the interaction; N_s, $N_{mic,s}$, and N_p are the total molar amount of surfactant injected, the molar amount of surfactant injected in micellar form, and the total molar amount of polymer in the calorimetrical cell, respectively. Then, $X_s = N_s /(N_s + N_p)$ is the mole fraction of surfactant, and $X_p = N_p /(N_s + N_p)$ is the mole fraction of polymer in the assemblies. The value $\Delta H_{mic,s}$ is the enthalpy of surfactant micellization. The term βRT corresponds to the mixing excess enthalpy and defines the difference between the experimental enthalpy and the value expected for ideal mixing. Insertion of eq 21 into eq 14 yields the normalized heat of injection and can be used for the further fitting procedure.

2. AIMS OF THE STUDY

There is a great interest in the investigation of polymer-surfactant interactions. The reason for such interest is the widespread use of polymer-surfactant systems in technology, pharmacy and some other applications. However, while the homopolymer-surfactant interactions are characterized well enough, the same interactions for block copolymers are poorly described. The main development in the latter topic has been achieved for Pluronic molecules (block copolymers of PEO and PPO) in the presence of variety of surfactants. Interestingly, the Pluronic molecules, due to the structure complexity, exhibit a thermo-responsive and surface-active behavior and in some occasions can be considered as a cosurfactant. In our work we took an attempt to expand our knowledge about polymer-surfactant interactions to the more complex systems and to figure out the driving forces for such processes.

In the present work we focus on structural and thermodynamic interpretation of processes between complex stimuli-responsive block copolymers and surfactants. Due to unprecedented complexity of the copolymers the analysis of their interaction with ionic and non-ionic surfactants has to be performed very thoroughly. To achieve that purpose, scattering techniques and the isothermal titration calorimetry method were exploited. Moreover, our sideline purpose was to shed light on the interpretation of titration curves obtained from ITC experiment.

The aims of the study are:

- ♣ The analysis of solution behavior of the statistical block copolymers PBuOZ-*co*-PiPrOZ in the presence and absence of polymeric nonionic surfactant F127;
- ♣ The structural characterization of hybrid nanoparticles formed by the copolymer PBuOZ-*co*-PiPrOZ of different composition ratios and polymeric surfactant F127. The study of temperature-dependent behavior in such nanoparticles;
- ♣ The analysis of solution behavior of the triblock copolymers PMeOZ-*stat*-(PBuOZ-*co*-PiPrOZ)-MeOZ with different ratios of hydrophilic, hydrophobic and thermosensitive blocks. The investigation of the temperature behavior of the triblock copolymers and their interactions with ionic surfactants (SDS, CTAB). The analysis of structure and thermodynamic evolution in the polymer/surfactant complex nanoparticles.
- ♣ The analysis of solution behavior of pH-sensitive amino acid based polymers in the presence and absence of nonionic surfactant Brij98. The structure and thermodynamic characterization of polymer/surfactant interactions and of the resulting complexes.

3. LIST OF PUBLICATIONS

Included articles:

Article 1:

Pánek, J.,Filippov, S.,Hrubý, M.,Rabyk, M.,Bogomolova, A.,Kučka, J.,Štěpánek, P.,

Thermoresponsive Nanoparticles Based on Poly(2-Alkyl-2-Oxazolines) and Pluronic F127.

Macromol. Rapid Commun., **2012**, 33, 1683-1689.

Article 2:

Bogomolova, A.,Hrubý, M.,Pánek, J.,Rabyk, M.,Turner, S.,Bals, S.,Steinhart, M.,Zhigunov, A.,Sedláček, O.,Štěpánek, P.,Filippov, S.,

Small-Angle X-ray Scattering and Light Scattering Study of Hybrid Nanoparticles Composed of Thermoresponsive Triblock Copolymer F127 and Thermoresponsive Statistical Polyoxazolines with Hydrophobic Moieties.

J. Appl. Crystallogr., **2013**, 46, 1690-1698.

Article 3:

Bogomolova, A., Filippov, S., Starovoytova, L., Angelov, B., Konarev, P., Sedlacek, O., Hruby, M., Stepanek, P.,

Study of Complex Thermosensitive Amphiphilic Polyoxazolines and Their Interaction with Ionic Surfactants. Are Hydrophobic, Thermosensitive, and Hydrophilic Moieties Equally Important?

J. Phys. Chem. B, **2014**, 118, 4940-4950.

Article 4:

Bogomolova, A., Keller, S., Klingler, J., Sedlak, M., Rak, D., Sturcova, A., Hruby, M., Stepanek, P., Filippov, S. K.,

Self-Assembly Thermodynamics of pH-Responsive Amino Acid-Based Polymers with a Non-Ionic Surfactant.

Langmuir, **2014**, 30, 11307-11318.

4. RESULTS

Thermoresponsive Nanoparticles Based on Poly(2-alkyl-2-Oxazolines) and Pluronic F127

Jiří Pánek, Sergey K. Filippov, Martin Hrubý,* Maria Rabyk, Anna Bogomolova, Jan Kučka, Petr Štěpánek

We synthesized statistical poly(2-isopropyl-2-oxazoline–*co*–2-butyl-2-oxazolines) (POXs) that are molecularly dissolved below their cloud point temperature in aqueous milieu and are incorporated into micellar nanoparticles of biocompatible Pluronic F127 (F127) after heating their solution above transition temperature, T_{tr}. A functional comonomer 2-(but-3-enyl)-2-oxazoline copolymerized into one of the POXs (polymer E) allows introduction of fenolic moieties and subsequent radionuclide labeling with iodine-125. Self-assembly of the polymer E with F127 leads to formation of radioactive nanoparticles with hydrodynamic diameter 20 nm in aqueous solution by heating to 37 °C. The nanoparticles are intended to be used as radioimaging tool in solid tumor diagnostics.

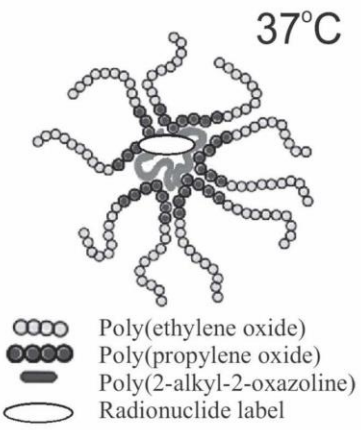

1. Introduction

Nanosized supramolecular structures such as micelles, nanoparticles, or liposomes are of a high interest in contemporary biomacromolecular research. Thermoresponsive systems based on self-assembly of thermosensitive polymers have the extra advantage that they may exist as molecular solutions at room temperature and form supramolecular nanoparticles after heating to body temperature (37 °C). Concerning biomedical applications, the particles may have an appropriate size for the enhanced permeation and retention (EPR) effect[1] (passive accumulation in solid tumor tisssue) while the corresponding unimers – which are in dynamic equilibrium with the particles[2] – can have molecular weights below the renal threshold, so they may be spontaneously eliminated by kidneys. It is possible, for example, to use a graft or block copolymer with thermoresponsive and hydrophilic blocks for this purpose. In another and easier way, as we have shown on a model poly(*N*-isopropyl acrylamide) with various surfactants,[3] the nanoparticles may be prepared by simple heating of a solution of the thermoresponsive polymer with a suitable surfactant forming a stabilized nanoemulsion. One of the possible uses of such systems is radiolabeling of molecularly dissolved thermoresponsive polymers with an appropriate radioisotope and their subsequent self-assembly into radioactive nanoparticles. Such a system exploiting the EPR effect may provide a sufficient contrast, for example, for diagnostics by noninvasive imaging techniques of nuclear medicine, which are attracting increasing interest nowadays.

In this paper, we describe new thermoresponsive nanoparticles based on self-assembly of a radiolabeled

J. Pánek, S. K. Filippov, M. Hrubý, M. Rabyk, A. Bogomolova, J. Kučka, P. Štěpánek
Institute of Macromolecular Chemistry ASCR, v. v. i., Heyrovsky Sq. 2, 162 06 Prague 6, Czech Republic
E-mail: mhruby@centrum.cz

Macromol. Rapid Commun. **2012**, *33*, 1683–1689
© 2012 WILEY-VCH Verlag GmbH & Co. KGaA, Weinheim

DOI: 10.1002/marc.201200254

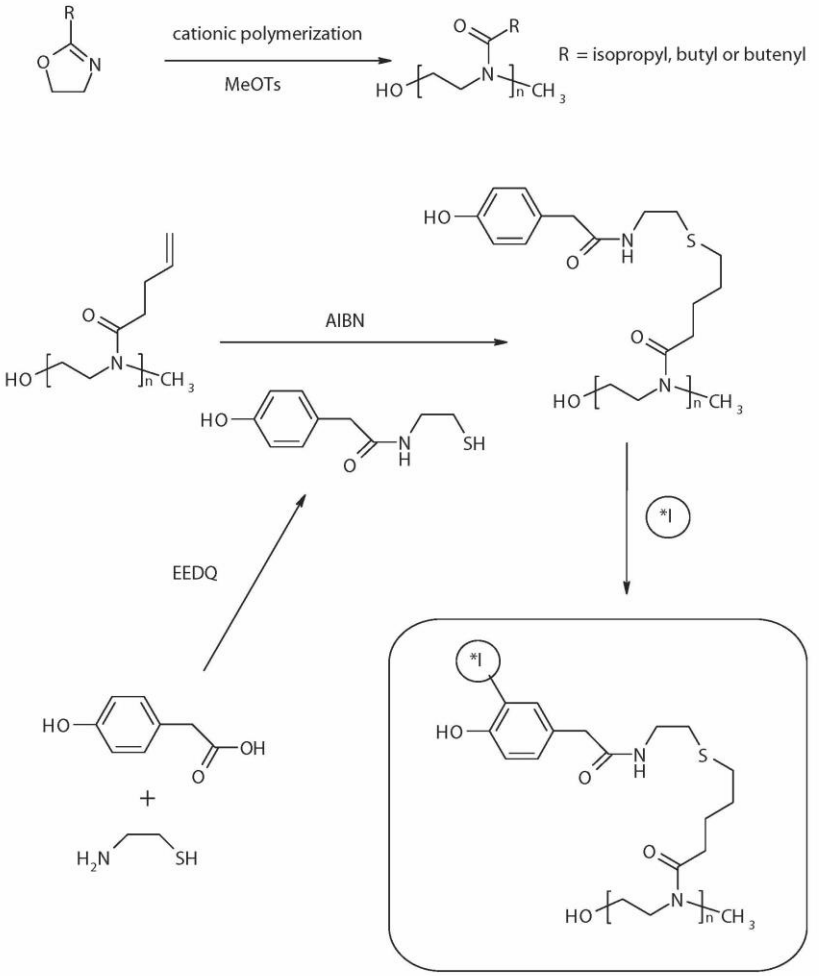

Scheme 1. Synthesis and radiolabeling of polymers.AIBN,azobis(isobutyronitrile); MeOTs,methyl *p*-toluenesulfonate; EEDQ, 2-ethoxy-1-ethoxykarbonyl-1,2-dihydroquinoline; *I, ^{125}I.

thermosensitive poly[2-isopropyl-2-oxazoline-*co*-2-butyl-2-oxazoline-*co*-2-(but-3-enyl)-2-oxazoline] with Pluronic F127 (F127) dissolved in aqueous milieu. Ring-opening cationic polymerization allows us to reach narrow molecular weight distributions of poly(2-alkyl-2-oxazolines) easily.[4] The thermoresponsive polymers based on 2-isopropyl-2-oxazoline (IprOX) have a peptide-related structure, they exhibit lower critical solution temperature[5] above which they become insoluble and their cloud point temperature (CPT) may be adjusted in a wide range by copolymerization of 2-butyl-2-oxazoline (BuOX). Moreover, functional comonomer 2-(but-3-enyl)-2-oxazoline (ENOX) allows to introduce double bonds, which may be further modified by the addition of thiols,[6] for example, with phenolic ring-containing thiols to allow radiolabeling by a model radionuclide (see Scheme 1). The system described in this paper (thermoresponsive statistical polyoxazoline with Pluronic F 127) has the advantage over block copolymers, described, for example, in ref.[7], in easier polymer synthesis, lower achievable polydispersities of the polyoxazolines, and the possibility to readily fine-tune nanoparticle properties due to modular multicomponent structure.

2. Experimental Section

2.1. Materials and Polymer Synthesis

Five statistical 2-alkyl-2-oxazoline copolymers (POXs, sing POX) were synthesised. Comonomers IprOX, BuOX, and ENOX were synthesized according to the method used in our previous paper,[5]

© 2012 WILEY-VCH Verlag GmbH & Co. KGaA, Weinheim

all other chemicals were purchased from Sigma–Aldrich Ltd. (Prague, Czech Republic). Triblock copolymer (ethylene oxide)$_{100}$–*block*-(propylene oxide)$_{65}$–*block*-(ethylene oxide)$_{100}$, with a commercial name Pluronic F127, was provided with a weight-average molecular weight, $\overline{M}_w$, of 12 600 Da. All the chemicals were used as obtained without additional purification.

Living cationic ring-opening polymerization of 2-alkyl-2-oxazolines in anhydrous acetonitrile using methyl *p*-toluenesulfonate as well as characterization of polymers (number- and weight-average molecular weight, content of monomeric units, CPT determination) were performed in analogy to the method described in our previous paper.[7] The polymerization conditions were set to obtain statistical copolymers containing theoretically 10 and 20 mol% BuOX in IprOX, respectively, and with theoretical molecular weights of 7.5 and 15 kDa. In the case of the polymer to be isotopically labeled, ENOX was used instead of equimolar part of BuOX to contain statistically one ENOX monomeric unit per polymer chain of the theoretical molecular weight. Addition of *N*-(2-sulfanylethyl)-2-(4-hydroxyphenyl)acetamide to double bonds of the ENOX monomeric unit was performed in analogy to our paper.[7]

The polymers were characterized by size-exclusion chromatography (SEC) and nuclear magnetic resonance (^{1}H NMR) in analogy to our previous paper.[7]

2.2. Radiolabeling

Radiolabeling and radiochemical stability study were carried out by electrophilic iodination by isotope ^{125}I with a chloramine method.[8] The radioactive polymer fraction was isolated from the reaction mixture by GPC separation using the PD-10 desalting column (loaded by gel Sephadex G-25). Radioactivity of individual fractions was determined by measurement on the ionization chamber VDC-404 (Veenstra Instruments, The Netherlands).

2.3. Preparation of Nanoparticles

Nanoparticles were prepared by heating of the POX/F127 aqueous solutions by either slow or fast heating procedures, 1 and 2:

(1) The measurement cuvette with a solution was kept in refrigerator at 8 °C at least for 2 h and then inserted into the sample holder of a light scattering instrument. It was heated in 1 °C steps, on every temperature change, the measurements were performed after reaching the steady conditions, typically after 20 min.
(2) The measurement cuvette with a solution was kept in refrigerator at 8 °C at least for 2 h and then immersed into a water bath at 37 °C for 20 min. The cuvette was then transferred to the preheated sample holder of a light scattering instrument.

2.4. Dynamic Light Scattering

Dynamic light scattering[9] (DLS) measurements were carried out at the scattering angle $\theta = 173°$ on a Zetasizer Nano-ZS, Model ZEN3600 (Malvern Instruments, UK), and the DTS (Nano) software, version 6.20, was used for data evaluation. The temperature was controlled within 0.05 °C interval. Values of hydrodynamic diameter, D_h, were calculated from volume distribution functions.

2.5. Isothermal Titration Calorimetry

Isothermal titration calorimetry[10] (ITC) experiments were carried out on the ITC-200 instrument (MicroCal, Inc., Northampton, MA). In samples for DLS characterization, the concentration of a POX was usually significantly lower than the concentration of F127; therefore, we chose the POX solution as a titrant in ITC. Each titration set consisted of 19 injections of a POX solution into a solution of F127 at intervals of 180 s. These injections were added at a constant volume of 2 μL. Measurements were conducted at temperatures below the CPT of the pure POXs to avoid phase separation of a POX prior to mixing. Experimental curves were corrected by the subtraction of the POX titration into water.

3. Results and Discussion

In summary, five POXs, (A, B, C, D, and E) with different content of BuOX – one of them also contained ENOX comonomer – and with different molecular weights were synthesized in order to characterize their temperature-dependent behavior. The hydrophobicity – that is, the content of the hydrophobic comonomer BuOX – was the same for polymers A, C and double for B, D, and E. The POXs were synthesized in high yields of ca. 90%, with average molecular weights slightly lower than theoretical and with a narrow molecular weight distributions – polydispersities, I, ca. 1.2, $I = \overline{M}_w/\overline{M}_n$, where $\overline{M}_w$ is the weight-average molecular weight and $\overline{M}_n$ is the number-average molecular weight. Characteristics of the synthesized POXs are given in Table 1.

Aqueous solutions of the POXs were mixed with several surfactants for the purpose of restriction on phase separation of the polymers above their CPT. Appropriate conditions for nanoparticle formation were found using F127, a well-known biocompatible surface-active copolymer exhibiting critical micellar concentration and critical micellar temperature (CMT).[11] Previously, F127 was also exploited for creation of nanostructures between surfactants and ionic liquids.[12] The formation of micelle-like nanoparticles composed of F127 and the POXs was achieved by heating POX/F127 mixtures above transition temperature, T_{tr}, of each mixture.

Although self-assembly of the POXs with several more surfactants (sodium dodecyl sulfate, sodium cholate, sodium taurocholate, Brij® 98, and Brij® 700) was tested, no nanoparticle formation was observed (data not shown) except for F127. That fact is ascribed to mutual compatibility of poly(2-alkyl-2-oxazoline) with poly(propylene oxide) chains of F127 (these structures may interact not only by hydrophobic interactions, but also because of

© 2012 WILEY-VCH Verlag GmbH & Co. KGaA, Weinheim

Table 1. Characteristics of the synthesized polymers. Statistical errors are within 5% of the measured value in all cases.

Polymer	Theoretical structure (remaining to 100% is IprOX)	$\overline{M}_n$ [a)]	$\overline{M}_w$ [b)]	I [b)]	BuOX [a)] [mol%]	CPT [c)] [°C]	$c_{37°C}$ [d)] [mg mL^{-1}]
A	10 mol% of BuOX [e)]	5600	6500	1.13	9.8	28.5	0.25
B	20 mol% of BuOX	5300	6200	1.16	19.2	21.5	0.05
C	10 mol% of BuOX	10 200	12 600	1.23	9.8	28.5	0.05
D	20 mol% of BuOX	8400	11 900	1.37	19.1	21.5	0.01
E	19 mol% of BuOX and 1 mol% of EnOX	5500	6700	1.18	18.0	21.5	0.05

[a)]From NMR; [b)]From size - exclusion chromatography (SEC), polydispersity (I) = $\overline{M}_w/\overline{M}_n$,$\overline{M}_w$ is weight-average molecular weight, $\overline{M}_n$ is number-average molecular weight from SEC; [c)]CPT is cloud point temperature at the polymer concentration c_{POX} = 5 mg mL^{-1}; [d)]Concentration of the polymer at which its CPT = 37 °C; [e)]IprOX is 2-isopropyl-2-oxazoline; BuOX is 2-butyl-2-oxazoline; ENOX is 2-(but-3-enyl)-2-oxazoline.

hydrogen bonding employing water incorporated or because of dipole–dipole interactions), whereas poly(2-alkyl-2-oxazoline) and hydrocarbon chains of the other surfactants were incompatible. These attractive forces may also contribute to the change of CPT in the presence of surfactant.

3.1. Dynamic Light Scattering

Below CMT (28 °C at c_{F127} = 10 mg mL^{-1}, taken as the center of the micellar transition), there are single macromolecular chains – unimers – with D_h of 5.5 nm present in the aqueous solution of F127 (see Figure 1b). Above CMT, a formation of micellar particles is observed, whose D_h is 19.9 nm and their content in volume distribution rises sharply up to 100%.

If F127 is added into an aqueous solution of a POX, it can prevent macrophase separation of the POX above its CPT. However, after exceeding f_{CRIT}, a critical value of the molar concentration ratio $f = C_{POX}/C_{F127}$, POX precipitates. The dependences of D_h on f for samples containg the POXs and F127 are shown in Figure 1a. For $f \leq f_{CRIT}$, there are nanoparticles in the solutions at 37 °C, but formation of aggregates and precipitation of the polymer occur for $f > f_{CRIT}$ at the same temperature. The values of f_{CRIT} are 0.48, 0.35, 0.22, and 0.14 for polymers A, B, C, and D, respectively. Thus, f_{CRIT} decreases gradually with rising hydrophobicity and the molecular weight of the POXs, the latter has a stronger influence on the decrease.

A comparison of temperature behavior of the pure F127 with behavior of the POX/F127 mixtures at $f < f_{CRIT}$ over a temperature interval 10–45 °C (heating procedure 1) is given in Figure 1b. D_h of the pure F127 micelles is 19.9 nm (c_{F127} = 10 mg mL^{-1}) at 37 °C and the size of micellar particles in the POX/F127 solutions (c_{F127} = 10 mg mL^{-1}, c_{POX} = 0.5 mg mL^{-1}) differs slightly from that value. No large aggregates or macrophase separation of the polymer was observed. Although a reproducible "overshoot" in D_h is observed for the higher-molecular-weight polymer D (plausibly caused by time dependence of nanoparticle formation and core dehydration in the course of the

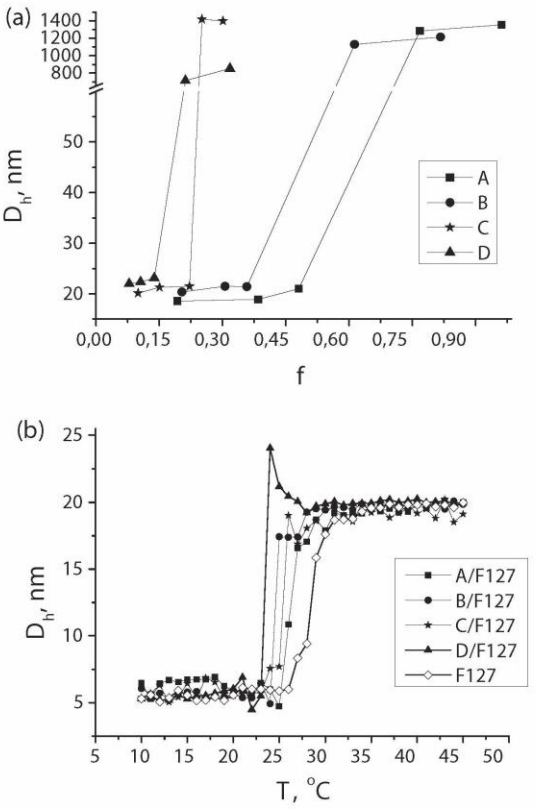

Figure 1. (a) Dependences of hydrodynamic diameter, D_h, on the molar ratio f for pure polymer solutions heated to 37 °C using heating procedure 2. (b) Temperature dependences of D_h for pure F127 and its mixtures with the POXs using heating procedure 1, c_{F127} = 10 mg mL^{-1}, c_{POX} = 0.5 mg mL^{-1}.

© 2012 WILEY-VCH Verlag GmbH & Co. KGaA, Weinheim

Table 2a. Hydrodynamic diameter, D_h, of POX/F127 and pure F127 solutions heated to 37 °C (heating procedure 2); c_{F127} = 10 mg mL^{-1}, c_{POX} = 0.5 mg mL^{-1}.

Sample	D_h [nm]	$\Delta D_h/D_h$ [a)]
A/F127	20.5	0.37
B/F127	20.9	0.35
C/F127	21.1	0.32
D/F127	22.5	0.23
E/F127	20.2	0.25
F127	19.6	0.32

[a)] ΔD_h is the full width at the half-maximum of D_h distribution. Statistical errors are within 5% of the measured value in all cases.

measurement), the nanoparticles for the D/F127 mixture are comparable to all the other systems above 28 °C. The temperatures T_{tr}, assessed for the POX/F127 solutions, correspond to the centers of transition regions where the micellar nanoparticles are formed. Their values are ca. 26.0, 24.5, 25.5, and 23.0 °C for the mixtures with polymers A, B, C, and D, respectively, so T_{tr} < CMT of the pure F127 (28 °C) at the the given concentrations. The hydrophobicity of the POXs influences a shift of T_{tr} values more than their molecular weight.

Using heating procedure 2 (fast heating) leads to the formation of nanoparticles with D_h bigger by 5%–11% in comparison with heating procedure 1, which could be ascribed to different formation kinetics. For both heating procedures, neither macrophase precipitation nor large aggregates were observed (visually and by DLS) in the POX/F127 solutions above their T_{tr}, indicating that the POXs are incorporated into the micellar nanoparticles of F127 above T_{tr}. The particle characteristics at 37 °C obtained by heating procedure 2 are given in Table 2a. Hydrodynamic radii for samples containing polymers with lower $\overline{M}_w$ (A, B, and E) are slightly lower than that for the other polymers and the pure F127.

A comparison of D_h of the pure A, B, and F127 with D_h of nanoobjects in the mixtures A/F127 and B/F127 measured at 10 °C is shown in Table 2b. Objects with D_h

Table 2b. Hydrodynamic diameter, D_h, of pure components and their mixtures at T = 10 °C; c_{F127} = 10 mg mL^{-1}, c_{POX} = 0.5 mg mL^{-1}.

Sample	D_h [nm]	$\Delta D_h/D_h$ [a)]
A	4.9	0.37
A/F127	6.4	0.24
B	4.5	0.27
B/F127	6.0	0.23
F127	5.5	0.23

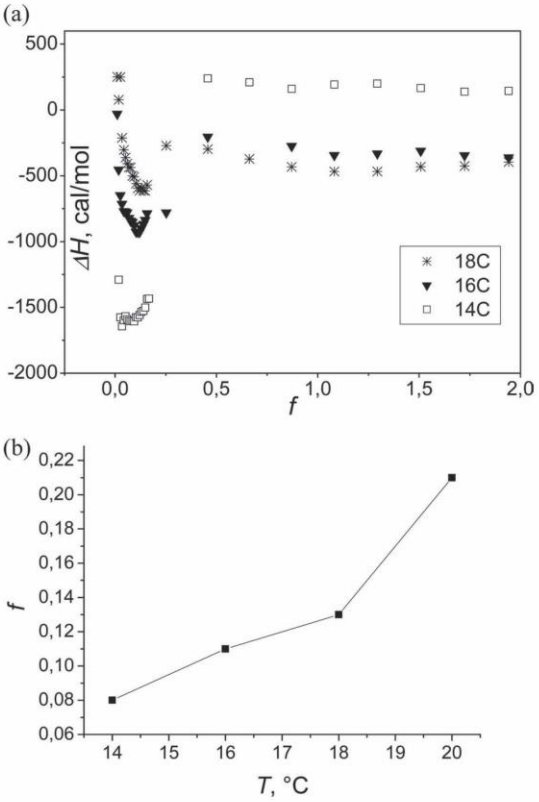

Figure 2. (a) Dependences of enthalpy increment on the molar ratio f for B/F127 mixture at three different temperatures. (b) Temperature dependence of the molar ratio f values that correspond to the enthalpy change minimum for B/F127 mixture.

of 6.4 and 6.0 nm were found in solutions A/F127 and B/F127, respectively, which means that the values are by ca. 10%–30% bigger than the values of D_h for single macromolecules of A, B, and F127. As DLS cannot unambigiously prove a formation of complexes between macromolecules of a POX and F127 below T_{tr} for given molar ratios f, a characterization by ITC technique was made.

3.2. Isothermal Titration Calorimetry

In Figure 2a, we can see a dependence of enthalpy change, ΔH, on the molar ratio $f = C_{POX}/C_{F127}$ for the polymer B. There is a distinct minimum on each of the three calorimetric titration curves corresponding to three different temperatures. Since F127 in solution at the concentration c_{F127} = 10 mg mL^{-1} and measurement temperature $T \leq 18$ °C do not form micelles, the negative ΔH values indicate an exothermic interaction and formation of complexes between F127 and polymer B. The position of the ΔH

© 2012 WILEY-VCH Verlag GmbH & Co. KGaA, Weinheim

minimum shifts toward higher values of f with increasing temperature, see Figure 2b, which could be explained by rising hydrophobicity of polymer B while approaching its CPT. For that reason, a higher number of POX molecules are bound to one F127 unimer. By extrapolation of the dependence in Figure 2b to T_{tr} of the polymer B, we get a value of f that corresponds to the f_{CRIT} determined by DLS. In summary, for $T < T_{tr}$, an exothermic interaction is observed between individual molecules of the compounds and we assume that the complexes formation below T_{tr} also participates in the following cooperative assembly of the POX/F127 micelle-like particles above the T_{tr} of each system. This is another proof that there exist a specific interaction between the POX and F127 molecules, probably not only by hydrophobic, but also because of hydrogen bonds or dipole–dipole interactions, and causing selective compatibility of POX and F127.

3.3. Radiolabeling

Radioiodination of the pure polymer E with ^{125}I radioisotope was carried out with standard chloramine method[7] with ca. 70% radiochemical yield. SEC has shown no significant effect of radiolabeling on molecular weights due to, for example, degradation. The radiochemical stability was 97% and 91% after 3 and 24 h, respectively, indicating that most of the radioiodine was bound to the polymer by a stable bond and only a minor part was released into low-molecular-weight fractions. The radiolabeled polymer E was subsequently dissolved together with F127 at f = 0.09 (c_{POX} = 0.5 mg mL^{-1} and c_{F127} = 10 mg mL^{-1}) in aqueous milieu and heated to 37 °C according to the heating procedure 2. Radioactivity and DLS measurements showed that radioactive micellar nanoparticles with D_h of 20.2 nm were successfully prepared and are identical in characteristics and behavior to nanoparticles prepared with polymer B. Functionalization and radiolabeling have thus negligible effect on nanoparticle characteristics obtained from DLS as expected, due to low weight content of radiolabelable groups and of the radionuclide in the polymer.

On the basis of the above-mentioned results, we propose a concept of the particle structure. Radiolabed POX mixed with F127 form micellar nanoparticles where the ^{125}I radioisotope bound to the POX is hidden inside the hydrophobic core, whereas the poly(ethylene oxide) blocks of F127 introduces surface PEGylation to the nanoparticles.

4. Conclusion

POXs, statistical thermosensitive poly(2-alkyl-2-oxazolines), were synthesized with different content of the hydrophobic comonomer BuOX, and their temperature-dependent self-assembly with Pluronic F127 was tested in aqueous milieu. Complexes formation between individual molecules of the POXs and F127 was observed by ITC below their T_{tr}. By heating the POX/F127 solutions (heating procedure 2) above T_{tr}, micellar nanoparticles were formed with D_h ranging from 20.2 to 22.5 nm at molar ratios of the compounds $f \leq f_{CRIT}$. The values of T_{tr} ranged from ca. 23 to 26 °C depending on the hydrophobicity (i.e., content of the BuOX comonomer) and molecular weight of the POXs. The POXs can be modified with functional comonomers, for example, for the puropose of radiolabeling. Polymer E — a radiolabelable variant poly[2-isopropyl-2-oxazoline-*co*-2-butyl-2-oxazoline-*co*-2-(but-3-enyl)-2-oxazoline] — was synthesized, and radioiodination with ^{125}I radioisotope was carried out with a good radiochemical yield and stability. Subsequently, radioactive biocompatible nanoparticles were prepared by simply heating the E/F127 solution above T_{tr} (ca. 24 °C). Such a system can serve, for example, as a model for further development of polymeric diagnostic systems for nuclear medicine imaging due to a suitable size for the EPR effect, surface PEGylation (and subsequent protection against entrapment in reticuloendothelial system), and physical biodegradability due to micelle–unimer equilibrium.

Acknowledgements: We acknowledge support by the Grant Agency of the Czech Republic (grants No. 202/09/2078 and No. P207/10/P054) and by the Academy of Sciences of the Czech Republic, grant No. M200501201.

Received: April 13, 2012; Revised: May 15, 2012; Published online: July 3, 2012; DOI: 10.1002/marc.201200254

Keywords: nanoparticles; pluronic F127; poly(2-alkyl-2-oxazoline)s; radiation; thermoresponsive polymer

[1] a) A. S. Hoffman, *J. Controlled Release* **2008**, *132*, 153; b) V. P. Torchilin, *Pharm. Res.* **2007**, *24*, 1; c) H. Maeda, *Bioconjugate Chem.* **2010**, *21*, 797.
[2] I. Goldmints, J. F. Holzwarth, K. A. Smith, T. A. Hatton, *Langmuir* **1997**, *13*, 6130.
[3] Č. Koňák, J. Pánek, M. Hrubý, *Colloid Polym. Sci.* **2007**, *285*, 1433.
[4] a) R. Hoogenboom, *Angew. Chem. Int. Edit.* **2009**, *48*, 7978; b) R. Hoogenboom, *Macromol. Chem.Phys.* **2007**, *208*, 18; c) R. Hoogenboom, M. W. M. Fijten, M. A. R. Meier, U. S. Schubert, *Macromol. Rapid Comm.* **2003**, *24*, 92.
[5] a) H. Uyama, S. Kobayashi, *Chem. Lett.* **1992**, *21*, 1643; b) C. Diab, Y. Akiyama, K. Kataoka, F. M. Winnik, *Macromolecules* **2004**, *37*, 2556; c) J. Zhao, R. Hoogenboom, G. Van Assche, B. Van Mele, *Macromolecules* **2010**, *43*, 6853; d) C. Weber, R. Hoogenboom, U. S. Schubert, *Prog. Polym. Sci.* **2012**, *37*, 686.
[6] a) A. Gress, A. Volkel, H. Schlaad, *Macromolecules* **2007**, *40*, 7928; b) C. Diehl, H. Schlaad, *Macromol. Biosci.* **2009**, *9*, 157; c) K. Kempe, R. Hoogenboom, U. S. Schubert, *Macromol. Rapid. Commun.* **2011**, *32*, 1484; d) K. Kempe,

© 2012 WILEY-VCH Verlag GmbH & Co. KGaA, Weinheim

T. Neuwirth, J. Czaplewska, M. Gottschaldt, R. Hoogenboom, U. S. Schubert, *Polym. Chem.* **2011**, *2*, 1737.
[7] M. Hrubý, S. K. Filippov, J. Pánek, M. Nováková, H. Macková, J. Kučka, D. Větvička, K. Ulbrich, *Macromol. Biosci.* **2010**, *10*, 916.
[8] Y. Koyama, M. Ishikawa, A. Ueda, A. Suginaka, *A. Polymer J.* **1993**, *25*, 355.
[9] P. Štěpánek, Č. Koňák, *Adv. Colloid Interfac.* **1984**, *21*, 195.
[10] a) I. Jelesarov, H. R. Bosshard, *J. Mol. Recognit.* **1999**, *12*, 3; b) K. Bouchemal, F. Agnely, A. Koffi, G. Ponchel, *J.Colloid Interf. Sci.* **2009**, *338*, 169.
[11] G. Wanka, H. Hoffmann, W. Ulbricht, *Macromolecules* **1994**, *27*, 4145.
[12] L. L. Ge, R. Guo, X. H. Zhang, *J. Phys. Chem. B* **2008**, *112*, 14566.

© 2012 WILEY-VCH Verlag GmbH & Co. KGaA, Weinheim

Journal of
Applied
Crystallography
ISSN 0021-8898

Received 18 March 2013
Accepted 2 October 2013

Small-angle X-ray scattering and light scattering study of hybrid nanoparticles composed of thermoresponsive triblock copolymer F127 and thermoresponsive statistical polyoxazolines with hydrophobic moieties[1]

Anna Bogomolova,[a]* Martin Hruby,[a] Jiri Panek,[a] Maria Rabyk,[a] Stuart Turner,[b] Sara Bals,[b] Milos Steinhart,[a] Alexander Zhigunov,[a] Ondrej Sedlacek,[a] Petr Stepanek[a] and Sergey K. Filippov[a]

[a]Institute of Macromolecular Chemistry, AV ČR, Heyrovsky Sq. 2, Prague 6, 162 06, Czech Republic, and [b]EMAT, University of Antwerp, Antwerp, B-2020, Belgium. Correspondence e-mail: aubogomolova@gmail.com

A combination of new thermoresponsive statistical polyoxazolines, poly[(2-butyl-2-oxazoline)-*stat*-(2-isopropyl-2-oxazoline)] [pBuOx-*co*-piPrOx], with different hydrophobic moieties and F127 surfactant as a template system for the creation of thermosensitive nanoparticles for radionuclide delivery has recently been tested [Pánek, Filippov, Hrubý, Rabyk, Bogomolova, Kučka & Stěpánek (2012). *Macromol. Rapid Commun.* **33**, 1683–1689]. It was shown that the presence of the thermosensitive F127 triblock copolymer in solution reduces nanoparticle size and polydispersity. This article focuses on a determination of the internal structure and solution properties of the nanoparticles in the temperature range from 288 to 312 K. Here, it is demonstrated that below the cloud point temperature (CPT) the polyoxazolines and F127 form complexes that co-exist in solution with single F127 molecules and large aggregates. When the temperature is raised above the CPT, nanoparticles composed of polyoxazolines and F127 are predominant in solution. These nanoparticles could be described by a spherical shell model. It was found that the molar weight and hydrophobicity of the polymer do not influence the size of the outer radius and only slightly change the inner radius of the nanoparticles. At the same time, molar weight and hydrophobicity did affect the process of nanoparticle formation. In conclusion, poly(2-oxazoline) molecules are fully incorporated inside of F127 micelles, and this result is very promising for the successful application of such systems in radionuclide delivery.

© 2013 International Union of Crystallography
Printed in Singapore – all rights reserved

1. Introduction

Poly(2-alkyl-2-oxazolines) have attracted increased attention in biomedical research owing to their peptide-like structure and wide range of adjustable physicochemical and biological properties, which depend on the alkyl substituent (Adams & Schubert, 2007; Park *et al.*, 2004; Hoogenboom, 2009; Sedlacek *et al.*, 2012). Their properties can include high hydrophilicity and biocompatibility for such polymers as poly(2-methyl-2-oxazoline) (Pidhatika *et al.*, 2008), thermal sensitivity in thermoresponsive polymers such as poly(2-ethyl-2-oxazoline) and poly(2-isopropyl-2-oxazoline) (Park *et al.*, 2004; Diab *et al.*, 2004), and hydrophobicity that is typical of hydrophobic aromatic or aliphatic polymers [poly(2-phenyl, butyl or nonyl-2-oxazoline)] (Adams & Schubert, 2007; Persigehl *et al.*, 2000). Moreover, copolymerization of different blocks allows the adjustment of the properties of such polymers and creates new copolymers with a wide range of properties.

Polymer micelles are very promising candidates for anti-cancer drug and radionuclide delivery systems (Mahmud *et al.*, 2007; Torchilin, 2007; Filippov, Konak *et al.*, 2010; Koňák *et al.*, 2007; Filippov, Starovoytova *et al.*, 2010; Filippov, Chytil *et al.*, 2012; Skodova *et al.*, 2011; Filippov, Hrubý *et al.*, 2008; Chekina *et al.*, 2011). An additional advantage of a thermoresponsive polymer is the simple process of formation of the micelles, with hydrophobic cores and hydrophilic coronae, by fast heating of an aqueous solution (Hruby *et al.*, 2009). Recently, it was shown that thermoresponsive copolymers, using a poly(2-alkyl-2-oxazoline) as a building block, could be successfully radiolabelled with the ^{125}I radioisotope (Hruby *et al.*, 2010). However, the copolymers do not form compact nanoparticles

[1] This article will form part of a virtual special issue of the journal, presenting some highlights of the 15th International Small-Angle Scattering Conference (SAS2012). This special issue will be available in late 2013/early 2014.

Table 1
Physico-chemical characteristics of polymers.

In all cases, statistical errors are within 5% of the measured values.

Polymer	Theoretical structure†	M_w	M_w/M_n	CPT (K)
A	10 mol% of BuOx	6500	1.13	301.7
B	20 mol% of BuOx	6200	1.16	294.7
C	10 mol% of BuOx	12600	1.23	301.7

† Remaining percentage is iPrOx.

and only exist as loose aggregates above the cloud point temperature (CPT) (Hruby *et al.*, 2010). A thermosensitive surfactant could be used to overcome the problem. This idea was fulfilled by Pánek *et al.* (2012), who used a Pluronic F127 triblock copolymer as a surfactant. Pluronic F127 consists of a central poly(propylene oxide) (PPO) block with terminal poly(ethylene oxide) (PEO) blocks and it forms micelles in aqueous solution above the critical micelle concentration (CMC) and critical micelle temperature (Bakshi & Sachar, 2006). F127 micelles have a hydrophilic corona of PEO and a hydrophobic core of PPO and, in contrast to other surfactants, have already been used to solubilize and transport hydrophobic drugs (Foster *et al.*, 2009; Sharma & Bhatia, 2004; Sharma *et al.*, 2008). Moreover, it has been shown that Pluronics are the least toxic among commercially available surfactants and are able to enhance the effect of carriers by sensitizing specific biological cells (Foster *et al.*, 2009; Sharma & Bhatia, 2004).

Previously, we described new hybrid nanoparticles that were designed for radionuclide delivery, consisting of thermoresponsive statistical poly(2-alkyl-2-oxazolines) with different numbers of hydrophobic BuOx (2-butyl-2-oxazoline) groups and Pluronic F127 (Pánek *et al.*, 2012).

Nevertheless, a number of fundamental questions remain unanswered:

How do F127 and poly(2-oxazolines) self-assemble below the CPT?

How important are the molecular weight and composition of poly(2-oxazolines) for the size and polydispersity of nanoparticles above the CPT?

Do the nanoparticles have internal structure? In other words, can poly(2-oxazolines) be effectively hidden inside of the F127 core?

The protection from enzymatic degradation of poly(2-alkyl-2-oxazolines) modified with radionuclides is a crucial requirement for successful radionuclide delivery.

Here, we have examined the structural changes produced as a result of interactions between statistical polyoxazolines and F127 surfactant over a certain temperature range by means of small-angle X-ray scattering (SAXS) and dynamic light scattering (DLS). The effects of molecular weight and hydrophobicity were also considered by studying samples of polymer containing different numbers of hydrophobic groups (pBuOx) as outlined in Table 1. Moreover, we exploited transmission electron microscopy (TEM) to prove the spherical form of hybrid nanoparticles.

The diversity of structures observed in our system requires a formulation of terminology adapted for the behaviour of thermosensitive compounds. The terminology recommended by IUPAC was chosen for characterization (Jones *et al.*, 2013). According to that, an aggregate is an irregular cluster of otherwise individual molecules or particles; a micelle is an aggregate of amphiphilic molecules or ions of colloidal dimensions having a core–shell structure with the solvophilic parts directed outwards and the solvophobic parts directed inwards that, under specific conditions, exists in equilibrium with the molecules or ions from which it is formed; a complex is a molecular entity formed by the mutual attraction of two or more component molecular entities, ionic or uncharged; a nanoparticle is any particle with a size of 1–100 nm.

2. Materials and methods

Polymers were synthesized according to the scheme published in our previous paper (Hruby *et al.*, 2010).

Pluronic F127 (Sigma–Aldrich) was used with an average molecular weight M_w of 12 600 g mol^{-1}. All experiments were carried out with component concentrations of c_{F127} = 10 mg ml^{-1} and $c_{polymer}$ = 0.5 mg ml^{-1}. The procedure for preparing the nanoparticles was also taken from our previous work (Pánek *et al.*, 2012).

2.1. Static and dynamic light scattering

Dynamic and static light scattering (SLS) measurements were performed to determine the average size and molecular weight of the nanoparticles. DLS experiments are widely used for these purposes (Filippov, Lezov *et al.*, 2008). Static and dynamic light scattering measurements were carried out on an ALV/CGS instrument equipped with a 22 mW He–Ne laser in the angular range from 30 to 150° and with an ALV 6010 multibit, multi-τ autocorrelator covering approximately 12 decades in the delay time τ. Normalized autocorrelation functions $g_2(t)$ were analyzed using the *GENDIST* software, which employs the REPES algorithm (Jakes, 1988) to perform the inverse Laplace transformation:

$$g_2(t) - 1 = \beta\left[\int G(\tau)\exp(-t/\tau)\mathrm{d}\tau\right]^2, \qquad (1)$$

where t is the delay time of the correlation function and β is an instrumental parameter known as contrast. The resulting $G(\tau)$ is a distribution of relaxation times that generally consists of several peaks representing individual dynamic processes. Finally, the apparent hydrodynamic radius R_h is derived from the relaxation times obtained using the well known Stokes–Einstein relation. The DLS data are taken from intensity-weighted distribution functions (Filippov, Lezov *et al.*, 2008). To account for the logarithmic scale on the R_h axis, all DLS distribution diagrams are displayed in the equal area representation, $R_hG(R_h)$ (Stepanek, 1993). The value of R_h for each system was averaged over three runs.

The static light scattering data were determined from a Zimm plot with the following equation:

$$\frac{Kc}{R(q)} = \frac{1}{M_w} + \frac{R_G^2 q^2}{3M_w} + 2A_2 c, \quad (2)$$

where $R(q)$ is the Rayleigh ratio of the scattering intensity, $q = (4\pi/\lambda)\sin\Theta/2$ (λ is the wavelength of light in the medium and Θ is the scattering angle between the incident and the scattered beam), K is the contrast factor containing the optical parameters, c is the weight concentration, M_w is the weight average of the molecular weight of the particles, A_2 is the second virial coefficient and R_G is the radius of gyration of the particles. The temperature was controlled to within 0.05 K. The prepared samples were filtered into a dust-free cell. Calibration to absolute units was performed using toluene as a calibration standard.

2.2. SAXS

SAXS experiments have previously been used for the successful characterization of nanoparticles (Pedersen *et al.*, 2003; Formariz *et al.*, 2007; Sato *et al.*, 2009; Angelov, Angelova, Filippov *et al.*, 2011; Jeworrek *et al.*, 2008; Angelov, Angelova, Mutafchieva *et al.*, 2011; Štěpánek *et al.*, 2011; Zhang *et al.*, 2011; Gromadzki *et al.*, 2009; Filippov, Sedlacek *et al.*, 2012).

SAXS experiments were conducted on beamline ID02 at the ESRF in Grenoble, France. Polymer solutions were sealed in a 1.5 mm borosilicate capillary. The scattered intensity is recorded using a fast-readout low-noise (FReLoN) CCD-based X-ray detector housed in an evacuated flight tube. The sample-to-detector distance can be varied between 0.8 and 10 m, which corresponds to an accessible q range of $6 \times 10^{-3} < q < 6.0$ nm^{-1} for $\lambda = 0.1$ nm. The FReLoN detector consists of a fibre optic coupled (2:1) CCD image sensor (Kodak KAF-4320) with an active area of 10 × 10 cm. Further description can be found in the paper by Sztucki *et al.* (2010). Temperature experiments were conducted using a home-made sample holder with Peltier elements.

Another set of SAXS experiments was performed using a pinhole camera (Molecular Metrology SAXS System) attached to a micro-focused X-ray beam generator (Osmic MicroMax 002) operating at 45 kV and 0.66 mA (30 W). The camera was equipped with a multiwire gas-filled area detector with an active area diameter of 20 cm (Gabriel design). Two experimental setups were used to cover the q range of 0.07–11 nm^{-1}. The scattering intensities were put on an absolute scale using a glassy carbon standard. Prior to the fitting analysis, the scattering from the capillary with solvent was subtracted. The background signals from the empty capillary were also subtracted.

Temperature experiments were performed by adjusting the control temperature stepwise to 318 K. The real temperature inside of the capillary was determined afterwards by placing a thermocouple into an empty capillary under similar conditions. The same procedure was performed for cooling experiments. In between cooling and heating cycles, the sample was equilibrated for 15 min. For each cycle, 150 frames were accumulated to monitor the self-assembly of the nanoparticles.

Table 2
Composition of the system for each component.

	Molar mass (g mol^{-1})	Molecular volume (nm^3)	Density (g cm^{-3})	SLD ($\times 10^{-5}$) (nm^{-2})
EO	44	0.064	1.127	104.2
PO	58	0.091	1.06	99.0
iPrOx	113	0.153	1.226	113.0
H_2O	18	0.030	1.00	94.45

The data were fitted using a spherical shell model implemented in the *SASfit* software (http://kur.web.psi.ch/sans1/SANSSoft/sasfit.html). The spherical shell model incorporates the following fitting parameters: overall radius of spherical shell (R_1), core radius (R_2), scattering length density (SLD) difference between shell and matrix (η), and SLD difference between core and matrix relative to the shell contrast (μ).

$$\mathrm{SLD_{shell}} - \mathrm{SLD_{matrix}} = \eta \quad (3)$$

and

$$\frac{\mathrm{SLD_{core}} - \mathrm{SLD_{matrix}}}{\mathrm{SLD_{shell}} - \mathrm{SLD_{matrix}}} = \mu. \quad (4)$$

To account for the polydispersity of the nanoparticles, the form factor was modified assuming a lognormal distribution for the outer radius R_1. The form factor and structure factor were combined to give the scattering intensity. The structure factor derived for hard sphere interaction (Percus–Yevick model) was used.

The actual composition of the samples in terms of the scattering length density for each sample component is given in Table 2.

2.3. Transmission electron microscopy

To prepare the samples for TEM investigation, a drop of diluted colloidal solution with a staining agent was heated above 318 K and placed on a carbon-coated copper grid and left to dry. High-resolution TEM experiments were carried out on an FEI Titan 80-300 Cubed microscope fitted with an aberration corrector for the imaging lens and operated at 80 kV to minimize knock-on damage to the sample. Uranium salt was added as a staining agent to increase the contrast of the solutions.

3. Results

3.1. Light scattering measurements

To preliminarily assess the solution properties of pure F127 and the F127/poly(2-alkyl-2-oxazoline) mixtures, we conducted DLS and SLS studies. The three general relaxation processes that can be discerned from the relaxation times in the DLS spectra will be referred to below as the fast, the middle and the slow modes. Assuming that all modes are of a diffusive nature, one can convert relaxation times to hydrodynamic radii.

For a solution of pure F127, the fast and slow modes could be discerned from the DLS data. At temperatures below the

CPT, single molecules of F127 (*ca* 3 nm) and their aggregates (*ca* 100–150 nm) were present in solution (Fig. 1, open circles). When the temperature increased above the CPT, the aggregates and single molecules transformed into 10 nm nanoparticles (Fig. 1).

Dynamic and static light scattering data for the mixed polymer A/F127 system are also presented in Figs. 1(*a*) and 1(*b*). One can see that the correlation curves reveal increasing complexity with the addition of polymer A to the F127 solution (Figs. 1*a* and 1*b*, filled circles). For both systems, large aggregates with R_h of *ca* 100–150 nm are observed. These large aggregates could be attributed to the compositional polydispersity of F127, *e.g.* the different lengths of PEO–PEP blocks. A smaller peak with an R_h value of *ca* 3 nm is traceable in both solutions. Thus, we assume that this peak is associated with single F127 molecules that are molecularly dissolved in the solution at low temperature.

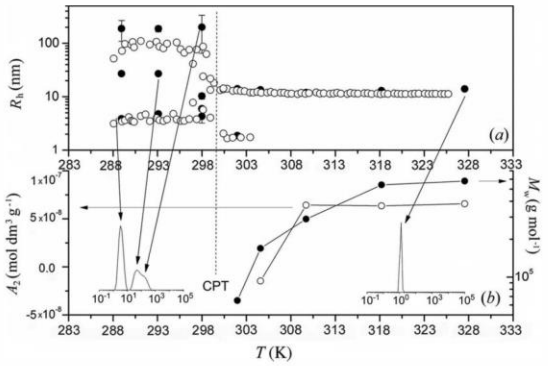

Figure 1
(*a*) DLS data: open circles represent pure F127 data, and filled circles are for the polymer A/F127 data, *c*(polymer)/*c*(F127) = 0.1. (*b*) SLS data for the polymer A/F127 system: open circles are second virial coefficient, A_2, data, and filled circles are data for the molecular weight of nanoparticles, M_w.

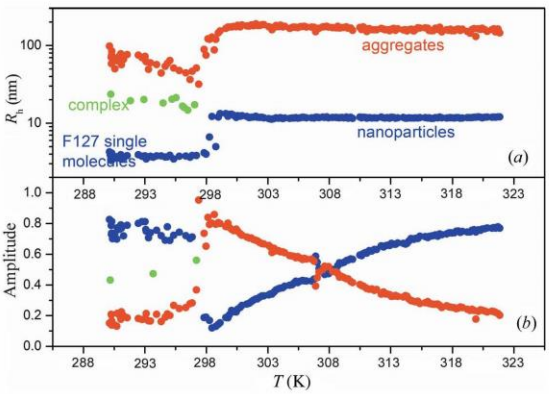

Figure 2
DLS data for the polymer C/F127 system. For the R_h data (*a*), the red filled circles are aggregates, green filled circles are complexes, and blue filled circles are single F127 molecules and nanoparticles, *c*(polymer)/*c*(F127) = 0.1. For the amplitude (*b*) data, the red filled circles are aggregates, the green filled circles are complexes, and the blue filled circles are single F127 molecules and nanoparticles.

Both the smaller and larger objects are reassembled into 10 nm nanoparticles with increasing temperature above the cloud temperature (Fig. 1*a*, filled circles). A fraction of smaller objects with R_h values of *ca* 2 nm remains in the solution within the transition region and they could be classified as single F127 macromolecules in a globular state. The negative value of the second virial coefficient, A_2, justifies such a hypothesis (see Fig. 1*b*). When the temperature is raised further above the CPT, these small objects disappear from the intensity distribution function and are believed to merge with the existing nanoparticles. This conclusion is further supported by the SLS data (Fig. 1*b*). The value of the apparent M_w of the nanoparticles rises steeply within the transition region and gradually above the transition region and it finally reaches a plateau. Moreover, the second virial coefficient, A_2, changes its sign from negative to positive over the transition region, which indicates that the quality of the solvent is changing from bad to good. A comparison of the nanoparticles that occur in polymer A/F127 with the ones that occur for pure F127 shows that they have almost the same size; this is not surprising because the ratio $f = c$(polymer)/c(F127) = −0.1 is very small. It is worth noting that a middle peak is sometimes traceable for the polymer A/F127 system. Keeping in mind that this signal is completely absent for pure F127 (Fig. 1*a*), one can explain the occurrence of the middle mode as the presence of complexes between the polymer A and F127 molecules.

It was observed that the polymer C/F127 system can produce aggregates over a wide temperature range and even above the CPT (Fig. 2*a*); however, the concentration of those aggregates does continuously decrease above the CPT (Fig. 2*b*). For polymer C, complexes between the polymer and F127 were also observed (Fig. 2*a*).

3.2. SAXS measurements

SAXS experiments were carried out on systems of 0.1% hydrophobic statistical copolymers (polymer C and polymer B) mixed with 1% F127 over a certain temperature range (Figs. 3 and 4, respectively). An analysis of the scattering curve for the polymer C/F127 system as a function of the scattering vector magnitude q and temperature allows us to highlight several different features. Some of these features were previously observed for a solution of pure F127 (Mortensen & Talmon, 1995). At temperatures below the CPT, the scattering function is relatively featureless. As the temperature rises to 295 K, we can observe the appearance of a side peak, which indicates either the formation of dense compact objects with a sharp interface or a decrease in polydispersity. This side peak becomes more pronounced with increasing temperature, and we believe it is related to the decreasing polydispersity during the heating process. Moreover, we discern a small peak for scattering vectors in the region of $q = 0.1$ nm^{-1} that occurs slightly above the CPT (302 K). Despite the low concentration of F127, we identify this change as the correlation peak

(structure factor) of interactions between neighbouring nanoparticles.

Another feature that should be noted is the behaviour of the intensity of scattered light in regions of low q. Regardless of the general tendency to see increased intensity with temperature due to self-assembly of polymer C/F127 into nanoparticles, we observed a slight decrease of intensity at temperatures below the CPT. It is logical to explain this behaviour by the presence of aggregates at temperatures below the CPT; the size of this aggregate can be assessed as a *ca* 40 nm. The existence of such aggregates with a size of 40–60 nm was proven by the DLS experiments (Fig. 2). Moreover, we also observed a slight upturn in intensity in the range of q = 0.03–0.07 nm^{-1} at temperatures above the CPT. These results correspond fully to the DLS experiments which showed that aggregates exist in the system over the whole temperature range.

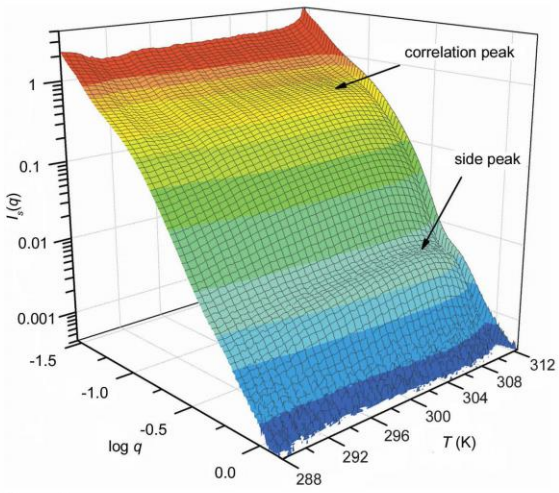

Figure 3
Three-dimensional plot of SAXS data as a function of the scattering vector magnitude and temperature for the polymer C/F127 system.

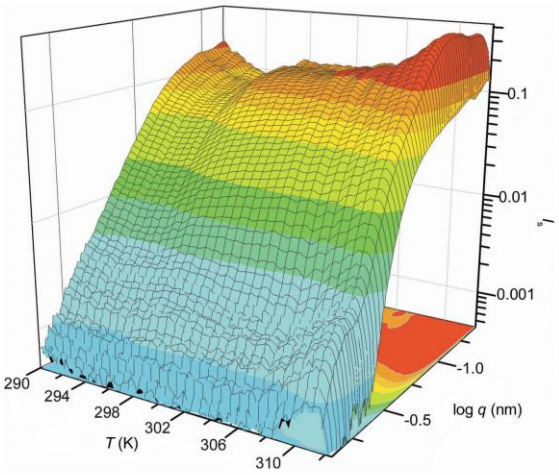

Figure 4
Three-dimensional plot of SAXS data as a function of the scattering vector magnitude and temperature for the polymer B/F127 system.

Polymer B is more hydrophobic (20% BuOx) than polymer C (10% BuOx) and it has a lower molecular weight. Nevertheless, we observed similar features between the polymer B/F127 and polymer C/F127 systems in the SAXS data. The distinction between the two systems is found only in the temperature values specific to some characteristic points. Thus, for the polymer B/F127 system, we find the appearance of side maximum and correlation peaks at 300 K. More significantly, the form of the scattering curve changes at temperatures above 310 K, and finally becomes fully identical to the SAXS data for pure F127 (Fig. 5*b*). At the same time, the polymer B/F127 system only manifests aggregates at temperatures below the CPT.

To obtain more information about the structural differences between the polymer B/F127 and polymer C/F127 systems, we made a comparison of the scattering curves for the two different polymers under similar conditions (Figs. 5*a* and 5*b*). The data are shown in two regimes: static and dynamic. In the

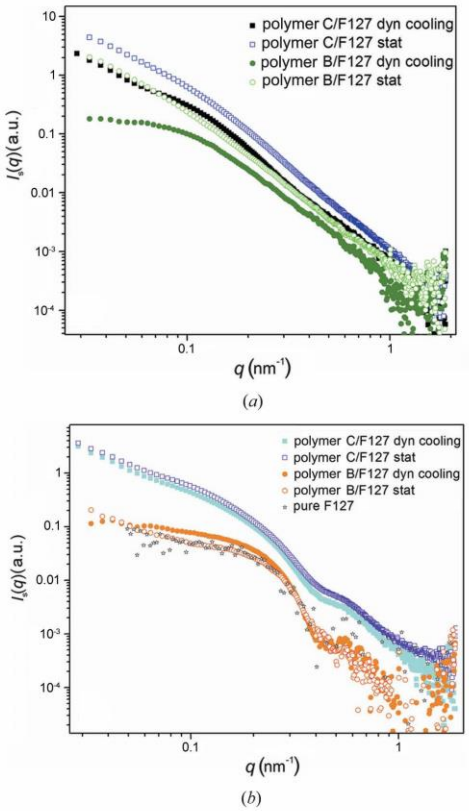

Figure 5
SAXS results from the polymer B/F127 and polymer C/F127 systems in different regimes at (*a*) 288 K and (*b*) 312 K.

static regime, the temperature was well defined, and the samples were thermostated before each measurement. Therefore, we can consider the state of the system in this condition as equilibrium. At the same time, the dynamic temperature experiment was performed by continuously increasing (decreasing) the temperature during consecutive measurements of the system at equal time intervals. The processes of heating and cooling were not uniform in time; they proceeded at a high rate in the beginning and achieved a steady-state value in the final stage. An analysis of the data at 288 K shows similar dependence for both polymers (Fig. 5*a*). A comparison of the data obtained in different q ranges shows that the scattered intensity has monotonic and featureless behaviour in the middle- and high-q ranges. In the low-q range, a strong intensity upturn is observed. On the basis of the above-reported DLS data, we conclude that both systems have small polydisperse objects with a tendency to aggregate.

A different situation was found at 312 K, where the form of the curves for different polymers differs significantly (Fig. 5*b*). Obviously, the result is related to the different hydrophobicities of the polymers. The form of the curve for polymer B is very similar to that for pure F127 as discussed above. It is worth mentioning that the behaviour of the polymers is similar in both static and dynamic regimes, which means that the state of the system in the dynamic regime at 312 K is close to equilibrium.

For quantitative characterization of structural changes, we tested several fitting models: spherical shell, sphere with attached Gaussian chains (Pedersen & Gerstenberg, 1996, 2003) and sphere with exponential shell. Two of these models, spherical shell and sphere with attached Gaussian chains, show good agreement with the experimental data. Usually, the sphere with attached Gaussian chains model is used for behavioural descriptions of different Pluronics and Pluronic-containing systems (Foster *et al.*, 2009; Mortensen & Talmon, 1995; Mortensen, 2001). In our case, this model showed good agreement for data at 288 and 312 K. However, an attempt to fit the intermediate temperatures showed lesser agreement with the experimental data than the fit results for the spherical shell model. The discrepancy might possibly be related to the experimental conditions, *i.e.* the dynamic regime of heating and cooling. We assume that the system reaches equilibrium only at the bordering points.

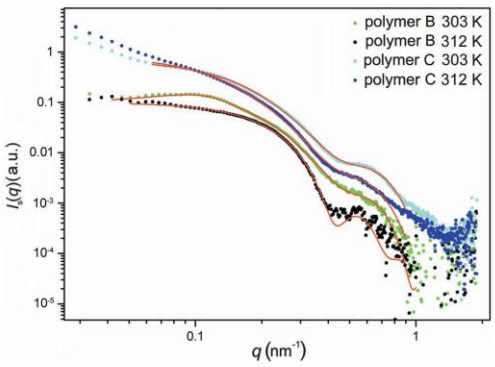

Figure 6
SAXS results from the polymer B/F127 and polymer C/F127 systems over a range of temperatures. Solid lines are fits to the spherical shell model.

Table 3
Fitting parameters (SAXS) for the polymer B/F127 system at a range of temperatures.

Temperature (K)	Outer radius (nm)	Inner radius (nm)	Poly-dispersity	Interaction radius hard sphere (nm)	Volume fraction hard sphere	η ($\times 10^{-5}$) (nm^{-2})	μ
298	13.2	3.9	0.31	24.5	0.08	4.2	7.2
303	13.1	4.5	0.2	25.1	0.09	3.9	6.45
308	13.6	4.7	0.17	26.7	0.09	4.1	6.6
310.9	13.5	4.2	0.25	27.8	0.11	5.5	7.26

Therefore, the spherical shell model was selected as the more plausible model to characterize all of the presented data. Fig. 6 shows the fitting results for the mixtures including polymers B and C at several temperatures. The hard sphere model was additionally used to describe the behaviour of the polymer B/F127 complex at high temperatures (311–312 K).

The SAXS data at low temperatures (below 295 K) are very difficult to analyse on the basis of one model; featureless monotonic curves allow the experimenter to fit these data with many types of models including the co-existence in solution of different types of particles. In fact, that explanation is the most plausible based on the DLS results. Fitting results are presented in Tables 2 and 3.

4. Discussion

F127 is a system that has been widely and thoroughly investigated over the past 20 years. It was established that F127 micelles occur at temperatures and concentrations above the CPT and critical micelle concentration, respectively. These micelles have a core composed of PPO block copolymer with a shell of PEO block copolymer. It was proven that these micelles are spherical (Attwood *et al.*, 1985; Wanka *et al.*, 1990; Mortensen & Talmon, 1995) with an apparent radius of 10–12.5 nm (Attwood *et al.*, 1985; Yu *et al.*, 1992). The reported size of these objects by several groups varies slightly owing to the differing experimental methods that are used to characterize the system. Nevertheless, there is agreement that the size of the micelles remains constant within a certain temperature range. This behaviour can be explained by theory (Attwood *et al.*, 1985; Wanka *et al.*, 1990), which indicates that the application of heat squeezes water from the solvated PPO and PEO groups and leads to pronounced micellar dehydration. This process is accompanied by continuous transfer of single F127 molecules from the solution into the micelles over a certain temperature range, which increases the aggregation number and, thereby, keeps the size of the micelles constant. In this process, micelles become more compact; this effect is accompanied by an increase in micellar molecular weight by a factor of more than three (Wanka *et al.*, 1990).

Table 4
Fitting parameters (SAXS) for the polymer C/F127 system at a range of temperatures.

Temperature (K)	Outer radius (nm)	Inner radius (nm)	Poly-dispersity	Interaction radius hard sphere (nm)	Volume fraction hard sphere	η ($\times 10^{-5}$) (nm^{-2})	μ
298	13.5	3.75	0.29			6.55	8.6
303	13.3	3.9	0.24	26.7	0.03	6.9	8.7
308	13.5	4	0.22	23.7	0.06	7.0	9.2
310.9	13.5	3.9	0.24	24.3	0.07	6.6	8.8

The current investigation fully confirms the data from previous studies for pure F127. In agreement with previous experiments, pure F127 molecules were shown to self-assemble into 11 nm particles above the CPT (Fig. 1*a*, open circles). The size of the particles is nearly constant over a certain temperature range. In the presence of hydrophobic copolymers, we also observed the transformation of 3 nm objects into hybrid nanoparticles with R_h values of *ca* 12 nm (Fig. 1*a*) from DLS measurements. The only difference between the pure F127 and the polymer/F127 systems is the presence of polymer–surfactant complexes, which were observed by DLS at temperatures below the CPT. One can consider statistical copolymers to be active centres of micelle formation (Brackman & Engberts, 1991, 1992). Hydrophobic blocks of butyloxazoline are insoluble in water, and they obviously play the role of centres for polymer–surfactant interaction.

From Tables 3 and 4, we see that the spherical shell model with a polydisperse outer radius distribution yields a nanoparticle radius of 13.5 nm. This nanoparticle size is a little larger than the size reported from the DLS experiments (Pánek *et al.*, 2012). However, the value becomes reasonable if the degree of polydispersity, as calculated in the SAXS experiment, is taken into account. Moreover, the nanoparticle core radius of 4.2–4.7 nm for the polymer B/F127 system is in good agreement within experimental error with a previously reported core size of 5 nm for pure F127 in water (Mortensen & Talmon, 1995). An analysis of the experimental data in terms of size (Tables 2 and 3) did not show any significant differences between the polymer B/F127 and polymer C/F127 systems even though the molar weights of the statistical polymers and their structures differed significantly. We detected only a small increase in value of the inner radius for the polymer B/F127 system as compared to the polymer C/F127 system, and both systems had a common tendency to decrease in polydispersity with increasing temperature. Thus, we conclude that the structure of these hybrid molecules is almost identical to the structure of the micelles of pure F127. The situation becomes different if we analyse the values of scattering length density of shell and core for systems of polymer/F127 and pure F127. Comparison of fitting values with the actual ones allows the influence of polymer hydrophobicity and molecular weight on the internal structure of hybrid nanoparticles to be characterized. For the pure F127, the calculated data are $\eta = 9.75 \times 10^{-5}$ nm^{-2} and $\mu = 0.41$. When the presence of the iPrOx group in the core of complex nanoparticles is taken into account, we can obtain the parameters $\eta = 9.75 \times 10^{-5}$ nm^{-2} and $\mu = 1.9$. The μ value of 1.9 is still less than the μ value that was found from the fitting of the experimental curve. One can suggest that the presence of statistical polymer inside the core of the F127 micelle significantly increases the scattering of the particles. Moreover, we observe that the scattering of the shell is less than was found from the calculation. According to our assumption, the shell of the particles is composed from the EO group, which shows a high hydrophilicity. This means that the shell could include some volume fraction of the solvent, reducing the scattering from 9.75×10^{-5} to $4–7 \times 10^{-5}$ nm^{-2}. We believe that a poly(2-alkyl-2-oxazoline) copolymer is fully incorporated into the F127 micelle (Fig. 7). The total incorporation of a copolymer is a crucial goal for successful radionuclide delivery.

Interestingly, different systems behave differently with temperature (Figs. 3 and 4), despite the fact that molar weight and hydrophobicity do not affect the size of the hybrid nanoparticles. By examining the kinetics of micelle formation and understanding thermosensitivity as a temperature-dependent process in time (Idziak *et al.*, 1999), it is possible to offer the following explanation of this behaviour. When the polymer C/F127 system is at a low temperature of 288 K, the surfactant starts to sit on the BuOx group and forms intermediate complexes. When the temperature rises to 296 K, more and more molecules of F127 transfer from the solution to the polymer, but the number of 2-isopropyl-2-oxazoline (iPrOx) groups is large enough and the process of their dehydration accelerates with increasing temperature. That leads to aggregation of some polymer molecules at 298.7 K (though some complex nanoparticles have already formed). The aggregation of the polymers increases the instantaneous concentration of surfactant in a limited volume and it becomes possible to observe correlations between different micelles of F127 at 302.9 K. Eventually, enough surfactant molecules are transferred to the polymers to cover them, and the number of aggregates and the correlation peak on the scattering curve both decrease. The same logic could be applied to the polymer A/F127 system, but in this case the number of iPrOx groups is smaller, which leads to an absence of aggregation. At temperatures above the CPT, new molecules of F127 incorporate into already-formed complex nanoparticles, which increase the molecular weight of the complexes as in the case of pure F127. The process of nanoparticle formation for polymer B/F127 seems to be very similar to that for polymer A/F127. Polymer B has a higher content of BuOx groups than polymer A. Nevertheless, the similarity of the processes for

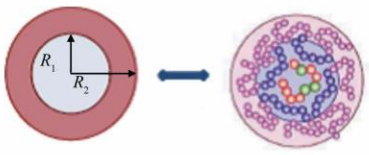

Figure 7
Schematic representation of hybrid nanoparticles.

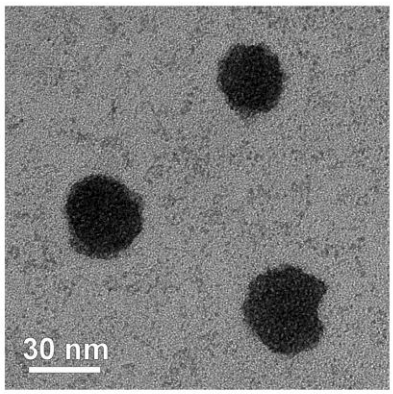

Figure 8
TEM image of polymer B/F127 hybrid nanoparticles.

polymer B/F127 and polymer A/F127 confirms the fact that, at 311 K, the scattering curve for the polymer B/F127 system is transforming from the spherical shell model to a sphere, and it eventually becomes fully identical to pure F127. A TEM image provided for the polymer B/F127 system supports the spherical-like structure of the hybrid nanoparticles (Fig. 8). One can see that nanoparticles formed above the CPT are nearly spherical, with some polydispersity in shape and size, in agreement with SAXS experiments. The core–shell structure could not be observed in TEM images, because of the presence of high-contrast uranium staining salts inside the nanoparticle.

5. Conclusion

By means of DLS and SAXS, we have studied the interactions between new thermoresponsive statistical polyoxazolines, poly[(2-butyl-2-oxazoline)-*stat*-(2-isopropyl-2-oxazoline)], with different hydrophobic moieties and the surfactant F127 as a template system for the creation of thermosensitive nanoparticles for radionuclide delivery. We have determined the internal structure and the solution properties of the nanoparticles over a temperature range from 288 to 312 K. It was proven that the poly(2-alkyl-2-oxazolines) and F127 form hybrid nanoparticles above the cloud point temperature and they could be described by a core–shell structure. We found that the molar weight and hydrophobicity of the polymer do not influence the outer radius and only slightly change the inner radius of the nanoparticles. At the same time, the molar weight and hydrophobicity affect the process of nanoparticle formation. Consequently, we conclude that poly(2-oxazoline) molecules are fully incorporated inside of the F127 micelles and the results are very promising for successful application of such systems to radionuclide delivery.

We gratefully acknowledge the ESRF (Grenoble, France) for the provision of synchrotron beam time (SC-3113). We thank J. Gummel and T. Narayanan for help with the SAXS measurements. The authors thank the Academy of Sciences of the Czech Republic for support under grant No. M200501201.The authors also acknowledge financial support (No. CZ09-DE06/2013–2014) from the ASCR–DAAD Programme PPP 2013–2014 and EU 7FP Program No. 262348 (European Soft Matter Infrastructure, ESMI). ST, SB and GVT gratefully acknowledge financial support from the Fund for Scientific Research Flanders (FWO) and the Belgian government through the Interuniversity Attraction Pole (IAP-PAI).

References

Adams, N. & Schubert, U. S. (2007). *Adv. Drug Deliv. Rev.* **59**, 1504–1520.
Angelov, B., Angelova, A., Filippov, S. K., Karlsson, G., Terrill, N., Lesieur, S. & Štěpánek, P. (2011). *Soft Matter*, **7**, 9714.
Angelov, B., Angelova, A., Mutafchieva, R., Lesieur, S., Vainio, U., Garamus, V. M., Jensen, G. V. & Pedersen, J. S. (2011). *Phys. Chem. Chem. Phys.* **13**, 3073–3081.
Attwood, D., Collett, J. & Tait, C. (1985). *Int. J. Pharm.* **26**, 25–33.
Bakshi, M. S. & Sachar, S. (2006). *J. Colloid Interface Sci.* **296**, 309–315.
Brackman, J. C. & Engberts, J. B. F. N. (1991). *Langmuir*, **7**, 2097–2102.
Brackman, J. C. & Engberts, J. B. F. N. (1992). *Langmuir*, **8**, 424–428.
Chekina, N., Horák, D., Jendelová, P., Trchová, M., Bene, M. M. H., Herynek, V., Turnovcová, K. & Syková, E. (2011). *J. Mater. Chem.* **21**, 7630–7639.
Diab, C., Akiyama, Y., Kataoka, K. & Winnik, F. M. (2004). *Macromolecules*, **37**, 2556–2562.
Filippov, S. K., Chytil, P., Konarev, P. V., Dyakonova, M., Papadakis, C., Zhigunov, A., Plestil, J., Stepanek, P., Etrych, T., Ulbrich, K. & Svergun, D. I. (2012). *Biomacromolecules*, **13**, 2594–2604.
Filippov, S., Hrubý, M., Konák, C., Macková, H., Spírková, M. & Stepánek, P. (2008). *Langmuir*, **24**, 9295–9301.
Filippov, S. K., Konák, C., Kopecková, P., Starovoytova, L., Spírková, M. & Stepánek, P. (2010). *Langmuir*, **26**, 4999–5006.
Filippov, S. K., Lezov, A. V., Sergeeva, O. Y., Olifirenko, A. S., Lesnichin, S. B., Domnina, N. S., Komarova, E. A., Almgren, M., Karlsson, G. & Štepanek, P. (2008). *Eur. Polym. J.* **44**, 3361–3369.
Filippov, S. K., Sedlacek, O., Bogomolova, A., Vetrik, M., Jirak, D., Kovar, J., Kucka, J., Bals, S., Turner, S., Stepanek, P. & Hruby, M. (2012). *Macromol. Biosci.* **12**, 1731–1738.
Filippov, S. K., Starovoytova, L., Konák, C., Hrubý, M., Macková, H., Karlsson, G. & Stepánek, P. (2010). *Langmuir*, **26**, 14450–14457.
Formariz, T., Chiavacci, L., Sarmento, V., Santilli, C., Tabosa do Egito, E. & Oliveira, A. (2007). *Colloids Surf. B Biointerfaces*, **60**, 28–35.
Foster, B., Cosgrove, T. & Hammouda, B. (2009). *Langmuir*, **25**, 6760–6766.
Gromadzki, D., Filippov, S., Netopilík, M., Makuška, R., Jigounov, A., Pleštil, J., Horský, J. & Štepánek, P. (2009). *Eur. Polym. J.* **45**, 1748–1758.
Hoogenboom, R. (2009). *Angew. Chem. Int. Ed.* **48**, 7978–7994.
Hruby, M., Filippov, S. K., Panek, J., Novakova, M., Mackova, H., Kucka, J., Vetvicka, D. & Ulbrich, K. (2010). *Macromol. Biosci.* **10**, 916–924.
Hruby, M., Konak, C., Kucka, J., Vetrik, M., Filippov, S. K., Vetvicka, D., Mackova, H., Karlsson, G., Edwards, K., Rihova, B. & Ulbrich, K. (2009). *Macromol. Biosci.* **9**, 1016–1027.
Idziak, I., Avoce, D., Lessard, D., Gravel, D. & Zhu, X. X. (1999). *Macromolecules*, **32**, 1260–1263.
Jakes, J. (1988). *Czech J. Phys. B*, **38**, 1305–1316.
Jeworrek, C., Pühse, M. & Winter, R. (2008). *Langmuir*, **24**, 11851–11859.

Jones, R. G., Ober, C. K., Hodge, P., Kratochvíl, P., Moad, G. & Vert, M. (2013). *Pure Appl. Chem.* **85**, 463–492.
Koňák, C., Pánek, J. & Hrubý, M. (2007). *Colloid Polym. Sci.* **285**, 1433–1439.
Mahmud, A., Xiong, X. B., Aliabadi, H. M. & Lavasanifar, A. (2007). *J. Drug Target.* **15**, 553–584.
Mortensen, K. (2001). *Polym. Adv. Technol.* **12**, 2–22.
Mortensen, K. & Talmon, Y. (1995). *Macromolecules*, **28**, 8829–8834.
Pánek, J., Filippov, S. K., Hrubý, M., Rabyk, M., Bogomolova, A., Kučka, J. & Stěpánek, P. (2012). *Macromol. Rapid Commun.* **33**, 1683–1689.
Park, J. S., Akiyama, Y., Winnik, F. M. & Kataoka, K. (2004). *Macromolecules*, **37**, 6786–6792.
Pedersen, J. S. & Gerstenberg, M. C. (1996). *Macromolecules*, **29**, 1363–1365.
Pedersen, J. S. & Gerstenberg, M. C. (2003). *Colloids Surf. A*, **213**, 175–187.
Pedersen, J. S., Svaneborg, C., Almdal, K., Hamley, I. W. & Young, R. N. (2003). *Macromolecules*, **36**, 416–433.
Persigehl, P., Jordan, R. & Nuyken, O. (2000). *Macromolecules*, **33**, 6977–6981.
Pidhatika, B., Möller, J., Vogel, V. & Konradi, R. (2008). *Chimia*, **62**, 264–269.
Sato, T., Sakai, H., Sou, K., Medebach, M., Glatter, O. & Tsuchida, E. (2009). *J. Phys. Chem. B*, **113**, 8418–8428.
Sedlacek, O., Monnery, B. D., Filippov, S. K., Hoogenboom, R. & Hruby, M. (2012). *Macromol. Rapid Commun.* **33**, 1648–1662.
Sharma, P. K. & Bhatia, S. R. (2004). *Int. J. Pharm.* **278**, 361–377.
Sharma, P. K., Reilly, M. J., Jones, D. N., Robinson, P. M. & Bhatia, S. R. (2008). *Colloids Surf. B Biointerfaces*, **61**, 53–60.
Skodova, M., Hruby, M., Filippov, S. K., Karlsson, G., Mackova, H., Spirkova, M., Kankova, D., Steinhart, M., Stepanek, P. & Ulbrich, K. (2011). *Macromol. Chem. Phys.* **212**, 2339–2348.
Štěpánek, M., Materějíček, P., Procházka, K., Filippov, S. K., Angelov, B., Šlouf, M., Mountrichas, G. & Pispas, S. (2011). *Langmuir*, **27**, 5275–5281.
Stepanek, P. (1993). *Dynamic Light Scattering: the Method and Some Applications*. Oxford: Clarendon Press.
Sztucki, M., Di Cola, E. & Narayanan, T. (2010). *J. Appl. Cryst.* **43**, 1479–1487.
Torchilin, V. P. (2007). *Pharm. Res.* **24**, 1–16.
Wanka, G., Hoffmann, H. & Ulbricht, W. (1990). *Colloid Polym. Sci.* **268**, 101–117.
Yu, G., Deng, Y., Dalton, S., Wang, Q., Attwood, D., Price, C. & Booth, C. (1992). *J. Chem. Soc. Faraday Trans.* **88**, 2537.
Zhang, J., Fan, H., Levorse, D. A. & Crocker, L. S. (2011). *Langmuir*, **27**, 9473–9483.

THE JOURNAL OF PHYSICAL CHEMISTRY B

Article

pubs.acs.org/JPCB

Study of Complex Thermosensitive Amphiphilic Polyoxazolines and Their Interaction with Ionic Surfactants. Are Hydrophobic, Thermosensitive, and Hydrophilic Moieties Equally Important?

Anna Bogomolova,[†] Sergey K. Filippov,*[,†] Larysa Starovoytova,[†] Borislav Angelov,[†] Petr Konarev,[‡] Ondrej Sedlacek,[†] Martin Hruby,[†] and Petr Stepanek[†]

[†]Institute of Macromolecular Chemistry AS CR, v.v.i, Heyrovsky Sq. 2, 162 06 Prague 6, Czech Republic

[‡]European Molecular Biology Laboratory, EMBL c/o DESY, Notkestrasse 85, Hamburg D-22603, Germany

Supporting Information

ABSTRACT: The temperature-driven self-assembly of nonionic amphiphilic tailor-made triblock copolymers has been studied by DLS, NMR, ITC, and SAXS. The composition of these triblock copolymers is more complex than that of the vast majority of poly(2-alkyl-2-oxazoline)s: a statistical thermoresponsive (iPrOx) and hydrophobic (BuOx) central block with terminal hydrophilic blocks (MeOx). In general, as temperature increases, nanoparticles form in a process starting with single molecules that become loose aggregates and ends with the formation of compact nanoparticles. Here, we first attempt to resolve the effects of each block on nanoparticle formation. It has been proven that the iPrOx/MeOx ratio determines the value of the cloud point temperature, whereas the different BuOx–iPrOx blocks determine the character of the process. Finally, we complete our investigation by presenting the thermodynamic and structural profiles of the complexation between these triblock poly(2-alkyl-2-oxazoline)s and two ionic surfactants. The addition of an ionic surfactant promotes a rearrangement of the polymer molecules and the formation of complexes followed by the appearance of polymer–surfactant hybrid micelles. Analysis of the interaction shows a strong and nonspecific reaction between the polymers and the anionic surfactant sodium dodecyl sulfate and weak but polymer-state-sensitive interactions between the polymer and the cationic surfactant hexadecyltrimethylammonium bromide.

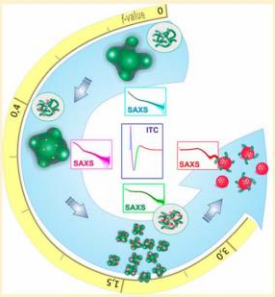

INTRODUCTION

Poly(2-alkyl-2-oxazoline)s are polymers that are currently widely and intensively investigated for biomedical purposes. Numerous articles have been devoted to the properties and applications of poly(2-alkyl-2-oxazoline)s in different fields, including drug delivery, tumor diagnostics, and antimicrobial agents.[1−4] The properties of these polymers depend on the alkyl group. The presence of a methyl or ethyl substituent (MeOx) makes the polymer hydrophilic, whereas poly(2-isopropyl-2-oxazoline) (iPrOx) shows thermoresponsive properties, and poly(2-butyl-2-oxazoline) (BuOx) and poly(2-phenyl-2-oxazoline) have hydrophobic natures.[2]

The synthesis of complex polymers from blocks with different structures makes it possible for the system to form specific structures.[5,6] It was previously shown that triblock copolymers constructed from a central block (statistical copolymer of BuOx and iPrOx) with terminal MeOx blocks can form a micelle-like structure as the temperature increases.[7] The onset of the transition from a molecular state to a micelle-like state has been defined as the cloud point temperature (CPT), and CPT has been shown to strongly depend on the ratio of thermoresponsive to hydrophilic blocks. Moreover, the introduction of a phenolic moiety into the copolymer allowed radionuclide labeling with iodine-125 for a promising use of the system in tumor diagnostics.

The structure of these copolymers appears to be very similar to the structure of Pluronic molecules, the triblock copolymers PEO–PPO–PEO, with their amphiphilic nature and the ability to self-assemble at a certain temperature.[8,9] Pluronic molecules have found wide application in biomedicine and are commonly used in a combination with normal ionic surfactants.[10] Recently, several experiments were performed using Pluronic systems in combination with ionic surfactants. It was shown that the ionic surfactants bind strongly with the polymer molecules and subsequently decrease the aggregation number of the block copolymer.[11−15]

Here, we investigate the behavior of the nonionic amphiphilic triblock copolymers MeOx-stat-(iPrOx-*co*-BuOx)-MeOx as the temperature increases. The backbone, which is constructed from poly(2-alkyl-2-oxazoline) units, makes this copolymer very attractive for biomedical applications. Its complex structure and similarity to Pluronic-like molecules allow for its use as an active species for tumor diagnostics. However, the units in the central block of this copolymer are arranged in a statistical manner, in contrast to the Pluronic molecules, making this system more complex. How does each

Received: January 31, 2014
Revised: April 15, 2014
Published: April 18, 2014

ACS Publications © 2014 American Chemical Society

dx.doi.org/10.1021/jp5011296 | J. Phys. Chem. B 2014, 118, 4940−4950

Scheme 1. Chemical Structure and Schematic Image of the Polymer under Investigation

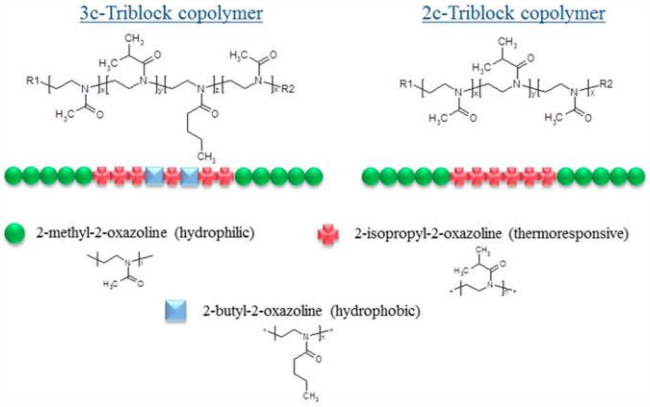

Table 1. Molecular Characteristics of the Polymers (c = 1.4 wt %)[a]

				n_{MeOx}		n_{iPrOX}		n_{BuOX}	
				NMR	NMR	NMR	NMR	NMR	NMR
polymers	type of polymer	2-butyl-2-oxazoline in thermoresponsive block, mol %	CPT, °C	H_2O	$CDCl_3$	H_2O	$CDCl_3$	H_2O	$CDCl_3$
MeOx	homopolymer	0	N/A		72				
IrOx	homopolymer	0	57				67		
oxBlock	2c-triblock copolymer	0	44	84	84	23	25.5		
ox(2:1)	3c-triblock copolymer	15	19	31.5	31.5	39	52.5	10	10.5
ox(1:1)	3c-triblock copolymer	15	17		52		40		8
ox(1:2)	3c-triblock copolymer	15	24	72	72	21	27	4.5	6

[a]The NMR data were obtained at 17 °C.

block in the molecule affect nanoparticle formation? To determine the answer to this question, we performed dynamic light scattering (DLS), small-angle X-ray scattering (SAXS), and nuclear magnetic resonance (NMR) experiments on three copolymers with different ratios of thermoresponsive to hydrophilic groups. Bearing in mind that a great attention was given for the characterization of Pluronic molecules in systems with ionic surfactants, we also analyzed the binding isotherm of copolymers with the anionic surfactant sodium dodecyl sulfate (SDS) and the cationic surfactant hexadecyltrimethylammonium bromide (CTAB) by isothermal titration calorimetry (ITC). Such knowledge will be extremely useful for understanding the nature of the interaction between amphiphilic poly(2-alkyl-2-oxazoline) molecules with the surfactant-like amphiphilic drugs that are used in micellar drug delivery systems; these drugs include the antibiotics doxorubicin (antineoplastic agent), monensin (a coccidiostat), amphotericin B, and nystatin (polyene antimycotic). To the best our knowledge, this study is the first in which the role of hydrophobic/hydrophilic/thermosensitive blocks and their interactions with surfactants were analyzed using polyoxazolines.

MATERIALS AND METHODS

Materials. Triblock copolymers were synthesized according to the scheme published in a previous article.[7] The chemical structure and composition of the polymers (three component (3c) and two component (2c) triblock copolymers) are indicated in Scheme 1 and Table 1. The 2c triblock was synthesized for comparative purposes; the 2c triblock copolymer possesses no hydrophobic BuOx groups. The molecular weights of polymers were ca. 10 kDa (roughly 100 monomeric units), and the polydispersities of the samples according to ref 7 were 1.39. Water was deionized with a Millipore Milli-Q water purification system. Sodium dodecyl sulfate and cetyltrimethylammonium bromide were purchased from Sigma-Aldrich Ltd. (Prague, Czech Republic). SDS was recrystallized from hexane, and the other chemicals were used without additional purification.

Methods. *Dynamic Light Scattering.* The temperature-induced micelle formation in aqueous solutions, the temperature dependences of the apparent hydrodynamic radius of particles, R_h, and the scattering intensity, I_s, were automatically measured at a scattering angle of $\theta = 173°$ on a Zetasizer Nano-ZS instrument, Model ZEN3600 (Malvern Instruments, UK). The DTS (Nano) program was used to evaluate the data. It provides an intensity-, volume-, and number-weighted R_h distribution function $G(R_h)$. A volume-weighted value of the apparent R_h was chosen to monitor the temperature changes in the system because it provides a realistic measure of the characteristic particle size in a solution. The temperature dependence of the nanoparticle formation was measured by heating from 5 to 55 °C in steps of 1 °C. Three measurements were taken after a steady-state condition was reached after each temperature change.

If not otherwise stated, all measurements were conducted with a polymer concentration of 1.4 mM (14 mg/mL) in water, and all solutions were filtered through a 0.22 mm PVDF syringe filter before measurement. The molecular characteristics of the polymers are presented in Table 1.

dx.doi.org/10.1021/jp5011296 | J. Phys. Chem. B 2014, 118, 4940−4950

Nuclear Magnetic Resonance (NMR). To characterize the behavior of the polymer system, the ^{1}H and ^{1}H spin−spin relaxation times T_2 were measured using NMR spectroscopy at different temperatures. Relaxation NMR spectroscopy is a useful tool for investigating polymer and solvent dynamics due to the fact that the transverse magnetization component is sensitive to changes in the mobility of polymer segments as well as the solvent.

^{1}H NMR measurements were performed with a Bruker Avance III 600 spectrometer operating at 600.13 MHz. The integrated intensities were determined with the spectrometer integration software at an accuracy of ±1%. In all measurements, the temperature was maintained at a constant value within ±0.2 K using a BVT 3000 temperature unit. The typical measurement conditions were as follows: 90 pulses with a width of 10 μs, relaxation delay of 10 s, spectral width of 5995.204 Hz, and 32 scans in the temperature range 17−57 °C. The ^{1}H spin−spin relaxation times T_2 for all components were measured using the CPMG pulse sequence $90°_x$-(t_d-$180°_y$-t_d)n-acquisition with t_d = 0.5 ms. Each experiment was conducted with 16 scans, a relaxation delay of 100 s, and a spectral width of 10 kHz.

Two types of deuterated solvents were used for the experiments. Chloroform, in which all of the polymer blocks are fully soluble, was used as the solvent for the structure analysis of each block in the copolymers. In aqueous solution, the intensity of the iPrOx and BuOx blocks is affected by the thermoresponsive behavior of the copolymer. The molecular parameters obtained for the polymers in water and in chloroform at 17 °C are presented in Table 1.

Isothermal Titration Calorimetry. The microcalorimetry study was performed using a MicroCal 200 isothermal titration calorimeter. The experiment was performed with consecutive injections of the concentrated surfactant solution into the calorimeter cell; the cell contained 280 μL of the polymer or water solution (14 mg/mL). A surfactant solution was added from a 40 μL injection syringe, the tip of which was modified to act as a stirrer. The chosen stirring speed was 1000 rpm. The injection volume varied between 1 and 2 μL. The time between injections was usually 5 min. The measurements were conducted at 15, 25, and 41 °C. The data were analyzed using Microcal ORIGIN software. The experimental enthalpy was obtained by integrating the raw data signal. The integrated molar enthalpy change per injection was obtained by dividing the experimentally measured enthalpy by the number of moles of surfactant added. The final enthalpograms are the plots of the integrated molar enthalpy as a function of total surfactant concentration in the calorimeter sample cell.

Small-Angle X-ray Scattering. Synchrotron SAXS experiments were performed at EMBL beamline P12 (Petra III, Hamburg, Germany) using a pixel detector (2 M PILATUS). The X-ray scattering images were recorded at a sample−detector distance 2.7 m, using a monochromatic incident X-ray beam (λ = 0.125 nm) covering the range of momentum transfer of 0.05 nm^{-1} < q < 3.5 nm^{-1} ($q = 4\pi \sin\theta/\lambda$, where 2θ is the scattering angle). No measurable radiation damage was detected in most of the samples, as determined by comparing 20 successive time frames that had 50 ms exposure times. In all cases reported in this paper, the two-dimensional scattering patterns were isotropic. The patterns were azimuthally averaged to determine the dependence of the scattered intensity $I_s(q)$ on the momentum transfer q. The solvent scattering was subtracted prior to the fitting analysis.

All data manipulations were performed using PRIMUS software.[16,17]

Another set of SAXS experiments was performed on the high brilliance beamline ID02 at ESRF (Grenoble, France). The SAXS setup utilizes a pinhole camera with a beam stop placed in front of a two-dimensional Frelon CCD detector. The X-ray scattering patterns were recorded for sample-to-detector distances of 1.5 and 8 m, using a monochromatic incident X-ray beam with an energy E = 12 460 eV (λ = 0.1 nm). The available wave vector range was q = 0.05−2.76 nm^{-1}. Online corrections were applied for the detector, and the sample/detector distance, center, transmission, and incident intensity were calibrated. All the cases reported in this paper have isotropic scattering; thus, azimuthal regrouping and radial averaging were also performed online to determine the dependence of the scattered intensity $I_s(q)$ on the scattering vector q in absolute units. The scattering from a capillary filled with Milli-Q water was measured for use as a background and subtracted from the scattering signals of the samples. Prior to the experiment, a representative sample was checked for radiation damage.

RESULTS AND DISCUSSION

DLS analysis of the systems of triblock copolymers was performed at a polymer concentration of 1.4 mM, which was considered appropriate for the subsequent ITC experiments. The previous DLS results for 3c-triblock copolymers (concentration 0.05 mM)[7] indicate the presence of single molecules of a polymer (radius ca. 2−3 nm) at temperatures below CPT and the formation of large aggregates as the temperature increased above CPT (radius ca. 100−300 nm) (Figure 1). However, in addition to the previous results, we observed a consecutive transformation of the aggregates into compact nanoparticles (ca. 25 nm) at the highest temperature, 50 °C. (Figure 1). One can suggest that the loose aggregates that initially formed at CPT shrank above CPT in the surrounding conditions as a result of the thermosensitivity of the polymers.

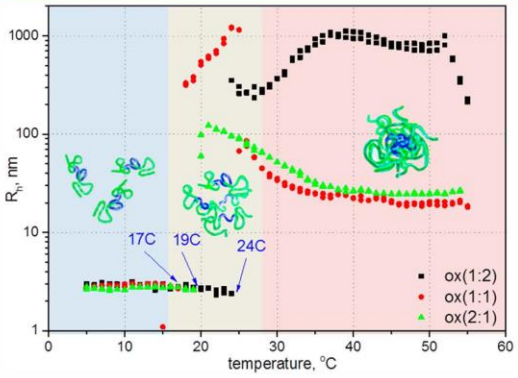

Figure 1. DLS data from pure 3c-triblock poly(2-alkyl-2-oxazoline)s, C = 14 mg/mL.

Comparing the DLS data from polymers with different ratios of hydrophobic/hydrophilic groups allows for an assessment of the influence of this ratio on the process of complex formation. The hydrophobic group content was slightly varied for all three

dx.doi.org/10.1021/jp5011296 | J. Phys. Chem. B 2014, 118, 4940−4950

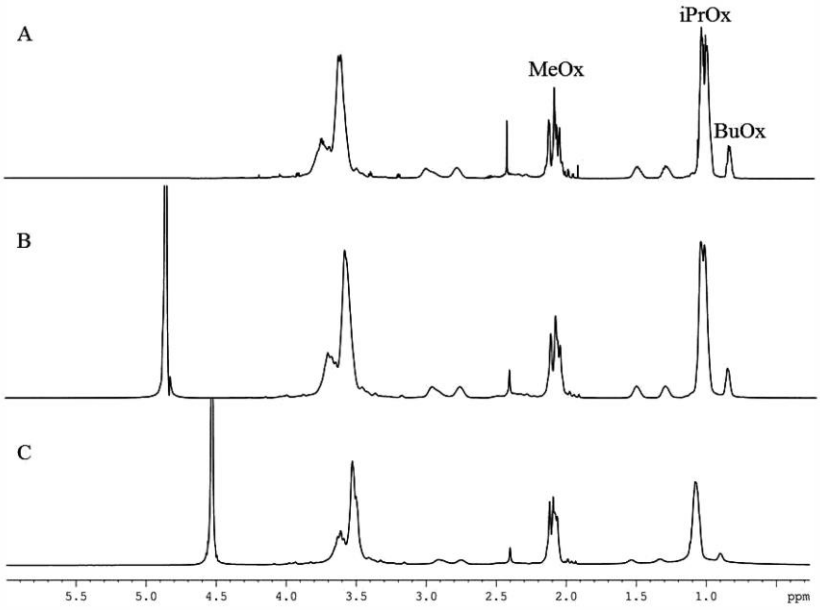

Figure 2. ^{1}H spectra of ox(2:1) copolymers (A) in $CDCl_3$ at 17 °C, (B) D_2O at 17 °C, and (C) D_2O at 57 °C.

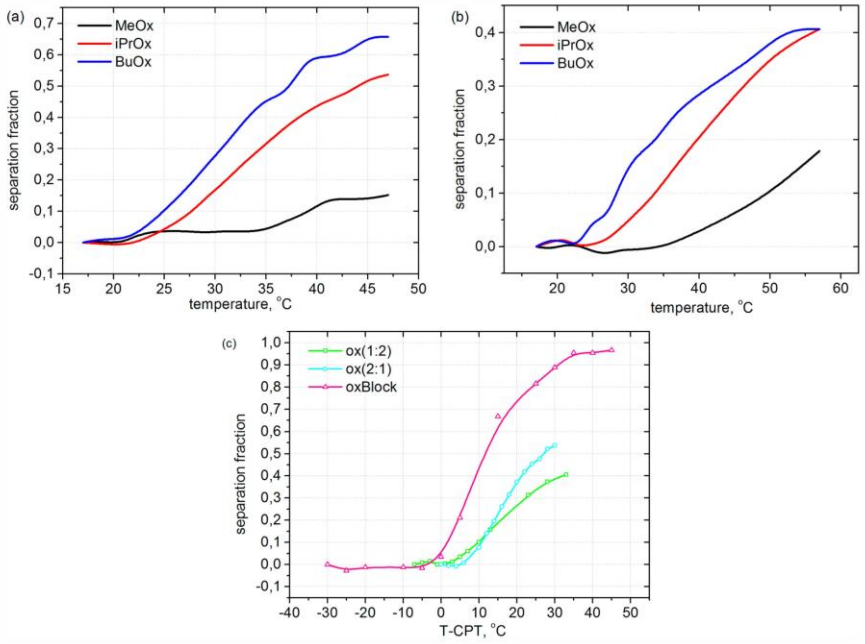

Figure 3. NMR data for the separation parameter as a function of temperature for (a) ox(2:1), (b) ox(1:2), and (c) iPrOx for ox(2:1), ox(1:2), and oxBlock.

investigated 3c-triblock copolymers (Table 1). There is only one significant difference in the experimental set—the ratio of units in the central and terminal blocks. An excess of hydrophobic and thermoresponsive groups leads to a decrease in CPT to 19 °C and to the formation of a rather compact structure right above the transition temperature. At the same time, increasing the number of hydrophilic groups contributes to the shift of the CPT to a higher value. The complex

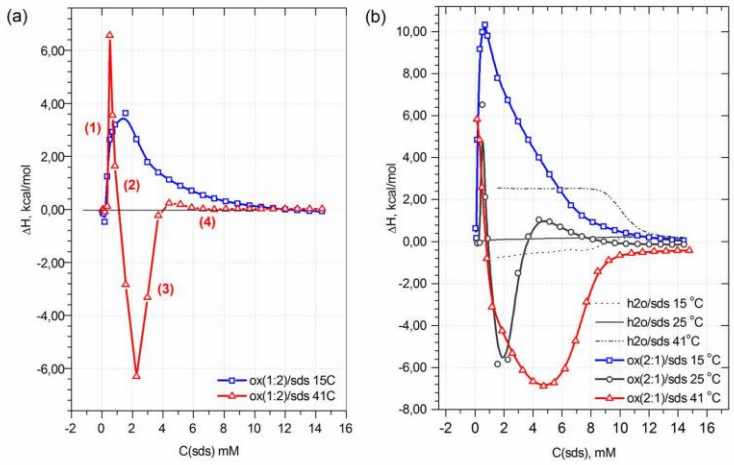

Figure 4. ITC curve for SDS titration of polymers at different temperatures: (a) ox(2:1) and (b) ox(1:2).

Table 2. Parameters of the Interaction between the Polymers and Surfactant

surfactant	cmc,[a] mM	cac[b] (molecular state), mM	cac (micellar state), mM	C_2, mM
SDS	8.4	0.15	0.35	12−14
CTAB	1.25	0.7	0.07	>20

[a]The cmc is taken from the blank titration of surfactant to water and does not show a significant variation with temperature. [b]The cac is an average value across all polymers; the molecular state and the micellar state correspond to the conformation of the polymer at 15 and 25 (or 41) °C, respectively.

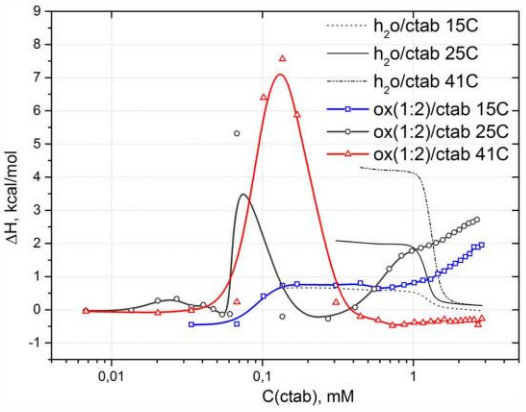

Figure 5. ITC curve for the titration of the polymer ox(1:2) with CTAB at different temperatures.

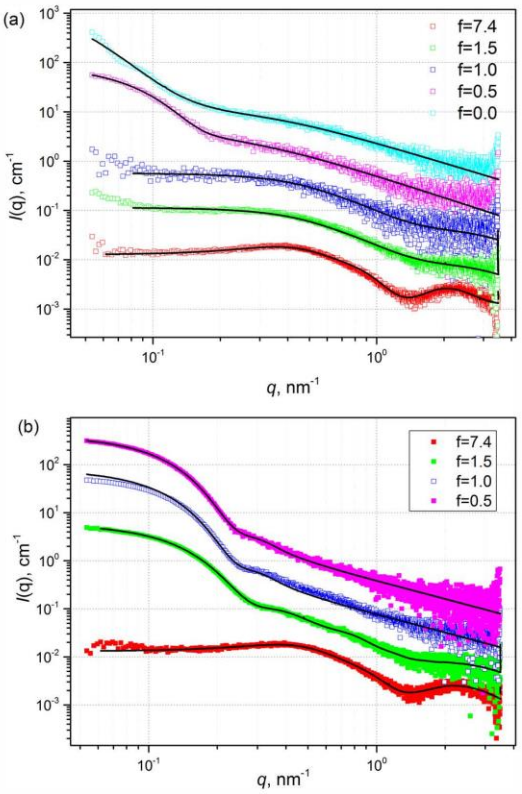

Figure 6. SAXS curves for solutions of the ox(1−1) copolymer and SDS taken at T = 25 °C (a) and T = 40 °C (b). The solid lines are fits. Each curve is shifted by a factor of 5 from top to bottom for clarity.

formation that is observed using DLS as the temperature increases can be described as a two-step process (red curve in Figure 1). In the first step, one can observe large aggregates with a hydrodynamic radius of up to 103 nm; with further temperature increases, the aggregates transformed into particles with a radius ca. 25−30 nm. For the ox(1:2) copolymer with the largest amount of hydrophilic MeOx groups, we detected an extended transition into compact structures (Figure 1). The

dx.doi.org/10.1021/jp5011296 | J. Phys. Chem. B 2014, 118, 4940−4950

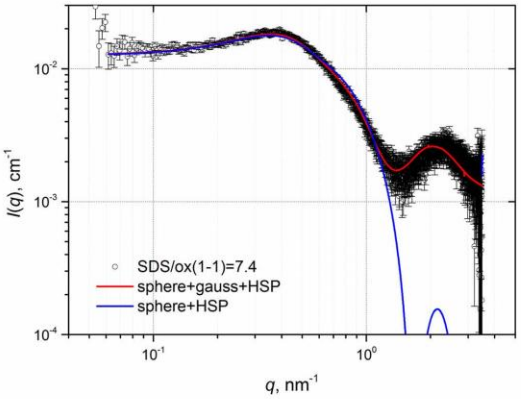

Figure 7. SAXS curve for solutions of ox(1:1) copolymer and SDS taken at T = 25 °C; f = 7.4.

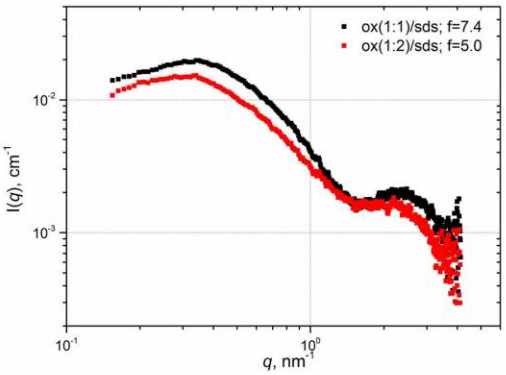

Figure 8. SAXS curves for solutions of ox(1:1) and of ox(1:2) polymers and SDS taken at T = 25 °C.

temperature dependence obtained for the 2c-triblock copolymer that was constructed from only the central thermoresponsive group with hydrophilic terminal groups exhibits similar behavior (Figure 1S, Supporting Information). One can conclude that addition of hydrophobic groups to the central block (at the same ratio of thermoresponsive/hydrophilic groups) causes the shift in the CPT value but does not influence the process of particle formation. Thus, we can consider the ox(1:2) sample to be a more hydrophilic polymer, whereas the ox(2:1) polymer demonstrates more hydrophobic properties.

NMR analysis was conducted for the pure polymers in the same conditions as mentioned above. The separation fraction was chosen to assess the mobility of the different groups as the temperature varied. The thermosensitivity of some polymer blocks restricted the mobility of polymer segments, thus causing the spectrum of a copolymer in water (Figure 2B,C) to differ from that in chloroform (Figure 2A). This restriction results in broadening and a significant decrease in the integrated intensity of the corresponding NMR signals. For comparative analysis, the values of the separation fraction p were calculated as

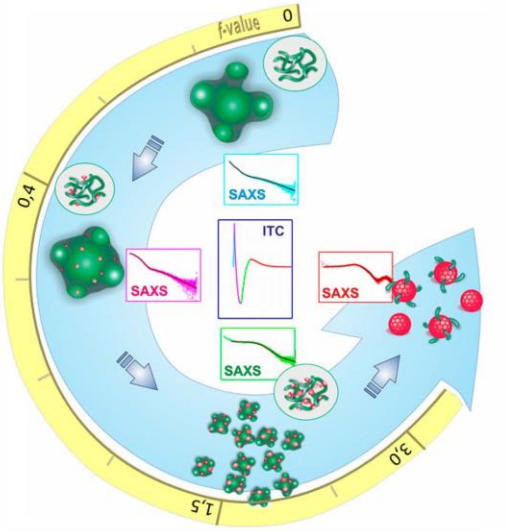

Figure 9. Structure sequence of the complexation process of triblock poly(2-alkyl-2-oxazolines) with increasing the concentration of surfactants.

$$p = 1 - I_T/I_0$$

where I_T is the integrated intensity of the polymer peak in a partly separated system and I_0 is the initial value of integrated intensity of the corresponding peak. The separation fraction p can be determined for all polymer segments separately.[18−22]

Preliminary analysis of the experimental data (Figure 3a,b) shows that the separation fraction, which corresponds to BuOx and iPrOx groups, sharply changes with temperature and reaches a value of 0.5−0.7 for the ox(2:1) copolymer (47 °C) and 0.4 for ox(1:2) (57 °C). We did not detect any significant differences in the temperature (21−23 °C) at which the group mobility began to decrease for the two polymers. This situation becomes clear if we account the fact that the NMR measurement was conducted in water and that the signal intensity of groups at 17 °C was taken as an initial parameter. Comparing the results obtained at 17 °C in water and in d-chloroform shows a very interesting fact: while the CPT for ox(2:1) was approximately 17 °C, the mobility of the iPrOx group at this temperature had already been reduced by a factor of 25%; this decrease was 22% for copolymer ox(1:2) at 24 °C (Table 1). At the same time, we did not observe any significant changes between the mobilities of the BuOx groups at 17 °C in water and in d-chloroform. Previous analysis and the fact that the separation fraction for the BuOx and iPrOx groups shows synchronous changes with increasing temperature support the initial suggestion about the statistical order of the units in the central block of copolymers. Thus, we can consider the central block to be a single entity and the whole copolymer to be similar to a Pluronic molecule with central thermoresponsive/hydrophobic blocks and terminal hydrophilic blocks. Moreover, we also observed some changes in the mobility of the MeOx group with increasing temperature. These changes most likely result from the aggregation of the central block that reduces the mobility of the nearby MeOx units and, as a result, slightly increases the separation fraction. Comparing the separation

dx.doi.org/10.1021/jp5011296 | J. Phys. Chem. B 2014, 118, 4940−4950

Table 3. Fitting Parameters for ox(1-1) and SDS at T = 25 and 40 °C

		form factor								
		big spherical particles, q > 0.2 nm^{-1}		generalized Gaussian coil		sphere with attaches Gaussian coil			structure factor	
f	T, C	R_{big}, Å ± 1	sigma ±0.01	R_g, Å	ν	R, Å	R_g, Å	sigma	RHS, Å ± 0.1	f_{bv} 10^{-2}
0	25	>200	0.86	37.3 ± 0.2	0.72 ± 0.02					
0.5	25	200	0.25	42.3 ± 0.3	0.66 ± 0.02					
0.5	40	167	0.19	37.5 ± 0.5	0.77 ± 0.04					
1.0	25					23 ± 4	4.8 ± 0.8	0.7 ± 0.2	63.9	2 ± 1
				33.7 ± 0.5	0.53 ± 0.03					
1.0	40	163	0.17			22 ± 2	1 ± 4	0.44 ± 0.08	93.2	8 ± 6
		163	0.15	56.2 ± 0.6	0.73 ± 0.02					
1.5	25					18.9 ± 0.4	5.4 ± 0.2	0.70 ± 0.08	70.6	3 ± 3
				33.0 ± 0.1	0.49 ± 0.01					
1.5	40	129	0.23			17.0 ± 0.4	3.5 ± 0.1	0.50 ± 0.03	76.3	14 ± 3
		142	0.18	34.7 ± 0.01	0.48 ± 0.03					
7.4	25					19.3 ± 0.5	1.1 ± 0.5	0.20 ± 0.01	66.4	7.3 ± 0.5
7.4	40					13 ± 1	5.1 ± 0.2	0.44 ± 0.03	60.9	7.6 ± 0.5

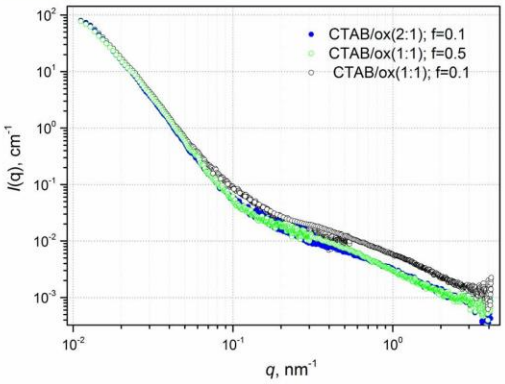

Figure 10. SAXS curves for solutions of ox(1:1), and ox(1:2) polymers and CTAB taken at T = 25 °C.

fraction for the iPrOx group in the different polymers allows for an assessment of the influence of the rest groups in the polymer on the thermosensitivity of iPrOx (Figure 3c). Considering our previous conclusion about the statistical arrangement of the BuOx and iPrOx groups in the central block of polymers and the independent character of the MeOx moieties, it makes sense to consider the influence of just the BuOx groups on the thermosensitivity of iPrOx. Here, we do not exclude the influence of the MeOx groups at all; instead, we attribute this influence solely to the shift in the position of CPT. The curve for iPrOx in the 2c-triblock copolymer reflects this situation (Figure 3c). Moreover, we detect a sharp transition in the separation fraction for the 2c-triblock copolymer as well. The addition of BuOx groups decreases the slope of the curve, and this change does not correlate with the BuOx group content in the polymer. We must thus consider some general factors related to the complex structure of the polymer molecules. While the thermosensitive groups promote a thermosensitive response of the hydrophobic groups and exert fewer effects on the hydrophilic groups, and the hydrophilic groups shift the transition temperature of the whole molecule, the hydrophobic groups could exert their effect by influencing the formation of hydrophobic microdomains. Consequently, the difference in the number of iPrOx and BuOx groups would define the hydrophobicity of the central block. A smaller difference would lead to a less thermoresponsive and more hydrophobic central block. The previous results confirm our assumption[7] (Supporting Information Table 1S). Thus, the slope of the curve in Figure 3 would reflect the hydrophobicity of the central entity. A smaller slope of the curve corresponds to a more hydrophobic central block.

The observed temperature behavior of the different blocks leads to new questions. Namely, will the difference in the nature of the blocks affect their interaction with amphiphilic molecules? To answer this question, we performed ITC experiments where pure polymer solutions were titrated by solutions of ionic surfactants (SDS or CTAB). These surfactants were chosen based on the different binding strengths that were recently reported for PNIPAM and PEO nonionic polymers.[23−26]

Three different temperatures were chosen for ITC analysis: 15, 25, and 41 °C; these temperatures correspond to the single molecule, large aggregate (or loose nanoparticle), and compact nanoparticle states of the polymer, respectively. The experiment was performed by sequentially adding the surfactant (SDS or CTAB) to the polymer solution. The previous data indicate that we can consider our 3c-triblock copolymers to be similar to Pluronic molecules with central thermosensitive/hydrophobic blocks and terminal hydrophilic blocks. This assumption allows us to use the system of Pluronic molecules with surfactants as a basis for further analysis of our systems.

Some experiments were conducted using thermoresponsive systems of PEO−PPO−PEO block copolymers with different

Table 4. Fitting Parameters for ox(1:1), ox (1:2), and SDS at T = 25 °C

copolymers	f	R, Å	sigma	R_g, Å	RHS, Å	f_{bv} 10^{-2}
ox(1−1)	7.4	19.3 ± 0.2	0.29 ± 0.01	1.7 ± 0.3	66.4 ± 0.1	7.0 ± 0.3
ox(1−2)	5.0	17.2 ± 0.9	0.47 ± 0.03	3.5 ± 0.3	78.8 ± 0.1	7.6 ± 0.3

dx.doi.org/10.1021/jp5011296 | J. Phys. Chem. B 2014, 118, 4940−4950

length of blocks in combination with SDS and CTAB.[11−13] We begin our consideration of the interaction between an ionic surfactant and nonionic 3c-triblock copolymer with the case of the anionic SDS. Analysis of the interaction of the F127 Pluronic molecule with SDS shows that the process can be described in a few stages. The number of stages depends on whether the polymer is in a state above or below the CPT. At temperatures below CPT, the polymer is in a dissolved state where single molecules can be detected. In this case, the ITC measurements are characterized by a single peak and two processes: an initial endothermic process followed by an exothermic process that finally proceeds to the formation of unimodal micelles of the surfactant.[11] This type of ITC curve is characteristic of a nonionic polymer and ionic surfactant. We observed similar behavior for our polymers at 15 °C (Figure 4a,b). Three important parameters could be determined from the ITC data: cac (critical aggregation concentration) = the concentration of the onset of the interaction between a polymer and surfactant, C_2 = the concentration at which micelles of the surfactant begin to form, and ΔH = the enthalpy of interaction. The data at 15 °C show a difference in the enthalpy of interaction: 3.6 kcal/mol for ox(1:2) and 10.4 kcal/mol for ox(2:1) (Figure 4a,b). Because we measured the transfer of the polymer from a bad solvent (water) to a good solvent (surfactant solution), one can conclude that this process should be more preferable for a more hydrophobic polymer, such as ox(2:1). The ox(1:2) at 15 °C was far from the CPT and did not show significant aggregation behavior.

As the temperature increases up to 25 °C, the polymers change their conformation from a single molecule to a large aggregate or a loose nanoparticle. In this situation, we can observe four processes in the ITC curve (Figure 4a,b): an initial endothermic process (1) followed by a strong exothermic process (2) with a subsequent strong endothermic process (3) and finally a weak exothermic process with merging of the measured curve to the curve for a pure surfactant (4). Similar behavior was observed in the interaction of F127 and other Pluronic molecules with SDS above CPT.[11,13,27] A very well-composed and reasoned explanation for such behavior was proposed by Li and Xu et al. The authors suggested that the first stage includes binding of the surfactant to the polymer aggregates and the formation of stable complexes. In the second stage, the sequential addition of SDS promotes the breakdown of the complexes to smaller mixed aggregates. This process continues until all aggregated structures are dissociated. The second stage may also include some interaction between the dissociated molecules of the polymer and the surfactant, but that process plays a leading role in the third stage. The last stage is the release of some bonding water from the polymer−surfactant hybrid micelles, followed by the formation of pure micelles of the surfactant (Figure 4b). Increases in the temperature up to 41 °C, where the polymer molecules are in a compact nanoparticle state, do not influence the form of the curve; the increases only make the exothermic process more explicit. In fact, the dimension of the exothermic peak is a function of particles compactness. The polymer ox(2:1) at 41 °C has more compact structure (ca. 25 nm) than the polymer ox(1:2) (ca. 1000 nm) and displays a more pronounced exothermic peak on the enthalpogram. It is worth to mention that we did not observe any significant changes in the values of cac and C_2 for ox(1:2) and ox(2:1) at 15 and 25 °C or at 41 °C. For our polymers, cac was almost constant in the range of 0.15−0.35 mM for any triblock copolymers and at any measured temperature (Figure 4a,b and Figure 2S). This result indicates that neither the hydrophobicity (hydrophilicity) nor the conformation of the polymer affects the strength of the interaction between SDS and the polymer. Moreover, the corresponding value of cac for F127 with SDS was found to be 0.35 mM. Because cmc = 8.4 mM for the pure SDS solution, one can conclude that the interaction of the SDS surfactant with the amphiphilic block copolymers is strong and non-specific (Table 2). Furthermore, we also detected the binding of SDS to the hydrophilic MeOx, which also supports our assumption about the nonspecific nature of the interaction of the SDS surfactant (Figure 3S).

The same analysis logic can be applied to the system of polymers with the cationic surfactant CTAB (Figure 5 and Figure 4S). We have observed the typical character of the curve for all polymers in the presence of CTAB.[13,27] However, there are some new and notable findings. The concentration dependence of the enthalpy changes shifted to a higher surfactant concentration than that for the case of the SDS experiment. Moreover, we did not detect any significant exothermic effect in the thermograms. Both of these factors could be explained by a weaker interaction with the compounds. Although ionic surfactants act in a similar manner, the differences in the size and charge of the headgroup may affect the strength of the interaction between the polymer and the surfactant. The parameter cac, which describes the onset of the binding process, is usually used to characterize the interaction strength. It is well-known that the cationic surfactant CTAB has a sterically more demanding ionic group (quaternary ammonium) at the end of the molecule compared with the ionic one (sulfate) in the anionic SDS.[12,13] This difference may explain why the interaction between the polymer and CTAB only starts at a cac = 0.7 mM surfactant concentration (cmc = 1.2 mM). In contrast, SDS did not show significant steric repulsions and the interaction began at a concentration of 0.35 mM (cmc = 8.4 mM). Another feature of the CTAB−polymer interactions is the existence of two different critical aggregation concentrations depending on the state of the polymer system. As mentioned above, the cac for the molecular conformation of a polymer was found to be 0.7 mM CTAB, while cac = 0.07 mM was detected for the polymer aggregates. This results reveals the complex but highly specific binding of CTAB to the macromolecule (Table 2).

To test the previously suggested mechanism for the interactions of the polymers with ionic surfactant, SAXS experiments were conducted. In these experiments, we tried to trace the evolution of the complexes as the composition ratio (f = C(surf.)/C(pol)) increased and to assess the temperature dependence of the process. For this reason, the f values for the experiment were selected in accordance with the characteristic processes on the ITC thermograms (Figure 4 and Figure 2S): 0.5 (C(sds) = 0.7 mM), 1.0 (1.4 mM), 1.5 (2.1 mM), and 7.4 (10.4 mM). The scattering curves for T = 25 °C show some changes with increasing composition ratio f (Figure 6a). At low q values, an upturn is visible for f = 0 and 0.5. At high q values, the scattering curve is a smooth function of q. With increasing SDS concentration, the upturn at low q values decreases, whereas at high q values, a side peak becomes clearly resolved. Similar behavior was observed at T = 40 °C (Figure 6b). The only difference between two temperatures is that the upturn is much more pronounced at T = 40 °C.

The interpretation of the scattering curves presented in Figure 6a,b is rather straightforward. The upturn at low values

dx.doi.org/10.1021/jp5011296 | J. Phys. Chem. B 2014, 118, 4940−4950

of q obviously results from the presence of large particles in the solution. The disappearance of the upturn should be related to particle decomposition. Moreover, the depression in the scattering intensity as $q \rightarrow 0$ at $f = 7.4$ and the appearance of a peak at $q = 0.4$ nm^{-1} for both temperatures are manifestations of the structure factor caused by the repulsion of the SDS micelles (Figure 7).

Previously, several SANS and SAXS experiments on the interaction of SDS with neutral polymers were reported.[28−35] In the classical work of Cabanne and Duplessix,[31] a contrast variation study was utilized to obtain structural information about PEO−SDS complexes. It was established that single PEO chains enhance the micellization of SDS molecules. Moreover, the structure of these complexes could be characterized by the hard-sphere model with SDS micelles of 2 nm with a separation distance of 9 nm between micelles. The presence of charged SDS micelles disrupts the conformation of PEO chains, making them more expanded and forming a pearl-necklace structure.

A similar conclusion was obtained for the PEO−SDS system by Suss et al. on the basis of cryo-TEM and SAXS experiments.[32] A hollow sphere model was used as a fitting function. The calculated radius was found to be 2.1 nm for SDS micelles in a mixture of 2 wt % SDS and 1% PEO and 2.5 nm for the pure 2.0% aqueous solution of SDS. A radius of 2.3−2.5 nm for the free SDS micelles was reported by Itri and Amral.[33,36] Similar results were also observed for the PVP−SDS system.[34]

To fit the scattering curves, several models could be utilized. In our work, we selected two models as the most appropriate ones: the model of a generalized Gaussian coil and the model of a sphere with an attached Gaussian coil. The generalized Gaussian coil model (parameters: R_g = radius of gyration of a polymer chain; ν = Flory exponent) was taken for the case of $f = 0$ and 0.5, whereas for $f > 0.5$, the sphere with an attached Gaussian coil model seems more plausible. This model was utilized instead of the hard sphere or hollow sphere model that previous authors utilized to analyze polymer−SDS aggregates.[32,33] As shown in Figure 7, the hard sphere fitting functions correctly describe the structure peak but vanish rapidly at $q > 1$ nm^{-1}, thus failing to describe the second peak. Because the scattering from the buffer was properly subtracted, there is a contribution to the scattered intensity apart from the hard sphere that should be taken into account. It is logical to assume that some pMeOx chains might be present on the surface of the SDS micelles. Therefore, the model of the sphere with an attached Gaussian coil was tested (parameters: R = radius of the core; R_g = radius of gyration of the outer shell; sigma = polydispersity). In some cases where an upturn at low q values was visible (T = 40 °C), we added a second contribution, the hard sphere model (R_{big} = radius of hard sphere; sigma = polydispersity) with Schultz−Zimm polydispersity. To account for the repulsive interactions, the classical Percus−Yevik structure factor was applied (parameters: RHS = hard sphere repulsion radius; f_b = volume fraction of hard spheres). The resulting fitting functions are presented in Figure 6.

Together with the Percus−Yevik structure factor, the fractal $\exp(-\alpha)$ structure factor described in ref35 was tried. That structure factor was not able to correctly describe the correlation peak of the curve. Thus, we can conclude that the pearl-necklace model is not applicable in our case due to the shorter contour length of polyoxazolines.

The fitting of the SAXS data also supports the conclusions drawn from the ITC experiments. The "structure-sequence" plot summarizes the obtained regularities for different concentrations of surfactants (Figure 9). At $f = 0.5$, which corresponds to the first exothermic process at 0.7 mM SDS (Figure 9, pink line, pink plot), the coexistence of the polymer in a coil conformation with 20.0 nm particles is visible in the SAXS data (Figure 7a and Table 3). The chain conformation of the copolymer at $f = 0.5$ is almost identical to the one in a surfactant-free solution ($f = 0$, Table 3) (Figure 9, blue line, blue plot). Moreover, the size and excluded volume exponent indicate that the ox(1:1) copolymer is in the swollen Gaussian chain conformation. The increase in the f value changes the SAXS pattern. At $f = 1$ (C(sds) = 1.4 mM) (Figure 9, green line, green plot), no large particles are observable on the SAXS curves at low q values at $T = 25$ °C (Figure 6a). Obviously, the large aggregates visible at $f = 0.5$ were disrupted with the higher SDS content, thus confirming the hypothesis drawn from the ITC data in which process 2 (Figure 9, pink line) is a breaking down of large mixed aggregates. Moreover, a small depression in the scattered intensity is witnessed at low q values (0.1−0.3 nm^{-1}), and a tiny upturn starts to grow at high q values ($q > 1$ nm^{-1}). This upturn is obscured by noise and is considered a deviation from Gaussian behavior. That fact impels us to find a more appropriative model to describe the visible features. The model of a sphere with an attached Gaussian coil seems more promising and seems to reflect the actual situation, as mentioned above. We also admit that the generalized Gaussian coil model is still applicable in this case (Table 2). A similar situation was observed for $f = 1.5$ as well. The only difference between the curves is a better manifestation of the peak at $q > 1$ nm^{-1}. All of these findings confirm our previous assumption from the ITC data about the manner of the interaction between the polymer and surfactant. Thus, one can propose that the disruption of the large aggregates and the formation of nonstoichiometric complexes between SDS and the copolymer occur in the second and third stages of the reaction (Figure 9, pink and green line, respectively).

The situation is not very different at $T = 40$ °C (Figure 6b and Table 3). Large particles coexist in the solution together with the single copolymer chains. However, in contrast with the situation at 25 °C, the large particles remain up to $f = 7.4$. The increase in the hydrophobicity of the copolymer due to the thermoresponsive nature of the iPrOx blocks plays a critical role here. The number of hydrophobic blocks increases to increase the number of large aggregates in the solution. The addition of 1.4 mM SDS ($f = 1.0$) is simply insufficient to break down all aggregates at this temperature.

The interpretation of the SAXS curves at $f = 7.4$ is straightforward (Figure 9, red line, red plot). The second peak is well resolved and indicates that hybrid micelles are formed in the solution. The core of such micelles is composed of SDS molecules bound to a copolymer chain. Moreover, no large particles are visible on the SAXS curves at either temperature. One can conclude that an ample amount of SDS was added to the solution, thus successfully preventing polymer aggregation. In contrast with the situation for high molecular weight homopolymers, such as PEO or PNIPAM, no pearl-necklace structure is formed for the copolymer ox(1:1), most likely due to the short length of the involved polymer chains. We have found that the size of the hybrid micelles 1.8−2.0 nm was in good agreement with the previously reported data for SDS−nonionic polymer complexes and less than the

dx.doi.org/10.1021/jp5011296 | J. Phys. Chem. B 2014, 118, 4940−4950

dimensions of pure SDS micelles in the polymer free solution. Interestingly, the dimension of the micellar core at 40 °C is less than that at 25 °C, while the radius of gyration of the Gaussian chains in the micellar shell and the polydispersity are higher. That fact can be explained again by the polymer thermosensitivity. As the polymer becomes more hydrophobic with increasing temperature, the tendency to move from the bad solvent (water) to the good one (surfactant micelles) increases. Finally, when the rearrangement is completed, the hydrophobic groups together with the surfactant molecules form a compact core, while the hydrophilic groups of the polymer extend to the water. The value f = 7.4 (10.4 mM of SDS) corresponds to process 4 (Figure 9, red line). It is the last process which brings about the interaction between the polymer and surfactant. Above that point, only pure micelles of the surfactant are observed to form.

The SAXS experiment shows that hybrid micelles could be formed for all copolymers regardless of their initial structure (Figure 8 and Table 4). The structure of such micelles is only determined by the amount of SDS in solution. In contrast, CTAB interacts much more weakly with the copolymer, as can be shown in the SAXS data (Figure 9). Large aggregates are observed on the SAXS curves even at high values of f.

■ CONCLUSIONS

We have investigated the temperature-dependent solution behavior of nonionic amphiphilic polymers with a complex nature. Triblock copolymers MeOx−(co-iPrOx-BuOx)−MeOx show thermoresponsive properties. As the temperature increase, the polymers transform from single molecules to loose aggregates to compact nanoparticles. We demonstrated that the ratio iPrOx/MeOx is a critical for the value of CPT, while the difference in BuOx-iPrOx can be attributed to the hydrophobicity of the central block of the polymers. Greater hydrophobicity in the central block of the polymer corresponded to the formation of looser aggregates at high temperature. The addition of ionic surfactant leads to a rearrangement of the polymer molecules and finally to the formation of complexes between the polymer and surfactant. The interaction process is described in detail along with the structure of the formed complexes. Analysis of the interaction shows a strong and nonspecific reaction with the anionic surfactant SDS, but the binding of cationic CTAB is weak but highly sensitive to the polymer state. Nevertheless, we can refer the structure of our polymers to the structure of the Pluronic molecule PEO−PPO−PEO despite the statistical arrangement of the hydrophobic (BuOx) and thermoresponsive (iPrOx) groups in the central part. These findings play a critical role in understanding the behavior of poly(2-alkyl-2-oxazoline)-based micellar drug delivery systems, where the solution behavior is driven by polymer−polymer, polymer−drug, and drug−drug interactions.

■ ASSOCIATED CONTENT

Supporting Information

DLS data for BlockOx; table of physicochemical characteristics of the block polyoxazolines; ITC data for ox(1:1) and SDS; ITC data for MeOx, SDS, and CTAB; ITC data for ox(1:1), ox(2:1), and CTAB. This material is available free of charge via the Internet at http://pubs.acs.org.

■ AUTHOR INFORMATION

Corresponding Author

*Tel + 420 296 809 291, Fax +420 296 809 410, e-mail filippov@imc.cas.cz (S.F.).

Notes

The authors declare no competing financial interest.

■ ACKNOWLEDGMENTS

We gratefully acknowledge the European Synchrotron Radiation Facility (Grenoble, France) for providing synchrotron beam time (SC3113) and the Grant Agency of the Czech Republic, Project P205/11/1657. The authors thank the Academy of Sciences of the Czech Republic, Grant No. M200501201; the Ministry of Industry and Trade, Grant MPO TIP No. FR-TI4/625 financial support No. CZ09-DE06/2013-2014 from the ASCR−DAAD Programme PPP 2013-2014 and the EU FP7 program, I3 access Grant BioStruct-X, project Number 283570.

■ REFERENCES

(1) Hoogenboom, R. Poly(2-oxazoline)s: A Polymer Class with Numerous Potentia Application. *Angew. Chem.* **2009**, *48*, 7978−7994.

(2) Sedlacek, O.; Monnery, B. D.; Filippov, S. K.; Hruby, M.; Hoogenboom, R. Poly(2-Oxazoline)s − Are They More Advantageous for Biomedical Applications Than Other Polymers? *Macromol. Rapid Commun.* **2012**, *33*, 1648−1662.

(3) Viegas, T. X.; Bentley, M. D.; Harris, J. M.; Z, F.; Yoon, K.; Dizman, B.; Weimer, R.; Mero, A.; Pasut, G.; Veronese, F. M. Polyoxazoline: Chemistry, Properties, and Applications in Drug Delivery. *Bioconjugate Chem.* **2011**, *22*, 976−986.

(4) Luxenhofer, R.; Han, Y.; Schulz, A.; Tong, J.; He, Z.; Kabanov, A. B.; Jordan, R. Poly(2-oxazoline)s as Polymer Therapeutics. *Macromol. Rapid Commun.* **2012**, *33*, 1613−1631.

(5) Zhang, N.; Luxenhofer, R.; Jordan, R. Thermo-Responsive Poly(2-oxazoline) Molecular Brushes by Living Ionic Polymerization: Kinetic Investigations of Pendant Chain Grafting and Cloud Point Modulation by Backbone and Side Chain Length Variation. *Macromol. Rapid Commun.* **2012**, *213*, 973−981.

(6) Zschoche, S.; Rueda, J.; Boyko, V.; Krahl, F.; Arndt, K.-F.; Voit, B. Thermo-Responsive Nanogels Based on Poly[NIPAAm-graft-(2-alkyl-2-oxazoline)]s Crosslinked in the Micellar State. *Macromol. Chem. Phys.* **2010**, *211*, 1035−1042.

(7) Hruby, M.; Filippov, S. K.; Panek, J.; Novakova, M.; Mackova, H.; Kucka, J.; Vetvicka, D.; Ulbrich, K. Polyoxazoline Thermoresponsive Micelles as Radionuclide Delivery Systems. *Macromol. Biosci.* **2010**, *10*, 916−924.

(8) Yu, G.; Deng, Y.; Dalton, S.; Wang, Q.; Attwood, D.; Price, C.; Booth, C. Micellisation and Gelation of Triblock Copoly(oxyethylene/oxypropylene/oxyethylene), F127. *J. Chem. Soc., Faraday Trans.* **1992**, *88*, 2537−2544.

(9) Wanka, G.; Hoffmann, H.; Ulbricht, W. The Aggregation Behavior of Poly-(oxyethylene)-poly-(oxypropylene)-poly-(oxyethylene)-Block-Copolymers in Aqueous Solution. *Colloid Polym. Sci.* **1990**, *268*, 101−117.

(10) Escobar-Chavez, J. J.; Lopez-Cervantes, M.; Naik, A.; Kalia, Y. N.; Quintanar-Guerrero, D.; Ganem-Quintanar, A. Applications of Thermoreversible Plyronic F-127 Gels in Pharmaceutical Formulations. *J. Pharm. Pharm. Sci.* **2006**, *9*, 339−358.

(11) Li, Y.; Xu, R.; Bloor, D. M.; Holzwarth, J. F.; Wyn-Jones, E. The Binding of Sodium Dodecyl Sulfate to the ABA Block Copolymer Pluronic F127 ($EO_{97}PO_{69}EO_{97}$)-Electromotive Force, Microcalorimetry and Light Scattering Studies. *Langmuir* **2000**, *16*, 10515−10520.

(12) Li, Y.; Xu, R.; Couderc, S.; Bloor, D. M.; Holzwarth, J. F.; Wyn-Jones, E. Binding of Tetradecyltrimethylammonium Bromide to the ABA Block Copolymer Pluronic F127 (EO97 PO69 EO97):

Electromotive Force, Microcalorimetry, and Light Scattering Studies. *Langmuir* **2001**, *17*, 5742−5747.
(13) Li, Y.; Xu, R.; Couderc, S.; Bloor, D. M.; Wyn-Jones, E.; Holzwarth, J. F. Binding of Sodium Dodecyl Sulfate (SDS) to the ABA Block Copolymer Pluronic F127 (EO97PO69EO97): F127 Aggregation Induced by SDS. *Langmuir* **2001**, *17*, 183−188.
(14) Hecht, E.; Hoffmann, H. Interaction of ABA Block Copolymers with Ionic Surfactants in Aqueous Solution. *Langmuir* **1994**, *10*, 86−91.
(15) Hecht, E.; Mortensen, K.; Gradzielski, M.; Hoffmann, H. Interaction of ABA Block Copolymers with Ionic Surfactants: Influence on Micellization and Gelation. *J. Phys. Chem.* **1995**, *99*, 4866−4874.
(16) Konarev, P.; Volkov, V.; Sokolova, A.; Koch, M.; Svergun, D. PRIMUS: a Windows PC-Based System for Small-Angle Scattering Data Analysis. *J. Appl. Crystallogr.* **2003**, *36*, 1277−1282.
(17) Konarev, P. V.; Petoukhov, M. V.; Volkov, V. V.; Svergun, D. I. ATSAS 2.1, a Program Package for Small-Angle Scattering Data Analysis. *J. Appl. Crystallogr.* **2006**, *39*, 277−286.
(18) Spevacek, J.; Dybal, J.; Starovoytova, L.; Zhigunov, A.; Sedlakova, Z. Temperature-induced Phase Separation and Hydration in Poly(N-vinylcaprolactam) Aqueous Solutions: a Study by NMR and IR Spectroscopy, SAXS, and Quantum-chemical Calculations. *Soft Matter* **2012**, *8*, 6110−6119.
(19) Aseyev, V. O.; Tenhu, H.; Winnik, F. M. Temperature Dependence of the Colloidal Stability of Neutral Amphiphilic Polymers in Water. *Adv. Polym. Sci.* **2006**, *196*, 1−85.
(20) Guillermo, A.; Addad, J. P.; Bazile, J. P.; Duracher, D.; Elaissari, A.; Pichot, C. NMR Investigations into Heterogeneous Structures of Thermosensitive Microgel Particles. *J. Polym. Sci., Part B* **2000**, *38*, 889−898.
(21) Hofmann, C.; Schonhoff, M. Dynamics and Distribution of Aromatic Model Drugs in the Phase Transition of Thermoreversible Poly(N-isopropylacrylamide) in Solution. *Colloid Polym. Sci.* **2012**, *290*, 689−698.
(22) Kriz, J.; Dybal, J. Cooperative Preassociation Stages of PEO−PPO−PEO Triblock Copolymers: NMR and Theoretical Study. *J. Phys. Chem. B* **2010**, *114*, 3140−3151.
(23) Loh, W.; Teixeira, L. A. C.; Lee, L. T. Isothermal Calorimetric Investigation of the Interaction of Poly(N-isopropylacrylamide) and Ionic Surfactants. *J. Phys. Chem. B* **2004**, *108*, 3196−3201.
(24) Abuin, E.; Leon, A.; Lissi, E.; Varas, J. M. *Colloids Surf., A* **1999**, *147*, 55−65.
(25) Nambam, J. S.; Philip, J. Effects of Interaction of Ionic and Nonionic Surfactants on Self-Assembly of PEO−PPO−PEO Triblock Copolymer in Aqueous Solution. *J. Phys. Chem. B* **2012**, *116*, 1499−1507.
(26) Niemiec, A.; Loh, W. Interaction of Ethylene Oxide−Propylene Oxide Copolymers with Ionic Surfactants Studied by Calorimetry: Random versus Block Copolymers. *J. Phys. Chem. B* **2008**, *112*, 727−733.
(27) Cardoso da Silva, R.; Olofsson, G.; Schillen, K.; Loh, W. Influence of Ionic Surfactants on the Aggregation of Poly(Ethylene Oxide)−Poly(Propylene Oxide)−Poly(Ethylene Oxide) Block Copolymers Studied by Differential Scanning and Isothermal Titration Calorimetry. *J. Phys. Chem. B* **2002**, *106*, 1239−1246.
(28) Almgren, M.; Brown, W.; Hvidt, S. Self-Aggregation and Phase Behavior of Poly(ethylene oxide)-poly(propylent oxide)-poly(ethylene oxide) Block Copolymer in Aqueous Solution. *Colloid Polym. Sci.* **1995**, *273*, 2−15.
(29) Almgren, M.; Garamus, V. M.; Asakawa, T.; Nan, J. Contrast Variation SANS Investigation of Composition Distributions in Mixed Surfactant Micelles. *J. Phys. Chem. B* **2007**, *111*, 7133−7141.
(30) Garamus, V. M. Formation of Mixed Micelles in Salt-Free Aqueous Solutions of Sodium Dodecyl Sulfate and $C_{12}E_6$. *Langmuir* **2003**, *19*, 7214−7218.
(31) Cabane, B.; Duplessix, R. Organization of Surfactant Micelles Adsorbed on a Polymer Molecule in Water: a Neutron Scattering Study. *J. Phys. (Paris)* **1982**, *43*, 1529−1542.
(32) Süss, D. C.; Cohen, Y.; Talmon, Y. The Microstructure of the Poly(ethylene oxide)/Sodium Dodecyl Sulfate System Studied by Cryogenic-Temperature Transmission Electron Microscopy and Small-Angle X-ray Scattering. *Polymer* **1995**, *36*, 1809−1815.
(33) Itri, R.; Amaral, L. C. Distance Distribution Function of Sodium Dodecyl Sulfate Micelles by X-ray Scattering. *J. Chem. Phys.* **1991**, *95*, 423−427.
(34) Cattoz, B.; de Vos, W. M.; Cosgrove, T.; Crossman, M.; Prescott, S. W. Manipulating Interfacial Polymer Structures through Mixed Surfactant Adsorption and Complexation. *Langmuir* **2012**, *28*, 6282−6290.
(35) Santos, S. F.; Zanette, D.; Fischer, H.; Itri, R. A Systematic Study of Bovine Serum Albumin (BSA) and Sodium Dodecyl Sulfate (SDS) Interactions by Surface Tension and Small Angle X-ray Scattering. *J. Colloid Interface Sci.* **2003**, *262*, 400−408.
(36) Almgren, M.; Gimel, J. C.; Wang, K.; Karlsson, G.; Edwards, K.; Brown, W.; Mortensen, K. SDS Micelles at High Ionic Strength. A Light Scattering, Neutron Scattering, Fluorescence Quenching, and CryoTEM Investigation. *J. Colloid Interface Sci.* **1998**, *202*, 222−231.

Langmuir

Article

pubs.acs.org/Langmuir

Self-Assembly Thermodynamics of pH-Responsive Amino-Acid-Based Polymers with a Nonionic Surfactant

Anna Bogomolova,[†] Sandro Keller,[‡] Johannes Klingler,[‡] Marian Sedlak,[§] Dmytro Rak,[§] Adriana Sturcova,[†] Martin Hruby,[†] Petr Stepanek,[†] and Sergey K. Filippov*[,†]

[†]Institute of Macromolecular Chemistry AS CR, v.v.i, 162 06 Prague, Czech Republic

[‡]Molecular Biophysics, University of Kaiserslautern, 67663 Kaiserslautern, Germany

[§]Institute of Experimental Physics SAS, 040 01 Kosice, Slovak Republic

Supporting Information

ABSTRACT: The behavior of pH-responsive polymers poly(*N*-methacryloyl-L-valine) (P1), poly(*N*-methacryloyl-L-phenylalanine) (P2), and poly(*N*-methacryloylglycyne-L-leucine) (P3) has been studied in the presence of the nonionic surfactant Brij98. The pure polymers phase-separate in an acidic medium with critical pH_{tr} values of 3.7, 5.5, and 3.4, respectively. The addition of the surfactant prevents phase separation and promotes reorganization of polymer molecules. The nature of the interaction between polymer and surfactant depends on the amino acid structure in the side chain of the polymer. This effect was investigated by dynamic light scattering, isothermal titration calorimetry, electrophoretic measurements, small-angle neutron scattering, and infrared spectroscopy. Thermodynamic analysis revealed an endothermic association reaction in P1/Brij98 mixture, whereas a strong exothermic effect was observed for P2/Brij98 and P3/Brij98. Application of regular solution theory for the analysis of experimental enthalpograms indicated dominant hydrophobic interactions between P1 and Brij98 and specific interactions for the P2/Brij98 system. Electrophoretic and dynamic light scattering measurements support the applicability of the theory to these cases. The specific interactions can be ascribed to hydrogen bonds formed between the carboxylic groups of the polymer and the oligo(ethylene oxide) head groups of the surfactant. Thus, differences in polymer−surfactant interactions between P1 and P2 polymers result in different structures of polymer−surfactant complexes. Specifically, small-angle neutron scattering revealed pearl-necklace complexes and "core−shell" structures for P1/Brij98 and P2/Brij98 systems, respectively. These results may help in the design of new pH-responsive site-specific micellar drug delivery systems or pH-responsive membrane-disrupting agents.

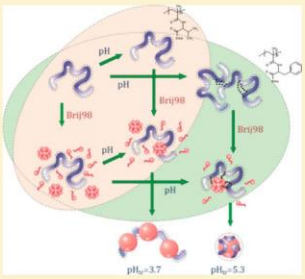

INTRODUCTION

pH-sensitive polymers are a new class of macromolecules that are able to change their conformation and solution properties and to undergo a controlled phase separation in response to changes in surrounding conditions (i.e., pH of the environment) .[1−3] These polymers have been widely developed recently because of their specific properties and their potential application as site-specific pH-responsive drug delivery systems.[4−14] It is well-known that each tissue in the human digestive system possesses its unique pH value. For example, the pH is 6.0−7.0 in the saliva, 4.0−6.5 in the upper stomach, 1.5−4.0 in the lower stomach, 7.0−8.5 in the duodenum, and 4.0−7.0 in the small intestine.[15] Moreover, tumors and inflamed cells are generally more acidic (pH ca. 6.5) due to the production of lactic acid and other acids under hypoxic conditions than normal tissues (pH 7.4).[10] Thus, creation of pH-responsive carriers would be very helpful for various biological applications.

Generally, polymers that phase separate from aqueous solution in response to an external pH change contain hydrophobic moieties, which drive phase separation and either weak bases (e.g., 2-diethylaminoethyl, which also introduces thermoresponsivity) or weak acids (e.g., carboxylic acid). An important parameter of a pH-sensitive polymer is its pK_a value. Ionizable polymers with a pK_a value between 4 and 8 are candidates for pH-responsive systems.[2,9] Polymers with weak base character deionize above their pK_a and ionize below it, causing an increase in hydrophilicity and electrostatic repulsion of the polymer molecules, whereas the opposite holds for polymers with weak acid character.[11] When the degree of ionization decreases, hydrophobic interactions begin to prevail. The pH-dependent protonation/deprotonation mechanism of the weak base/acid regulates the overall polarity (charge density) of the polymer and, together with Coulombic repulsion of identically charged chains, leads to pH-responsiveness.[16] The pK_a value of a polymer can be adjusted by controlling the molecular weight of the polymer,[16] changing

Received: August 5, 2014
Revised: September 5, 2014
Published: September 5, 2014

ACS Publications © 2014 American Chemical Society

the chemical environment of the ionizable groups, or copolymerizing monomers with different pK_a values.[4,6,7]

Block copolymers with one pH-sensitive building block have been extensively developed over the recent years. The main feature of these copolymers is their ability to form micelles at certain conditions. The physicochemical properties of such micelles are controlled by the mass ratio of hydrophobic and hydrophilic blocks.[2] Hydrophobic blocks aggregate to form a dense core for solubilization and protection of drug payload, whereas hydrophilic shell mainly confers aqueous solubility and steric stability to the ensembles. There are considerable numbers of reviews on the controlled release of hydrophobic drugs from block copolymer micelles with pH-sensitive blocks in aqueous solutions.[2,4−8,12−14] Conventionally, all pH-sensitive block copolymers can be categorized into several groups: thermosensitive−pH-sensitive blocks;[17−21] two pH-sensitive blocks with different pK_a values;[22−24] hydrophilic−pH-sensitive blocks;[25,26] hydrophobic−pH-sensitive blocks,[27,28] or even triblocks featuring some combination of the above-mentioned blocks.[29,30]

Modification of the chemical environment of ionizable groups is another tool for adjustment of pH sensitivity. The most frequently used pH-sensitive acidic polymers are polyacrylates. Among them, poly(acrylic acid) (PAA) and its derivative poly(methacrylate acid) (PMAA), which have pK_a values of about 4−5, are the most representative. The introduction of different substituents on the polymeric chain allows variation of the physicochemical and biological properties of polymers toward hydrophobicity, biocompatibility, or swelling behavior.[15,31−39] Modification can be performed at the carboxylic group of the side chain or by the variation of an alkyl group at C═C bond. By the second method, polyethylacrylic, polypropylacrylic, and polybutylacrylic acids and their copolymers can be obtained, which have been found to be pH-responsive membrane-disrupting permeabilizers.[31−35] Both acrylic esters (amides) obtained by the first type of modification and their copolymers are developed more intensively.[15,35−39] For example, the copolymer of methyl methacrylate and acrylic acid, Eudragit S 100, is already widely used for intestine/colon delivery, because it is insoluble in the acidic milieu of the stomach, while it is readily dissolved in the neutral to mildly alkaline environment of the intestine.[39] The presence of relatively hydrophobic substituents such as hydrophobic amino acids in side chains of every monomer unit allows more accurate adjustment of hydrophobicity. α-nitrogen-attached amino acids preserve the acidic character of the polymer molecule and create a possibility for variation in amino acid substituent as an additional tool for adjusting polymer hydrophobicity. Moreover, the introduction of amino acids can also increase the biocompatibility of a polymer. In the present work, we investigate, from a thermodynamic point of view, how different substituents in the side chain of a polymer affect the hydrophobicity of the entire polymer and solution behavior in the presence of the nonionic surfactant Brij98.

The presence of Brij98 in solution is crucial for two reasons. First, the surfactant promotes the rearrangement of polymer molecules, resulting in well-defined particles with low polydispersity. Second, it stabilizes the resulting particles from the following separation tendency and in some occasions can be considered as a model system for nonionic amphiphilic drugs.

Thus, our investigation is devoted to pH-sensitive polymers on the basis of polymethacrylic acids in the backbone and amino acid residues in the side chains and to the characterization of their interactions with the nonionic surfactant Brij98. To this end, we have analyzed three polyamino acids, namely, poly(*N*-methacryloyl-L-valine), poly(*N*-methacryloyl-L-phenylalanine) and poly(*N*-methacryloyl glycyl-L-leucine). Bearing in mind the differences in hydrophobicity of the amino acid residues in polymers, we expected some extent of variation in their behavior with Brij98. Nanoparticles of a narrow size distribution have been obtained and display reversible transition behavior with increasing or decreasing acidity.[40,41] However, one important question remains unanswered: how does the variation in amino acid structure influence the properties of formed nanoparticles? Deeper understanding of the intermolecular interactions between the polymer and the surfactant is required for complete characterization of the system and a prediction of the shape and features of the nanoparticles below the transition pH. We continued our investigation with an objective to characterize the type of interaction between polymer and surfactant and to shed light to the physical processes that are in charge of nanoparticle formation. Isothermal titration calorimetry (ITC), electrophoretic light scattering, small-angle neutron scattering measurements (SANS), and infrared spectroscopy (FTIR) were used for that purpose.

MATERIALS AND METHODS

Materials. The polymers used in the present study were synthesized according to the scheme published previously.[40] Initially, each particular amino acid was methacrylated by a modification procedure followed by a polymerization reaction. The chemical structures and molecular characteristics (molecular weight of the polymers, M_w, and molecular weight of the corresponding polymer unit, MM_{unit}, number of units, N_{unit}, and transition pH value for the pure polymer, pH_{tr}) of polymers are indicated in Scheme 1 and Table 1.

Scheme 1. Chemical structure of Poly(*N*-methacryloyl-L-valine) (P1), Poly(*N*-methacryloyl-L-phenylalanine) (P2), and Poly(*N*-methacryloyl glycyl-L-leucine) (P3) (sodium salt forms)

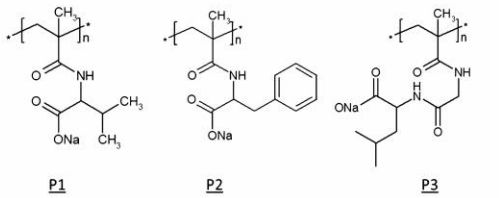

Water was deionized with a Millipore Milli-Q water purification system. The nonionic surfactant Brij98 with the chemical structure $C_{18}EO_{20}$−OH was purchased from Sigma-Aldrich Ltd (Prague, Czech

Table 1. Molecular Characteristics of the Polymers (c = 0.2 w%)

	P1	P2	P3
name	poly(*N*-methacryloyl-L-valine)	poly(*N*-methacryloyl-L-phenylalanine)	poly(*N*-methacryloylglycyl-L-leucine)
M_w	78 000	29 000	30 000
MM_{unit}	207	255	278
N_{unit}	377	113	108
pH_{tr} (pK_a)	3.7	5.3	3.4

Republic). All other chemicals were used without additional purification. Polymer solutions were obtained by dissolving the sodium salt form of the polymer in deionized water.

General Experimental Procedure. Generally, two kinds of experiments were performed. First, acid titrations of 1:1 mixtures of polymer and surfactant were conducted by consecutive addition of small amounts of 0.2 M hydrochloric acid. Second, a solution of pure polymer was adjusted to the desired pH and titrated with a surfactant solution of the same pH. All experiments were performed at 25 °C.

The latter preparation method was chosen for the ITC analysis to avoid undesirable effects of protonation. All concentrations are given in weight percent.

Methods. *Dynamic Light Scattering.* The pH dependency of the hydrodynamic radius of particles, R_h, and the scattering intensity, I_s, were measured at a scattering angle of $\theta = 173°$ with a Zetasizer Nano-ZS instrument, model ZEN3600 (Malvern Instruments, U.K.). The DTS (Nano) program was used to evaluate the data. It provides intensity-, volume-, and number-weighted R_h distribution functions $G(R_h)$. The volume-weighted value of the apparent R_h was chosen to monitor the pH-dependent changes in the system. Three measurements were performed after each pH change.

If not otherwise stated, all measurements were conducted with a polymer and surfactant concentration of 0.2 wt % each (0.07 mM for polymer; 1.74 mM for surfactant) in water, and all solutions were filtered through a 0.45 μm PVDF syringe filter before measurement. The molecular characteristics of the polymers are presented in Table 1.

Zeta-Potential Measurements. Electrophoretic mobility was measured with the same Zetasizer Nano-ZS instrument used for dynamic light scattering measurements. The DTS software was used to compute the zeta-potential through the Henry equation (eq 1). The electrophoretic mobility of a spherical particle is related to the zeta-potential by

$$U_E = \frac{\zeta 2\varepsilon_p f(ka)}{3\eta} \tag{1}$$

where ε, is the dielectric constant of the sample, η is the dynamic viscosity (Pa s), and ζ is the zeta-potential (V); $f(ka)$ is Henry's function, which is calculated within the approximation of Smoluchowski ($f(ka) = 1.5$) for aqueous solutions with moderate ionic strength. Each mobility value presented in the text is an average of 15 up to 100 values.

Isothermal Titration Calorimetry. Microcalorimetric experiments were performed using a MicroCal VP-ITC isothermal titration calorimeter (GE Healthcare, Uppsala, Sweden). The experiment was performed with consecutive injections of 10 or 15 μL of a concentrated surfactant solution into the calorimeter cell, which contained 1.4 mL of a polymer (20 mg/mL) or water solution. In total, the injection syringe contained 300 μL surfactant solution, the stirring speed was 300 rpm, and the time between injections was 5 min. Automated baseline adjustment and peak integration were accomplished using NITPIC.[42] The molar reaction heat per injection was obtained by dividing the experimentally measured reaction heat by the molar amount of surfactant added. The final curves display the molar reaction heat as a function of total surfactant concentration in the calorimeter sample cell. Experimental data were fitted according to regular solution theory by nonlinear least-squares fitting using a spreadsheet program based on Microsoft Excel with the Solver add-in.[43]

Small-Angle Neutron Scattering. SANS experiments were performed at FRM II on the KWS-2 beamline. Measurements were made on a 128 × 128 multidetector (pixel size 0.5 cm × 0.5 cm) using a nonpolarized, monochromatic (wavelength λ set by a velocity selector) incident neutron beam collimated with rectangular apertures for three sample-to-detector distances, namely 2, 8, and 24 m (with λ = 0.6 nm). With this setup, the investigated q-range was 0.02−3 nm^{-1}. In all cases, two-dimensional scattering patterns were isotropic and were azimuthally averaged resulting in the dependence of the scattered intensity $I_s(q)$ on q. The curves were corrected for background scattering and detector efficiency. The intensities of neutron scattering are given in absolute units. The experiment was conducted for the polymer/surfactant solution in H_2O with a mass ratio of components 1:1.

Fourier transform Infrared (FTIR) Spectroscopy. FTIR spectra were collected on a Thermo Nicolet 6700 Advanced Gold spectrometer equipped with a DLaTGS detector with a KBr window. Samples were measured on a MIRacle ATR unit (Pike) with a Si/ZnSe prism. Spectral resolution was 4 cm^{-1}. ATR spectra were processed by ATR correction. In order to avoid strong contributions from H_2O to the IR spectra, all measurements were done in D_2O solutions. Spectra of D_2O were digitally subtracted. Polymer solutions were prepared by dissolving the sodium salt form of the polymer in D_2O. The same solutions were then prepared with the addition of surfactant Brij 98. Compounds were taken in concentration of 2 wt % to achieve the best resolution of experiment. The experiment followed to the first experimental procedure, when 0.1 M DCl was sequentially added to the mixed solution. Titration of pure polymer solution was performed with the same titration step like for the mixed solution for the comparison.

THEORY

Regular solution theory was applied for the analysis of the experimental ITC data.[44,45] This model is based on the assumption of uniform complex formation. Thus, the addition of one component to the other leads to the formation of one type of complexes irrespective of their mixing ratios. Further addition of a component promotes a rearrangement of the existing complexes. The process takes place until the full exhaustion of the added component.

The general equation for the regular solution theory can be written as

$$q(i) = N_s\Delta H = (N_s - N_{mic,s})\Delta H_{mic,s} + \frac{N_p N_s \beta RT}{N_p + N_s} \tag{2}$$

where $q(i)$ is the absolute heat of reaction; ΔH is the enthalpy of the interaction; N_s, $N_{mic,s}$, and N_p are the total molar amount of surfactant injected, the molar amount of surfactant injected in micellar form, and the total molar amount of polymer in the calorimetrical cell, respectively. Then, $X_s = N_s/(N_s + N_p)$ is the mole fraction of surfactant, and $X_s = N_p/(N_s + N_p)$ is the mole fraction of polymer in the assemblies. The value $\Delta H_{mic,s}$ is the enthalpy of surfactant micellization. Since the value $\Delta H_{mic,s}$ is very low for the surfactant Brij98, as can be seen from the blank titration (Figure 2b), and since cmc(Brij98) = 0.02 mM is also very low, we can rewrite eq 2 as

$$q(i) = N_s\Delta H = \frac{N_p N_s \beta RT}{N_p + N_s} \tag{3}$$

where the term βRT corresponds to the mixing excess enthalpy and defines the difference between the experimental enthalpy and the value expected for ideal mixing.

Directly from the experiment, one can obtain the value of the normalized heat of injection:

$$Q(i) = \frac{q(i)}{\Delta V(i) c^{syr}} + Q_{dil} \tag{4}$$

where $\Delta V(i)$ is the injected volume; c^{syr} is the concentration of the added component (component in the syringe); Q_{dil} is the normalized heat of dilution. Insertion of eq 3 into eq 4 yields the fitting function, with β and a scaling factor for the molar amount of polymer, X, as fitting parameters.

RESULTS

DLS experiments were conducted first to obtain overall information on the polymers under investigation and mixtures of polymer/Brij98 solutions. The results for pH dependences of the scattered light intensity (I_s) and the hydrodynamic radius

dx.doi.org/10.1021/la5031262 | Langmuir 2014, 30, 11307−11318

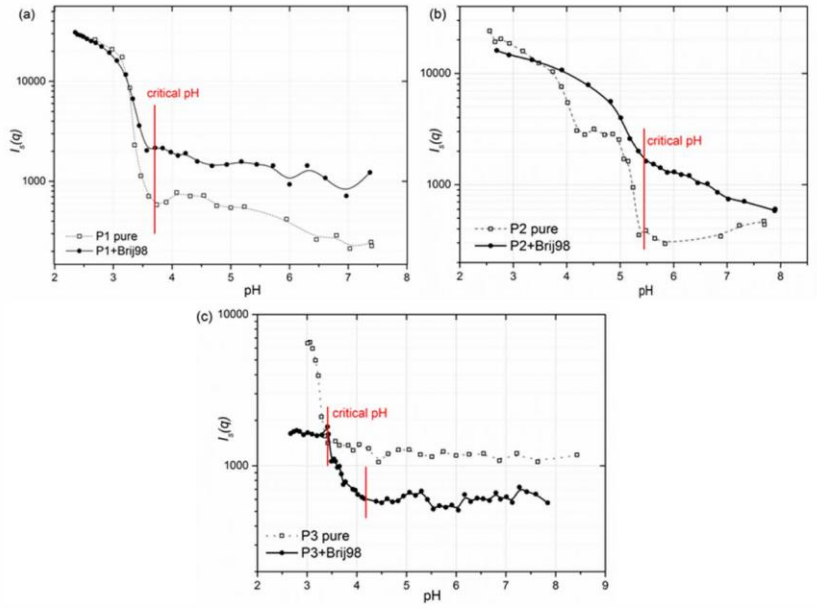

Figure 1. pH dependence of the scattered light intensity $I_s(q)$ (θ = 173°) for solutions of (a) polymer P1, (b) polymer P2, and (c) polymer P3. Open squares, pure polymers; filled circles, polymer/Brij98 mixture.

(R_h) are shown in Figure 1 and Supporting Information Figure S1.

The scattered intensity of pure polymers displays a sharp transition upon decreasing pH value. The value of the corresponding critical pH is characteristic of the polymeric structure and eventually of the type of amino acid residue: 3.7 for the polymer P1 (valine), 5.5 for the P2 (phenylalanine), and 3.4 for the polymer P3 (glycine-leucine). While the transition for the polymers P1 and P3 is a one-step process, the polymer P2 exhibits two stages of transition. Moreover, the critical pH remains unchanged in the cases of P1/Brij98 and P2/Brij98 with respect to the critical pH value for the pure polymer solutions, while it is shifted to a value of 4.1 for the mixture P3/Brij98. Further data analysis for the polymer/Brij98 mixture revealed new features. The data for systems P1/Brij98 and P3/Brij98 display the sharp transition of scattered intensity with decreasing pH similar to the respective pure polymers. At the same time, the transition for the system P2/Brij98 becomes smoother; some differences between the pure polymer and the polymer/Brij98 system could be detected in spite of similarity in critical pHs. These results imply the complex mechanism of interaction between the polymers and the surfactant. It is well-known that protonated polyalkylacrylic acids easily form hydrogen bonds in water environment.[46,63,64] Introduction of amino acids in the polymer chain has two consequences: it enhances hydrophobicity and keeps the carboxylic group accessible for hydrogen bonding (There are oligo(ethylene oxide groups) in the hydrophilic part of Brij98, which can also form hydrogen bonds). The protonated form of poly(acrylic acid) readily assembles into strong insoluble complexes with poly(ethylene oxide) due to multiple zipper-like hydrogen bonding. Similarly, the protonated form of polymethacrylic acid was found to form complexes with poly(ethylene oxide) in poly(methacrylic acid)-*block*-poly(ethylene oxide) copolymers.[47−49] However, in the case of the polymers P1, P2 and P3 the situation is sterically more complex. Thus, one can suggest the type of polymer/surfactant interaction is a result of the mutual influence of several contributions: the ability of each particular amino acid to the formation of inter-, intramolecular hydrogen bonds, the predominance of hydrophobic intermolecule interactions on hydrogen bonding and the nature of surfactant which affects the strength and efficiency of hydrophobic polymer/surfactant interactions.

The pH dependence of the hydrodynamic radius additionally reveals the impact of some particular amino acid on the solution behavior of polymer. For each polymer/Brij98 system at initial pH, the presence of ca. 50 nm particles could be detected, along with 4 nm nanoparticles. The size of the smaller particles fully corresponds to the size of pure Brij98 micelles. Therefore, one can associate the 50 nm particles with the polyelectrolyte slow mode effect occurring traditionally in low salt polyelectrolyte solutions irrespective of the concrete chemical structure of particular polymer.[50] When the salt concentration is low, dynamic light scattering experiments show two relaxation times in the correlation functions. This behavior is denoted as "extraordinary" behavior or slow mode dilemma, described and discussed in many instances in the past years.[51−59] As the salt concentration was increasing above a certain characteristic concentration, c_s*, the correlation functions become single exponential. Below the critical pH, only one sort of particles is detected; 21 nm for the polymer P1, 13 nm for the polymer P2, and almost unchanged 5 nm particles for the polymer P3 were found (Supporting Information Figure S1).

For deeper investigation of the interactions between the ionic pH-sensitive polymers and the nonionic surfactant, ITC

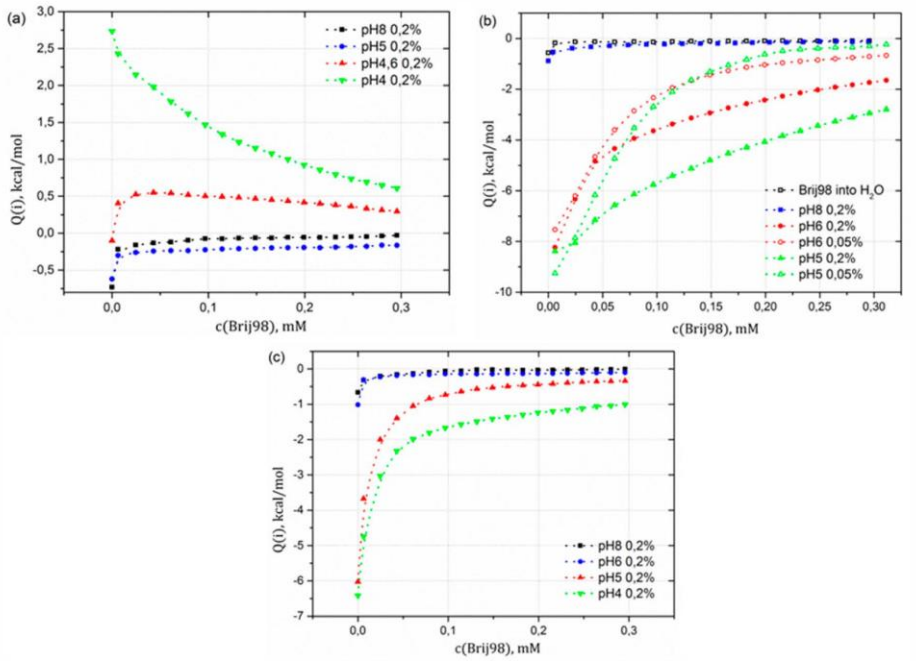

Figure 2. ITC curves for the titration of the polymers: (a) P1 solution, (b) P2 solution, and (c) P3 solution with surfactant Brij98 at different concentrations and pH values (T = 25 °C).

experiments were performed. The isotherms obtained for all three polymers are shown in Figure 2.

ITC data confirm the preliminary conclusions drawn from the DLS part about the different manner of interactions between polyamino acids and nonionic Brij98. Figure 2 illustrates the exothermic effect of the interaction between Brij98 and the polymers P2 and P3 and the endothermic effect for the polymer P1. The pattern obtained from titration of P1 with Brij98 is typical of the interactions of nonionic polymers with ionic surfactants (Figure 2a).[60,61] These interactions are characterized by two processes; the first endothermic process is followed by exothermic process and finally merges with the curve for blank titration of Brij98 into water. By contrast, the behavior of the polymers P2 and P3 cannot be interpreted unambiguously. Only one process was observed in the isotherms (Figure 2b, c). This behavior might have several reasons: either polymeric micelles[62,63] or mixed micelles of surfactant and polymer are formed,[64,65] or a reaction between polymer and surfactant through the formation of some specific bonds takes place. We can exclude the formation of polymeric micelles in the system due to the absence of any uniform particles on the DLS data at pH 6 and 5 for the pure polymer P2 and at pH 5 and 4 for the pure polymer P3 and on the basis of the chemical structure of the polymers (Supporting Information Figure S1). Other possible reasons will be discussed later.

It is worth noting that at initial pH all systems behave similarly to the titration of pure Brij98 into water (Figure 2b). There are no interactions observed. The same situation repeats at pH 5 for the polymer P1; only at pH 4.6 are the interactions detectable (Figure 2a). The situation is similar for polymer P3, where at pH 5 an onset of interactions is observed (Figure 2c). One can attempt to explain that behavior in terms of hydrophobicity and hydrogen bonding. Then the hydrophobicity should rise in the order P1 < P3 < P2. The hydrogen bonds can be formed only in the protonated form of polymer; therefore, the degree of protonation has been calculated for each particular system at each experimental condition (Table

Table 2. Physicochemical Characteristics of Polymers at Different pHs

polymer	pH	C(Pol), mM	C(Pol), wt %	degree protonation, α' %
P1	6.8	0.026	0.2	5
	6	0.026	0.2	12
	5	0.026	0.2	24
	4.6	0.026	0.2	36
	4	0.026	0.2	41
P2	6	0.07	0.2	12
		0.035	0.1	19
		0.0175	0.05	24
	5	0.07	0.2	38
		0.035	0.1	45
		0.0175	0.05	47
P3	6	0.07	0.2	20
	5.1	0.07	0.2	33
	4.9	0.0165	0.05	39
	4.1	0.07	0.2	53
	4.1	0.0165	0.05	59

Table 3. Fitting Parameters for the Systems Polymer/Brij98

polymer	C(Pol), wt %	pH	degree protonation, α', %	X	β	βRT, kcal/mol	Q_{cip}, cal/mol
P1	0.2	6.8	5	3.6	−0.4	−0.24	−34
	0.2	6	12	6.7	−0.2	−0.12	−246
	0.2	5	24	9.3	−0.3	−0.18	−148
	0.2	4.6	36	10.0	1.2	0.71	250
	0.2	4	41	13.4	4.4	2.61	19
P2	0.2	6	12	1.5	−11.5	−6.8	−1690
	0.1		19	4.9	−12.2	−7.2	−675
	0.05		24	5.2	−13.4	−7.9	−328
	0.2	5	38	5.5	−12.7	−7.5	−909
	0.1		45	5.9	−14.3	−8.5	−510
	0.05		47	6.6	−18.4	−10.9	569
P3	0.2	6	20	0.8	−0.5	−0.3	−115
	0.2	4.9	33	0.4	−12.7	−7.52	−294
	0.05	5.1	39	0.9	−8.1	−4.8	−158
	0.2	4	53	0.6	−10.8	−6.4	−1115
	0.05	4	59	5.9	−5.0	−2.96	−191

2). The degree of protonation was calculated according to the equation:

$$\alpha' = \frac{n_{COOH}}{n_{COO^-}} \times 100\%$$

where α' is the degree of protonation; n_{COOH} is the number of moles of a polymer in the protonated state, as calculated from the amount of hydrochloric acid added to adjust the pH of system to a certain value; n_{COO^-} is the number of moles of a polymer in the charged state.

From Table 2, one can define the degree of protonation at the pH where the interactions between the compounds were observed: 36% at pH = 4.6 for P1, 12% at pH = 6 for P2, and 33% at pH = 5 for P3. It is well-known that the protonated form of ionic polymers is more hydrophobic than the charged one. Then how to explain the highest hydrophobicity of polymer at the lowest degree of protonation or vice versa? The formation of inter- and intramolecular hydrogen bonds has to be taken into account. These two contributions, hydrophobicity and hydrogen bonds, act simultaneously in a similar way by decreasing the solubility of the polymer in the solution and promote polymer/surfactant interactions. It is almost impossible to provide full picture of interactions in the systems, but we can try to figure out the dominant ones for each of them.

To provide further information about the interactions in the systems, a fit of the experimental ITC curves was performed. Regular solution theory was chosen for this purpose. This theory has already been successfully applied to systems consisting of nonionic surfactants and amphipol molecules.[65,45] Fitting results are shown in Table 3 and Figure 3.

The parameter β reflects the nonideality of mixing. β-values in the range of -10 to +10 have been reported in the literature, with strongly negative values being indicative of specific interactions.[45] In our case, we determined such strongly negative values β for the systems P2/Brij98 and P3/Brij98. Thus, one can assume the presence of specific interaction in these systems. Moreover, the fitting results for the system P1/Brij98 yielded only low absolute values of β indicating near-ideal mixing. The comparison of the fitting results for β with the value of the degree of protonation provides new insights. For the system P1/Brij98, we observe a small increase of β with

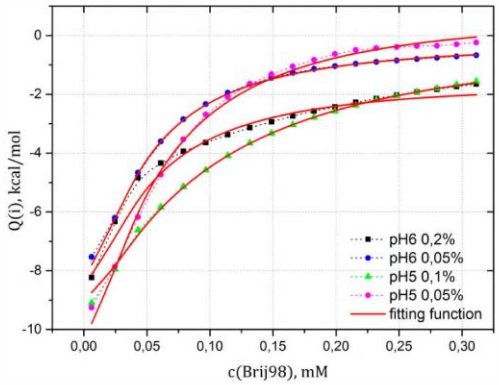

Figure 3. ITC curve for the titration of the polymer P2 by surfactant Brij98 at different concentrations and pH values.

an increasing degree of protonation. At the same time, an increase in the degree of protonation for system P2/Brij98 led to a reduction in β to even more negative values. We interpret this behavior as a manifestation of specific interactions that become more pronounced. The behavior of β in the system P3/Brij98 is more complex and seems to be a combination of the previous two; nevertheless, the large variability in the fitted values complicates a detailed analysis.

To confirm the assumptions deduced from the previous two parts, electrophoretic measurement has been conducted. Zeta-potential obtained from electrophoretic measurement is very sensitive to the surface charge of the polymer/surfactant complexes and therefore could specify the particular structure of each polymer system. The electrophoretic measurement was performed in both experimental regimes, which were mentioned above in Materials part. The second regime is beneficial in some respects. The addition of hydrochloric acid results in the formation of NaCl in aqueous environment and can change the ionic strength of the solution. At the same time, the performance of the experiment at a fixed pH allows to avoid this effect and, moreover, to compare in direct manner the

dx.doi.org/10.1021/la5031262 | Langmuir 2014, 30, 11307−11318

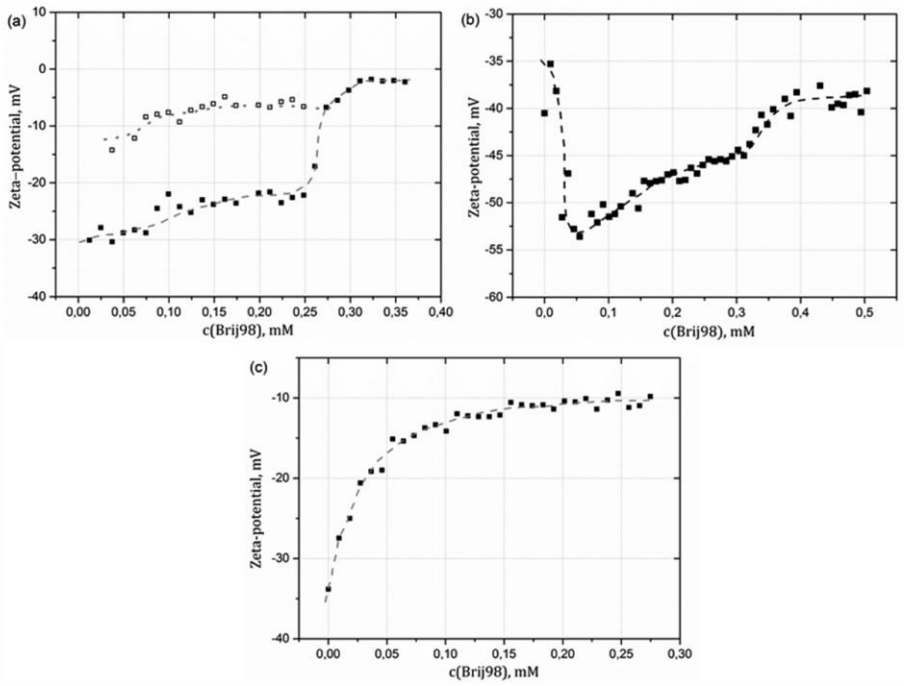

Figure 4. Zeta potential values as a function of the surfactant concentration: (a) P1, pH = 5; (b) P2, pH = 6; P3, pH = 5. For the zeta potential data (a), the open squares are first peak and filled squares are second peak as a function of the surfactant concentration.

results from ITC with electrophoretic measurements. Results obtained from electrophoretic experiments are presented in Figure 4 and Supporting Information Figure S2. The pH for each experiment was chosen above the pH_{tr} but low enough to allow for polymer/surfactant interactions: pH = 5 for P1/Brij98 and P3/Brij98 and pH = 6 for P2/Brij98.

At initial conditions, in the pure polymer solution, the value of zeta-potential corresponds to the charge of pure polymer aggregates, −(30−40) mV. The first few injections of surfactant up to 0.025 mM (cmc of Brij98) result in the formation of surfactant micelles which causes a change in the zeta-potential of system. This change is either positive (P1, P3) or negative (P2). Nevertheless, further addition of surfactant increases the value of the zeta-potential until it reaches a plateau. Interestingly, the final value of zeta-potential is not a constant and strongly depends on the system: −3 mV for P1/Brij98 system, −38 mV for P2/Brij98, and −10 mV for P3/Brij98. Comparison of the final zeta-potentials of the surfactant titration with those found at the same pH in the acid titration (Supporting Information Figure S2) showed a good convergence of results. Some deviations in the values can be explained by the kinetics of complex formation or by the effect of ionic strength as mentioned above.

The addition of surfactant into the polymer solution of P1 at pH = 5 leads to the appearance of two signals in the zeta-potential plot. These signals could be attributed to aggregates of pure polymer (ca. −30 mV) and polymer/surfactant complexes (ca. −10 mV). Finally, the two signals merge at the Brij98 concentration 0.27 mM and particles with surface charge of −3 mV form. In contrast, one can detect only one signal for the polymer solution P2 in the presence of Brij98. The value of that mode (ca. −50 mV) corresponds to the signal of pure aggregates of the polymer (ca. −55 mV at pH = 6 (Supporting Information Figure S3)). However, the first few points (ca. −35 mV) on the curve deviate from the general tendency. Thus, one can assume that even a small amount of surfactant (free molecules of surfactant) results in a complete reorganization of the polymer aggregates and complex mixed structures are formed. Hereinafter, when the first rearrangement process in the polymer is completed, the charge of the structures is continuously increasing during the titration, and this fact confirms the applicability of regular solution theory used to the analysis of ITC data. Interestingly, whereas the polymer aggregates in the solution of P1 are continuously transforming to polymer/surfactant complexes, data from the titration of solution P2 suppose the formation of highly charged polymer/surfactant complexes. Different mechanism of complex formation can be assumed. The titration of the polymer solution P3 by Brij98 displays a similar behavior as the titration of P2 by Brij98. The zeta-potential continuously grows upon addition of Brij98, but no deviation in negative side has been observed.

It has to be noted that while the interaction between polymers and surfactant (P2/Brij98 at pH = 6 and P3/Brij98 at pH = 5) has been demonstrated by ITC, in the system P1/Brij98 the presence of any interactions at pH = 5 is still a question under consideration. No significant heat effect was shown from ITC experiments but, nevertheless, the zeta-potential in the system reaches almost zero through the

surfactant titration. This may be explained by covering of polymer charges by surfactant micelles.

Previous results from the ITC and electrophoretic measurements reveal differences in the mechanism of complex formation between different types of polymers and surfactant. That fact necessitates performing a structural analysis of the systems and assessing the structural variations in the complexes.

The solutions of P1/Brij98 and P2/Brij98 at pH = 3.5 were chosen for SANS measurements. SANS and SAXS techniques served as a powerful tool for analyzing nanoparticle structures and suspensions of both concentrated and diluted polymer solutions.[66−68] Figure 5 shows the scattering vector q

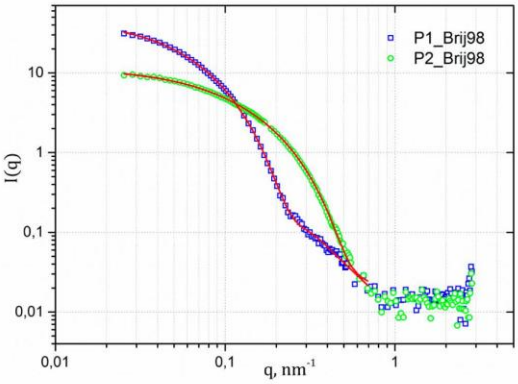

Figure 5. Scattered intensity I_s as a function of the scattering vector q at pH = 3.5 for P1/Brij98 and P2/Brij98 samples. Solid lined are fits.

dependence of the intensity of neutron scattering I_s for these systems. Both curves display a plateau at $q > 0.8$ nm^{-1}, which can be explained by the presence of low-molecular-weight compounds in the solution compare to the pure solvent. Besides that, a small upturn is visible at $q = 0.4$ nm^{-1} for the P1/Brij98 system. For P2/Brij98, one can neglect the interparticle interactions in system, so $I(q) = P(q)$, where $P(q)$ is a nanoparticle form factor. We were able to fit the experimental curve for P2/Brij98 by the spherical shell model (fitting parameters: R, core radius; dR, dimension of the shell; η_c, scattering length density (SLD) of the core, η_s, SLD of the shell; s, polydispersity of the shell radius). Several models were tested for the P1/Brij98 system. The application of the mass-fractal structure factor together with the spherical shell form-factor exhibits the best results for the whole scattering curve. The model includes the parameters: R, core radius; dR, thickness of the shell; η_c, SLD of the core, η_s, SLD of the shell; s, polydispersity of the shell radius; R_{sg}, radius of complex; D, mass fractal dimension of complex) That approach has already been successfully applied for the fitting of experimental data in a BSA/SDS (LDS) system, where the form factor for sphere or ellipsoid was used.[69,70] According to that approach, the structure of a complex is described in terms of micellar-like aggregates that are randomly distributed along the polymer chain or pearl-necklace model. The resulting fitting functions for the systems P1/Brij98 and P2/Brij98 are presented in Figure 5. Furthermore, we were able to get direct information about the nanoparticle structure from the scattering curves by inverse Fourier transformation using GNOM.[71] The pair distance distribution function (PDDF) and radial distribution function of intensity of scattered light display a good agreement with the models used for the fitting (Supporting Information Figure S4). The appearance of a second maximum on the radial distribution function of intensity for P2/Brij98 is usually interpreted as a core−shell structure, and an asymmetric form of the PDDF function with an expanded tail for P1/Brij98 is characteristic of the pearl-necklace model.

The fitting parameters are presented in Table 4. Here, it is worth noting that the resolution of our SANS data, which is

Table 4. Fitting Parameters of SANS curves for Different Systems

fitting parameters/system	P1/Brij98	P2/Brij98
R, nm	3.9	4.5
dR, nm	1.6	7.1
η_c, nm^{-1}	-6.1×10^{-4}	4.8×10^{-4}
η_s, nm^{-1}	1.35×10^{-3}	1.3×10^{-3}
s	0.6	0.7
R_{sg}	21.7	
D	2.6	

determined by the sampling theorem, $D = \pi/q$, is 1 to 125 nm, but the presence of the plateau at high values of q reduces the experimental range of particle dimension to 3.5 up to 125 nm. That fact introduces a certain degree of ambiguity on the interpretation of inner nanoparticle structure.

Previous data obtained from SAXS and SANS experiments for the homologues of Brij98, Brij35 ($C_{12}E_{23}$), and Brij700 ($C_{18}E_{100}$) reveal a core−shell spherical or ellipsoidal structure for the pure water surfactant solutions. The size of surfactant micelles varies from 4.0 to 10.0 nm and depends strongly on the length of hydrophilic corona, which is highly hydrated by surrounding water molecules. Nevertheless, the dimension of micellar core varies only slightly in the range of 1.5−1.8 nm.[72−74]

For our system, DLS data taken from the mixed polymer/surfactant solution (P1 and P3) at initial conditions (pH = 8) display the appearance of particles with the size of 4 nm (Supporting Information Figure S1a, b) that is in a good agreement with the previously reported data for the micelles of Brij35. Moreover, the fitting parameters from the SANS experiment for the systems P1/Brij98 and P2/Brij98 also agree with the size of pure surfactant micelles; the radius of "pearls" in P1/Brij98 is 5.5, and 4.5 nm is the size of the particle core (Table 4). The polymer definitely has an effect on the surfactant dimension and expands it. One can assume that the pearls and the core in a simple core−shell model have a deeper inner structure like micelles of pure Brij surfactant, but their characterization is limited by the resolution of the SANS experiment.

FTIR experiment was chosen to examine the nature of specific interactions observed in the cases of P2/Brij98 and P3/Brij98 systems. FTIR spectra from the solutions of P2 and P2/Brij98 are presented in Figure 6.

The bands at 1596 and 1400 cm^{-1} correspond to the asymmetric stretching and symmetric stretching vibrations of the free (nonbonded) COO^- groups, respectively. The band at 1596 is also slightly shifted to 1600 cm^{-1}. The band detected at 1717 cm^{-1} is assigned to the carbonyl stretching vibration in the COOD group hydrogen bond in the dimer COOD···COOD, possibly hydrated (hydrogen bond to water).[75,76]

dx.doi.org/10.1021/la5031262 | Langmuir 2014, 30, 11307−11318

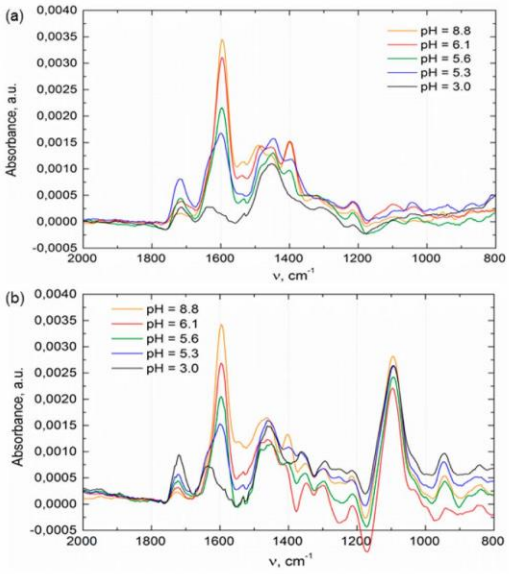

Figure 6. FTIR spectra from the solutions (a) pure P2 and (b) P2/Brij98 at different values of pH (T = 25 °C).

Other peaks in Figure 6a result from the presence of peptide bonds in the side chains of the polymer.

The following tendency was found during the acidic titration of the pure polymer. The bands attributed to the vibration of the free COO^- dominate the spectra of the sample with $\alpha = 0$ (pH = 8.8) while their intensity is strongly decreasing in the spectra of samples with gradually increasing degree of protonation α (decreasing pH).[75,76] By contrast, the intensity of carbonyl stretching vibration in the hydrogen bonded COOD groups increases with decreasing pH, which could be explained by the fact that the concentration of COOD groups increases upon deuteration of COO^- groups. However, a downturn in this trend is observed for the pure P2 solution when going from pH= 5.3 to pH= 3.0 that corresponds to the onset of polymer aggregation (Figure 6a). The appearance of the downturn (the decrease of the absorption band at 1717 cm^{-1}) might be related to the situation where COOD groups are in aggregates, less hydrated (water partially expelled from the neighborhood of carboxylic groups in aggregates) and less mutually hydrogen bonded due to the sterical hindrance. For the system P2/Brij98, new bands arising from the presence Brij98 were found below 1200 cm^{-1} that might be attributed to −C−O− stretching vibrations nonsensitive to pH (Figure 6b). Regarding the band from the polymer, the same vibration bands at almost the same wavenumbers are observed. A significant difference is found in the development of amplitude of the peak at 1719 cm^{-1} that corresponds to the carbonyl stretching vibration of the hydrogen bond COOD groups. While in solution without surfactant the intensity of this band increases with gradually increasing α (decreasing pH) followed by a downturn in this trend, here a steady increase of the band intensity is observed upon increasing α. In this case, the concentration of hydrogen bonded carboxylic groups is not decreased upon the onset of aggregation since surfactant gets actively involved in aggregates/complexes and is hydrogen bonded with carboxylic groups. Analysis of infrared spectra from the pure P3 displays a similar dependency and is presented in the Supporting Information Figure S5.

DISCUSSION

The question about the interactions between polyoxyethylated nonionic surfactants of the Brij-type and various polymers (ionic and nonionic) has been raised frequently during the past decade. The results of the wide investigation on this topic is that polyoxyethylated nonionic surfactants reveal some interactions with polymers and form complexes only in pure surfactant solutions, in solutions of polyacids, or as a result of cooperation with another surfactant (hydrophobically modified polymer).[64,65,77−81] The explanation of this behavior is still ambiguous. Mostly it is connected with weak repulsion of surfactant headgroups, which is manifested by a much lower cmc value compared to that for ionic surfactants. Moreover, it is accepted that the interaction between polyoxyethylated nonionic Brij and polyacids is based on specific bonds in system, whereas the interaction in pure Brij or in the presence of side surfactant is based on the hydrophobic mechanism. It has been shown by a number of methods that the formation of complexes between poly(acrylic acid) and Brij-type surfactants proceeds through the formation of hydrogen bonds in the carboxylic group of the polymer and the oxyethylene group of the surfactant, and is enhanced by the hydrophobic association between the alkyl chains of the last one. The polymer wraps around the micelle of surfactant, and complex polymer/surfactant clusters are formed.[77−81] The addition of a cosurfactant has another pronounced effect on the behavior of surfactant solution. Cosurfactant (ionic or nonionic) promotes the rearrangement of molecules in the system and results in the appearance of mixed micelles. That process is accomplished by an exothermic reaction and obeys the regular solution theory.[64,65,81]

As was mentioned above, the introduction of amino acid residues keeps the polymer theoretically available to hydrogen bonding with surfactant. Moreover, data obtained from DLS experiments allow asserting the formation of complexes between polymers and surfactant. These complexes are stable and display good reversibility in a pH dependent manner.[41,42] Nevertheless, the type of amino acid used for polymer modification has a certain effect to the pH_{tr} and the size of the finally formed particles. The ITC data confirm a significant effect of the amino acid nature on the behavior of the whole polymer.

ITC data for the polymer P1with L-valine amino acid residues exhibit a behavior typical of hydrophobic interactions in polymer/surfactant systems. Fitting by regular solution theory revealed that a small endothermic effect and a weak dependency on the degree of protonation. Both of these factors suggest the absence of hydrogen bonds in the system. Even more, pH dependency of scattered intensity in DLS experiments for pure and mixed solutions has a similar pattern in both cases, there is one single process, and no additional contributions. One can conclude, the micelles of Brij98 are assembled on polymer chain and protect the hydrophobic protonated parts of the polymer. In our case, we deal with the polymer P1 with high enough molecular weight of 78 kDa, and keeping in mind the statistical distribution of protonated group during the pH drop, the pearl-necklace model can be simply assumed. The fitting from SANS experiment confirms that model. The pearl-necklace model can also explain the screening

of charges on the polymer molecule, which has been observed in zeta-potential measurements.

The situation becomes different in the case of the polymer P2 with L-phenylalanine amino acid residue. Here, we clearly define the appearance of hydrogen bonding; a slight shift of pH_{tr} to higher values, a smooth rather than step process of complex formation in the curve of scattered intensity, an exothermic effect of polymer/surfactant interaction in ITC experiments, and strong dependence of the β-value (nonideality of mixing) with an increase in degree of protonation are observed. A good convergence of the results with the previously reported data for the PAA/Brij system enables us to make assumptions about the inner particle structure. According to the reference data, the polymer wraps around the surfactant micelle, which is compatible with the core−shell structure derived from SANS experiment. Then, following the electrophoretic measurements, the mechanism of complex formation can be formulated: even a small amount of surfactant in the polymer solution screens partly the charge on the polymer molecule. However, the appearance of surfactant micelles promotes the rearrangement of polymer molecules in the system. They are moving to the micellar surface as reflected in a significant decrease of zeta-potential. The more micelles are produced in solution, the more effective rearrangement of charges is observed.

Furthermore, we define more complex mechanism of association in the system P3/Brij98 with glycine-L-leucine amino acid sequence and the appearance of both contributions mentioned above. The dependence of scattered light intensity displays a distinct shift in the position of pH_{tr} value. Change in the mechanism of association can be suggested. Data from ITC measurements partially support that statement: although the β-values vary, there is an obvious trend toward less negative values with increasing degree of protonation. This effect might be interpreted with respect to specific interactions, which are gradually replaced by hydrophobic ones. However, the negative surface charge of −10 mV was observed for the P3/Brij98 assemblies in the zeta potential measurement, in contrast with the P1/Brij98 system. The surfactant micelles were not able to cover all polymer chains, which keeps the polymer charge partly distributed on the micellar surface. Hence, the presence of two amino acid residues creates the variability in the polymer/surfactant interactions and requires further analysis.

■ CONCLUSION

The behavior of the pH-responsive polymers poly(*N*-methacryloyl-L-valine), poly(*N*-methacryloyl-L-phenylalanine), and poly(*N*-methacryloylglycyne-L-leucine) in the presence of the nonionic surfactant Brij98 has been studied. The addition of the surfactant prevents phase separation and promotes rearrangement of the polymer molecules. It was established that the nature of the interaction between polymer and surfactant is a competitive mechanism of several contributions, namely, the hydrophobicity of the amino acid, the ability to form hydrogen bonds, and Coulombic interactions. The results may help construct, for example, new pH-responsive site-specific micellar drug delivery systems or pH-responsive membrane-disrupting agents.

■ ASSOCIATED CONTENT

Supporting Information

pH-dependence of the hydrodynamic radius for mixtures: P1/Brij98, P2/Brij98 and P3/Brij98. pH-dependence of the zeta-potential for mixtures: P1/Brij98, P2/Brij98 and P3/Brij98. Zeta-potential as a function of pH for pure polymer solutions of P1, P2, P3. PDDF plot for P1/Brij98 and P2/Brij98 system; radial distribution function of scattered light for system P2/Brij98. FTIR spectra from the pure P3 and P3/Brij98 solutions at different pHs (T=25 °C). This material is available free of charge via the Internet at http://pubs.acs.org

■ AUTHOR INFORMATION

Corresponding Author

*Mailing address: Institute of Macromolecular Chemistry AS CR, v.v.i, Heyrovsky Sq. 2, 162 06 Prague 6, Czech Republic. Tel.: + 420 296 809 291. Fax: +420 296 809 410. E-mail: filippov@imc.cas.cz.

Notes

The authors declare no competing financial interest.

■ ACKNOWLEDGMENTS

The authors also acknowledge financial support No. CZ09-DE06/2013-2014 from the ASCR-DAAD Programme PPP 2013-2014, grant of Academy of Sciences of the Czech Republic (Grant No. M200501201), and grant of The Ministry of Education, Youth and Sports (MŠMT) No. LH14292. M.S. and D.R. acknowledge Support of the Slovak Research and Development Agency (Grant No. 048610) and Scientific Grant Agency VEGA (Grant No. 2/0182/14).

■ REFERENCES

(1) Dai, S.; Ravi, P.; Tam, K. C. pH-Responsive Polymers: Synthesis, Properties and Applications. *Soft Matter* **2008**, *4*, 435−449.
(2) Schmaljohann, D. Thermo- and pH-Responsive Polymers in Drug Delivery. *Adv. Drug Delivery Rev.* **2006**, *58*, 1655−1670.
(3) Huh, K. M.; Kang, H. C.; Lee, Y. J.; Bae, Y. H. pH-Sensitive Polymers for Drug Delivery. *Macromol. Res.* **2012**, *20*, 224−233.
(4) Li, Y.; Gao, G. H.; Lee, D. S. Stimulus-Sensitive Polymeric Nanoparticles and Their Applications as Drug and Gene Carriers. *Adv. Healthcare Mater.* **2013**, *2*, 388−417.
(5) Hoffman, A. S. Stimuli-Responsive Polymers: Biomedical Applications and Challenges for Clinical Translation. *Adv. Drug Delivery Rev.* **2013**, *65*, 10−16.
(6) Mano, J. F. Stimuli-Responsive Polymeric Systems for Biomedical Applications. *Adv. Eng. Mater.* **2008**, *10*, 515−527.
(7) Onaca, O.; Enea, R.; Hughes, D. W.; Meier, W. Stimuli-Responsive Polymersomes as Nanocarriers for Drug and Gene Delivery. *Macromol. Biosci.* **2009**, *9*, 129−139.
(8) Felber, A. E.; Dufresne, M. H.; Leroux, J. C. pH-Sensitive Vesicles, Polymeric Micelles, and Nanospheres Prepared with Polycarboxylates. *Adv. Drug Delivery Rev.* **2012**, *64*, 979−992.
(9) Park, I. K.; Snigha, K.; Arote, R. B.; Choi, Y. J.; Kim, W. J.; Cho, C. S. pH-Responsive Polymers as Gene Carriers. *Macromol. Rapid Commun.* **2010**, *31*, 1122−1133.
(10) Bawa, P.; Pillay, V.; Choonara, Y. E.; Toit, L. C. Stimuli-Responsive Polymers and Their Applications in Drug Delivery. *Biomed. Mater.* **2009**, *4*, 1−15.
(11) Rijcken, C. J. F.; Soga, O.; Hennink, W. E.; van Nostum, C. F. Triggered Destabilisation of Polymeric Micelles and Vesicles by Changing Polymers Polarity: An Attractive Tool for Drug Delivery. *J. Controlled Release* **2007**, *120*, 131−148.
(12) Ganta, S.; Devalapally, H.; Shahiwala, A.; Amiji, M. A Review of Stimuli-Responsive Nanocarriers for Drug and Gene Delivery. *J. Controlled Release* **2008**, *126*, 187−204.
(13) Xu, L.; Zhu, Z.; Borisov, O. V.; Zhulina, E. B.; Sukhishvili, S. A. pH-Triggered Block Copolymer Micelle-to-Micelle Phase Transition. *Phys. Rev. Lett.* **2009**, *103*, 1−4.

(14) Chen, G.; Hoffman, A. S. Graft Copolymers That Exhibit Temperature-induced Phase Transitions over a Wide Range of pH. *Nature* **1995**, *373*, 49−52.
(15) Sevimli, S.; Sagnella, S.; Kavallaris, M.; Bulmus, V.; Davis, T. P. Synthesis, Self-Assembly and Stimuli Responsive Properties of Cholesterol Conjugated Polymers. *Polym. Chem.* **2012**, *3*, 2057−2069.
(16) Laguecir, A.; Ulrich, S.; Labille, J.; Fatin-Rouge, N.; Stoll, S.; Buffle, J. Size and pH Effect on Electrical and Conformational Behavior of Poly(acrylic acid): Simulation and Experiment. *Eur. Polym. J.* **2006**, *42*, 1135−1144.
(17) Rahane, S. B.; Floyd, J. A.; Metters, A. T.; Kilbey, S. M. Swelling Behavior of Multiresponsive Poly(methacrylic acid)-*block*-poly(*N*-isopropylacrylamide) Brushes Synthesized Using Surface-Initiated Photoiniferter-Mediated Photopolymerization. *Adv. Funct. Mater.* **2008**, *18*, 1232−1240.
(18) Li, G.; Song, S.; Guo, L.; Ma, S. Self-Assembly of Thermo- and pH-Responsive Poly(acrylic acid)-*b*-poly(*N*-isopropylacrylamide) Micelles for Drug Delivery. *J. Polym. Sci., Part A: Polym. Chem.* **2008**, *46*, 5028−5035.
(19) Zhang, X. Q.; Li, J. G.; Li, W.; Zhang, A. Synthesis and Characterization of Thermo- and pH-Responsive Double-Hydrophilic Diblock Copolypeptides. *Biomacromolecules* **2007**, *8*, 3557−3567.
(20) Mori, H.; Kato, I.; Endo, T. Dual-Stimuli-Responsive Block Copolymers Derived from Proline Derivatives. *Macromolecules* **2009**, *42*, 4985−4992.
(21) Andre, X.; Zhang, M.; Muller, A. H. E. Thermo- and pH-Responsive Micelles of Poly(acrylic acid)-*block*-poly(*N*,*N*-diethylacrylamide). *Macromol. Rapid Commun.* **2005**, *26*, 558−563.
(22) Lee, A. S.; Gast, A. P.; Butun, V.; Armes, S. P. Characterizing the Structure of pH Dependent Polyelectrolyte Block Copolymer Micelles. *Macromolecules* **1999**, *32*, 4302−4310.
(23) Sumerlin, B. S.; Lowe, A. B.; Thomas, D. B.; McCormick, C. L. Aqueous Solution Properties of pH-responsive AB Diblock Acrylamido Copolymers Synthesized via Aqueous RAFT. *Macromolecules* **2003**, *36*, 5982−5987.
(24) Butun, V.; Billingham, N. C.; Armes, S. P. Unusual Aggregation Behavior of a Novel Tertiary Amine Methacrylate-Based Diblock Copolymer: Formation of Micelles and Reverse Micelles in Aqueous Solution. *J. Am. Chem. Soc.* **1998**, *120*, 11818−11819.
(25) Bae, Y.; Fukushima, S.; Harada, A.; Kataoka, K. Design of Environment-Sensitive Supramolecular Assemblies for Intracellular Drug Delivery: Polymeric Micelles that are Presponsive to Intracellular pH Change. *Angew. Chem., Int. Ed.* **2003**, *42*, 4640−4643.
(26) Kim, M. S.; Hwang, S. J.; Han, J. K.; Choi, E. K.; Park, H. J.; Kim, J. S.; Lee, D. S. pH-Responsive PEG-Poly(beta-amino ester) Block Copolymer Micelles with a Sharp Transition. *Macromol. Rapid Commun.* **2006**, *27*, 447−451.
(27) Xu, C.; Wayland, B. B.; Fryd, M.; Winey, K. I.; Composto, R. J. pH-Responsive Nanostructures Assembled from Amphiphilic Block Copolymers. *Macromolecules* **2006**, *39*, 6063−6070.
(28) Wu, J.; Eisenberg, A. Proton Diffusion across Membranes of Vesicles of Poly(styrene-*b*-acrylic acid) Diblock Copolymers. *J. Am. Chem. Soc.* **2006**, *128*, 2880−2884.
(29) Soppimath, K. S.; Tan, D. C-W.; Yang, Y.-Y. pH-Triggered Thermally Responsive Polymer Core−Shell Nanoparticles for Drug Delivery. *Adv. Mater.* **2005**, *17*, 318−323.
(30) Klaikherd, A.; Nagamani, C.; Thayumanavan, S. Multi-Stimuli Sensitive Amphiphilic Block Copolymer Assemblies. *J. Am. Chem. Soc.* **2009**, *131*, 4830−3838.
(31) Chakraborty, S.; Somasundaran, P. Sequestration of Drugs Using Poly(acrylic acid) and Alkyl Modified Poly(acrylic acid) Nanoparticles. *Soft Matter* **2006**, *2*, 850−854.
(32) Kyriakides, T. R.; Cheung, C. Y.; Murthy, N.; Bornstein, P.; Stayton, P. S.; Hoffman, A. S. pH-Sensitive Polymers That Enhance Intracellular Drug Delivery in Vivo. *J. Controlled Release* **2002**, *78*, 295−303.
(33) Hoffman, A. S.; Stayton, P. S.; Press, O.; Murthy, N.; Lackey, C. A.; Cheung, C.; Black, F.; Campbell, J.; Fausto, N.; Kyriakides, T. R.; Bornstein, P. Design of "Smart" Polymers That Can Direct Intracellular Drug Delivery. *Polym. Adv. Technol.* **2002**, *13*, 992−999.
(34) Hoffman, A. S.; Jones, R. A.; Cheung, C. Y.; Black, F. E.; Zia, J. K.; Stayton, P. S.; Wilson, M. R. Poly(2-alkylacrylic acid) Polymers Deliver Molecules to the Cytosol by pH-Sensitive Disruption of Endosomal Vesicles. *Biochem. J.* **2003**, *372*, 65−75.
(35) Cotonda, P.; Wright, D. B.; Tyler, M.; O'Reilly, R. K. A Comparative Study of the Stimuli-Responsive Properties of DMAEA and DMAEMA Containing Polymers. *J. Polym. Sci., Part A: Polym. Chem.* **2013**, *51*, 3333−3338.
(36) Fournier, D.; Hoogenboom, R.; Thijs, H. M. L.; Paulus, R. M.; Schubert, U. S. Tunable pH- and Temperature-Sensitive Copolymer Libraries by Reversible Addition-Fragmentation Chain Transfer Copolymerizations of Methacrylates. *Macromolecules* **2007**, *40*, 915−920.
(37) Van de Wetering, P.; Moret, E. E.; Schuurmans-Nieuwenbroek, N. M.; Van Steenbergen, M. J.; Hennink, W. E. Structure-Activity Relationships of Water-Soluble Cationic Methacrylate/Methacrylamide Polymers for Nonviral Gene Delivery. *Bioconjugate Chem.* **1999**, *10*, 589−597.
(38) Pietsch, C.; Mansfeld, U.; Guerrero-Sachez, C.; Hoeppener, S.; Vollrath, A.; Wagner, M.; Hoogenboom, R.; Saubern, S.; Thang, S. H.; Becer, C. R.; Chiefari, J.; Schubert, U. S. Thermo-Induced Self-Assembly of Responsive Poly(DMAEMA-*b*-DEGMA) Block Copolymers into Multi- and Unilamellar Vesicles. *Macromolecules* **2012**, *45*, 9292−9302.
(39) Kislalioglu, M. S.; Khan, M. A.; Blount, C.; Goettsch, R. W.; Bolton, S. Physical Characterization and Dissolution Properties of Ibuprofen-Eudragit Coprecipitates. *J. Pharm. Sci.* **1991**, *80*, 799−804.
(40) Filippov, S. K.; Hruby, M.; Konak, C.; Mackova, H.; Spirkova, M.; Stepanek, P. Novel pH Responsive Nanoparticles. *Langmuir* **2008**, *24*, 9295−9301.
(41) Filippov, S. K.; Starovoytova, L.; Konak, C.; Hruby, M.; Mackova, H.; Karlsson, G.; Stepanek, P. pH Sensitive Polymer Nanoparticles: Effect of Hydrophobicity on Self-Assembly. *Langmuir* **2010**, *26*, 14450−14457.
(42) Keller, S.; Vargas, C.; Zhao, H.; Piszczek, G.; Brautigam, C. A.; Schuck, P. High-Precision Isothermal Titration Calorimetry with Automated Peak-Shape Analysis. *Anal. Chem.* **2012**, *84*, 5066−5073.
(43) Kemmer, G.; Keller, S. Nonlinear Least Squares Data Fitting in Excel Spreadsheets. *Nat. Protoc.* **2010**, *5*, 267−281.
(44) Heerklotz, H. H.; Binder, H.; Schmiedel, H. Excess Enthalpies of Mixing in Phospholipid-Additive Membranes. *J. Phys. Chem. B* **1998**, *102*, 5363−5368.
(45) Diab, C.; Winnik, F. M.; Tribet, C. Enthalpy of Interaction and Binding Isotherms of Non-ionic Surfactants onto Micellar Amphiphilic Polymers (Amphipols). *Langmuir* **2007**, *23*, 3025−3035.
(46) Tanaka, N.; Kitano, H.; Ise, N. Raman Spectroscopic Study of Hydrogen Bonding in Aqueous Carboxylic Acid Solution. 3. Polyacrylic Acid. *Macromolecules* **1991**, *24*, 3017−3019.
(47) Holappa, S.; Karesoja, M.; Shan, J.; Tenhu, H. Solution Properties of Linear and Branched Block Copolymers Consisting of Acidic and PEO Blocks. *Macromolecules* **2002**, *35*, 4733−4738.
(48) Holappa, S.; Andersson, T.; Kantonen, L.; Plattner, P.; Tenhu, H. Soluble polyelectrolyte complexes composed of poly(ethylene oxide)-block-poly(sodium methacrylate) and poly(methacryloyloxyethyl trimethylammonium chloride). *Polymer* **2002**, *44*, 7907−7916.
(49) Konak, C.; Sedlak, M. pH-Sensitive Micelles Formed by Interchain Hydrogen Bonding of Poly(methacrylic acid)-block-Poly(ethylene oxide) Copolymers. *Macromol. Chem. Phys.* **2007**, *208*, 1893−1899.
(50) Sedlak, M. What Can be Seen by Static and Dynamic Light Scattering in Polyelectrolyte Solutions and Mixtures? *Langmuir* **1999**, *15*, 4045−4051.
(51) Schmitz, K. S.; Lu, M.; Singh, N.; Ramsay, D. J. Ordinary Extraordinary Phase-Transition of Poly(Lysine). *Biopolymers* **1984**, *23*, 1637−1646.

(52) Lin, S. C.; Lee, W. I.; Schurr, J. M. Brownian-Motion of Highly Charged Poly(L-Lysine) - Effects of Salt and Polyion Concentration. *Biopolymers* **1978**, *17*, 1041−1064.
(53) Schmitz, K. S.; Ramsay, D. J. Qels-Sef Study On Poly(Lysine) in the Extraordinary Phase - Effect of Electric-Field Strength on the Apparent Diffusion-Coefficient. *Biopolymers* **1985**, *24*, 1247−1256.
(54) Drifford, M.; Dalbiez, J. P. Effect of Salt on Sodium Polystyrene Sulfonate Measured by Light-Scattering. *Biopolymers* **1985**, *24*, 1501−1514.
(55) Sedlak, M.; Amis, E. J. Concentration and Molecular Weight Regime Diagram of Salt-Free Polyelectrolyte Solutions as Studied by Light Scattering. *J. Chem. Phys.* **1992**, *96*, 826−834.
(56) Filippov, S.K.; Seery, T. A. P.; Černoch, P.; Pánek, J.; Štěpánek, P. Behavior of Polyelectrolyte Solutions in a Wide Temperature Range. *Eur. Polym. J.* **2011**, *47*, 1410−1415.
(57) Filippov, S.K.; Seery, T. A. P.; Černoch, P.; Hruby, M.; Pánek, J.; Kříž, J.; Štěpánek, P. Collective Polyelectrolyte Diffusion as a Function of Counterion Size and Dielectric Constant. *Polym. Int.* **2013**, *62*, 1271−1276.
(58) Noskov, B. A.; Bilibin, A.Yu.; Lezov, A.V.; Loglio, G.; Filippov, S.K.; Zorin, I.M.; Miller, R. Dynamic surface elasticity of polyelectrolyte solutions. *Colloids Surf., A* **2007**, *298*, 115−122.
(59) Sedlak, M. Generation of Multimacroion Domains in Polyelectrolyte Solutions by Change of Ionic Strength or pH (Macroion Charge). *J. Chem. Phys.* **2002**, *116*, 5256−5262.
(60) Li, Y.; Xu, R.; Bloor, D. M.; Holzwarth, J. F.; Wyn-Jones, E. The Binding of Sodium Dodecyl Sulfate to the ABA Block Copolymer Pluronic F127 ($EO_{97}PO_{69}EO_{97}$): An Electromotive Force, Microcalorimetry, and Light Scattering Investigation. *Langmuir* **2000**, *16*, 10515−10520.
(61) Bogomolova, A.; Filippov, S. K.; Starovoytova, L.; Angelov, B.; Konarev, P.; Sedlacek, O.; Hruby, M.; Stepanek, P. Study of Complex Thermosensitive Amphiphilic Polyoxazolines and Their Interaction with Ionic Surfactant. Are Hydrophobic, Thermosensitive, and Hydrophilic Moieties Equally Important? *J. Phys. Chem. B* **2014**, *118*, 4940−4950.
(62) Bouchemal, K.; Agnely, F.; Koffi, A.; Ponchel, G. A Concise Analysis of the Effect of Temperature and Propanediol-1, 2 on Pluronic F127 Micellization Using Isothermal Titration Microcalorimetry. *J. Colloid Interface Sci.* **2009**, *338*, 169−176.
(63) Bouchemal, K. New Challenges for Pharmaceutical Formulations and Drug Delivery Systems Characterization Using Isothermal Titration Calorimetry. *Drug Delivery Today* **2008**, *13*, 960−972.
(64) Li, Y.; Xu, R.; Bloor, D. M.; Penfold, J.; Holzwarth, J. F.; Wyn-Jones, E. Moderation of the Interactions between Sodium Dodecyl Sulfate and Poly(vinylpyrrolidone) Using the Nonionic Surfactant Hexaethyleneglycol Mono-n-dodecyl Ether $C_{12}EO_6$: an Electromotive Force, Microcalorimetry, and Small-Angle Neutron Scattering Study. *Langmuir* **2000**, *16*, 8677−8684.
(65) Couderc, S.; Li, Y.; Bloor, D. M.; Holzwarth, J. F.; Wyn-Jones, E. Interaction between the Nonionic Surfactant Hexaethylene Glycol Mono-n-dodecyl Ether($C_{12}EO_6$) and the Surface Active Nonionic ABA Block Copolymer Pluronic F127 ($EO_{97}PO_{69}EO_{97}$)-Formation of Mixed Micelles Studied Using Isothermal Titration Calorimetry and Differential Scanning Calorimetry. *Langmuir* **2001**, *17*, 4818−4824.
(66) Gromadzki, D.; Filippov, S.K.; Netopilik, M.; Makuska, R.; Jigounov, A.; Plestil, J.; Horsky, J.; Stepanek, P. Combination of "Living" Nitroxide-Mediated and Photoiniferter-Induced "Grafting From" Free-Radical Polymerizations: From Branched Copolymers to Unimolecular Micelles and Microgels. *Eur. Polym. J.* **2009**, *45*, 1748−1758.
(67) Angelov, B.; Angelova, A.; Filippov, S. K.; Narayanan, T.; Drechsler, M.; Nicolas, V.; Stepanek, P.; Couvreur, P.; Lesieur, S. DNA/Fusogenic Lipid Nanocarrier Assembly: Millisecond Structural Dynamics. *J. Phys. Chem. Lett.* **2013**, *4*, 1959−1964.
(68) Filippov, S. K.; Chytil, P.; Konarev, P.; Dyakonova, M.; Papadakis, C. M.; Jigounov, A.; Plestil, J.; Stepanek, P.; Etrych, T.; Ulbrich, K.; Svergun, D.I. Macromolecular HPMA-Based Nanoparticles with Cholesterol for Solid-Tumor Targeting: Detailed Study of the Inner Structure of a Highly Efficient Drug Delivery System. *Biomacromolecules* **2012**, *13*, 2594−2604.
(69) Chen, S.-H.; Teixeira, J. Structure and Fractal Dimension of Protein-Detergent Complexes. *Phys. Rev. Lett.* **1986**, *57*, 2583−2586.
(70) Santos, S. F.; Zanette, D.; Fischer, H.; Itri, R. A Systematic Study of Bovine Serum Albumin (BSA) and Sodium Dodecyl Sulfate (SDS) Interactions by Surface Tension and Small Angle X-ray Scattering. *J. Colloid Interface Sci.* **2003**, *262*, 400−408.
(71) Svergun, D. I. Determination of the regularization parameter in indirect-transform methods using perceptual criteria. *J. Appl. Crystallogr.* **1992**, *25*, 495−503.
(72) Preu, H.; Zradba, A.; Rast, S.; Kunz, W.; Hardy, E. H.; Zeidler, M. D. Small Angle Neutron Scattering of D_2O-akcohol-Brij 35 Solution and Their Modelling Using the Percus-Yevick Integral Equation. *Phys. Chem. Chem. Phys.* **1999**, *1*, 3321−3329.
(73) Tomsic, M.; Bester-Rogac, M.; Jamnik, A.; Kunz, W.; Touraud, D.; Bergmann, A.; Glatter, O. Nonionic Surfactant Brij35 in Water and in Various Simple Alcohols: Structural Investigations by Small-Angle X-ray Scattering and Dynamic Light Scattering. *J. Phys. Chem. B* **2004**, *108*, 7021−7032.
(74) Sommer, C.; Pedersen, J. S. Structure and Interactions of Block Copolymer Micelles of Brij 700 Studied by Combining Small-Angle X-ray and Neutron Scattering. *Langmuir* **2005**, *21*, 2137−2149.
(75) Sedlak, M.; Konak, C.; Dybal, J. Heat-set Poly(ethylacrylic acid) Nanoparticles: Combined Light Scattering, Calorimetric, and FTIR Study. *Macromolecules* **2009**, *42*, 7439−7446.
(76) Sedlak, M. Homopolymer Self-assembly into Stable Nanoparticles: Concerted Action of Hydrophobic Association and Hydrogen Bonding in Thermoresponsive Poly(alkylacrylic acid)s. *J. Phys. Chem. B* **2012**, *116*, 2356−2364.
(77) Robb, I. D.; Stevenson, P. Interaction Between Poly(acrylic acid) and an Ethoxylated Nonionic Surfactant. *Langmuir* **2000**, *16*, 7168−7172.
(78) Anghel, D.; Winnik, F. M.; Galatanu, N. Effect of the Surfactant Head Group Length on the Interactions between Polyethylene Glycol Monononylphenyl Ethers and Poly(acrylic acid). *Colloids Surf., A* **1999**, *149*, 339−345.
(79) Bandyapadhyay, P.; Ghosh, A. K.; Bandyapadhyay, S. Brij-micelle and Polyacrylic Acid Interaction Investigated by Cu^{2+} - induced Pyrene Fluorescence: Effect of Brij-micelle Structure. *Chem. Phys. Lett.* **2009**, *476*, 244−248.
(80) Vasilescu, M.; Anghel, D. F.; Almgren, M.; Hansson, P.; Saito, S. Fluorescence Probe Study of the Interactions between Nonionic Poly(oxyethylenic) Surfactants and Poly(acrylic acid) in Aqueous Solutions. *Langmuir* **1997**, *13*, 6951−6955.
(81) Deo, P.; Somasundaran, P. Interactions of Hydrophobically Modified Polyelectrolytes with Nonionic Surfactants. *Langmuir* **2005**, *21*, 3950−3956.

5. DISCUSSION

The above presented original articles are a collection of results obtained in a mixture of surfactant and stimuli-responsive polymers. In Discussion Part we will try to summarize the important results and to make some conclusions on this topic.

The idea of controlled phase separation was explored for all of our systems. That idea assumes the careful adjustment of separation process through the change in surrounding conditions. Two external variables were chosen for investigation, temperature and pH. The polymer, indeed, has been used as an object for thermo- or pH-sensitivity.

5.1. Thermoresponsive Polymer Systems

In the current part, we would like to monitor through the Articles 1, 2 and 3 the sequential modification of block copolymers built from poly(2-alkyl-2-oxazoline) and the effect that has such modification on the interaction activity between polymers and surfactants. General structures of block copolymers are shown in Scheme 5.1. There are two main objects here, the statistical diblock copolymer, PBuOZ-*co*-PiPrOZ, and a more complex triblock PMeOZ-*stat*-(PBuOZ-*co*-PiPrOZ)-MeOZ. Moreover, the latter polymer was synthesized from the former one by addition of the terminal MeOZ units. The polymers studied on the present work were synthesized by O. Sedlacek and M. Hruby from Department of Supramolecular Polymer Systems in Institute of Macromolecular Chemistry.

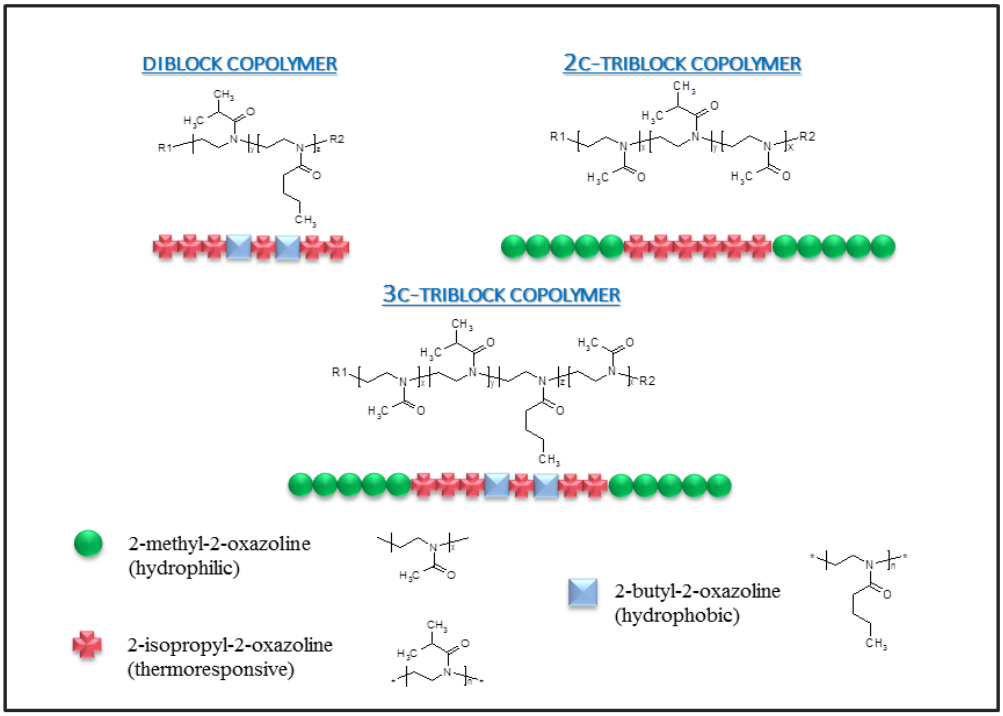

Scheme 5.1. Chemical structure and schematic image of poly(2-alkyl-2-oxazoline)s block copolymers.

Table 5.1. Molecular characteristics of the polymers

Polymers	type of polymer	2-butyl-2-oxazoline in thermoresponsive block, mol %	M_w	*cpt*, °C	n_{MeOx}	n_{iPrOX}	n_{BuOX}
A	diblock copolymer	10	6500	28.5[a]	-	51	6
B	diblock copolymer	20	6200	21.5[a]	-	44	11
C	diblock copolymer	10	12600	28.5[a]	-	99	11
ox(2:1)	3c-triblock copolymer	15	10100	19[b]	31.5	52.5	10.5
ox(1:1)	3c-triblock copolymer	15	10300	17[b]	52	40	8
ox(1:2)	3c-triblock copolymer	15	10000	24[b]	72	27	6

[a] *cpt* at the polymer concentration c=0.5 wt%, [b] *cpt* at the polymer concentration c=1.4 wt%.

The statistical diblock copolymer, PBuOZ-co-PiPrOZ, consists only from hydrophobic (BuOZ) and thermo-responsive (PiPrOZ) part with absence of any hydrophilic one (Table 5.1.). The absence of hydrophilic part creates a high instability of polymer in the condition of temperature increase and results in abrupt micro-phase separation in system. Thus, our purpose was the creation of stable system with the ability to regulate the phase separation process. We used polymeric surfactant F127 for that purpose. Polymeric structure of F127 surfactant effectively stabilizes the polymer and solubilizes it inside of micellar hydrophobic core. Interestingly, not only the polymer but also the surfactant displays thermo-responsive properties in this case. That leads to the extra complexity in the analysis of such mixed system.

We have found that the interactions between statistical polymer and F127 can be detected long before the transition temperature of the polymer as well as that of the surfactant. The premicellar complexes were observed by DLS and ITC technics (Figure 5.1. a, b, c). Moreover, the polymer composition has essential effect to the structure of resulting complexes.

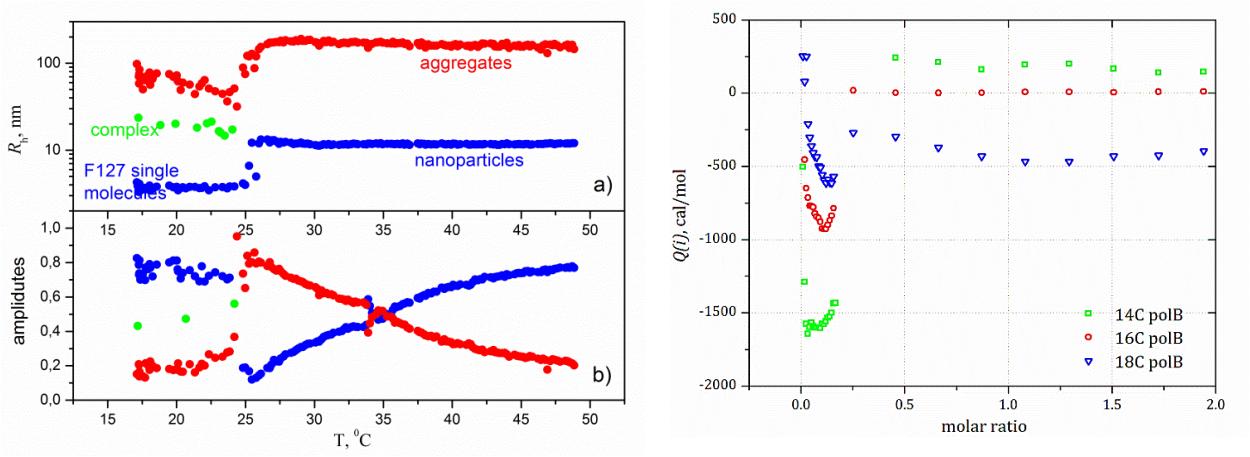

Figure 5.1. DLS data for the Polymer C+F127 system. a) R_h data for: (●) – aggregates, (●)- complexes and (●)- single F127 molecules and nanoparticles ; c(pol)/c(F127) = 0.1; b) Amplitudes data: (●) – aggregates; (●)- complexes, (●)- single F127 molecules and nanoparticles, c) ITC curves for titration F127 by Polymer B, molar ratio = c(pol)/c(F127).

It was observed that the hydrophobicity of the polymers in particular is more important than the thermosensitivity of them in respect to the strength of interactions. While the process of interaction for the hydrophobic and for the thermo-responsive polymers is the same, the final structure of more hydrophobic polymer/F127 nanoparticles would be more compact (at equal amount of surfactant). The evolution of polymer/surfactant complexes as a function of temperature is presented on Figure 5.2 in the form of a SAXS curves. It is possible to interpret the structure sequence in the polymer/surfactant complexation process in the following way.

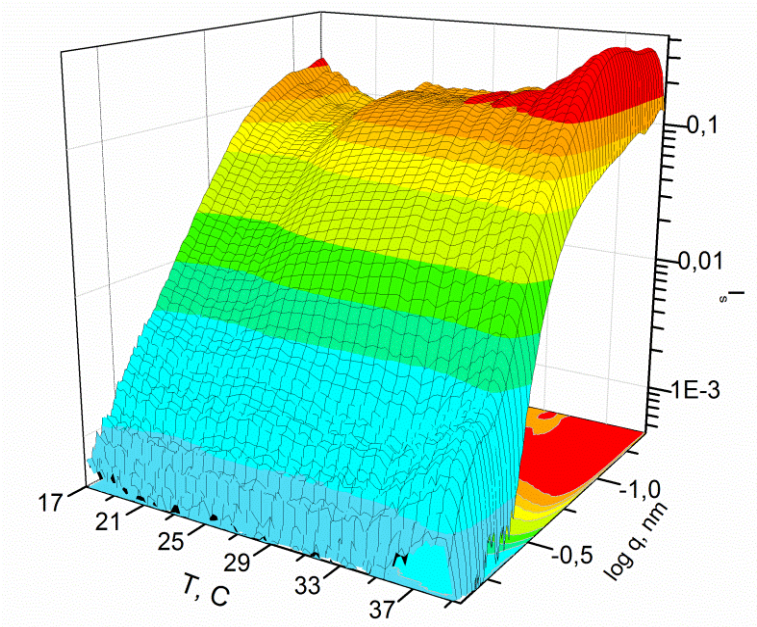

Figure 5.2. 3D plot of SAXS data as a function of scattering vector and temperature for the Polymer B/F127 system.

F127 at low temperature identifies the hydrophobic moieties (BuOZ) of macromolecule and forms intermediate complexes. When the temperature rises, more and more molecules of F127 transfer from the solution to the polymer. However, since the polymer as well as the surfactant has thermo-sensitive properties, and thermosensitivity is a temperature-dependent process in time, there is certain competition between homo- and hetero-association. One can assume, when the association process began (at *cpt*) the presence of hydrophobic moieties in polymer makes the process of homo-association in polymer more preferable. That leads to aggregation of some polymer molecules. The aggregation of the polymer molecules increases the instantaneous concentration of surfactant in a limited volume, and it becomes possible to observe correlations between different molecules of F127. Eventually, enough surfactant molecules are transferred to the polymers to cover them, the correlation of molecules disappears and the shape of complexes becomes fully identical to pure F127 micelles. Finally, the structure of hybrid (mixed) nanoparticles can be referred to a spherical shell model, where the core consist of the statistical polymer and the PPO group of F127, and the shell is a sequence of the PEO group of F127 (Figure 5.3)

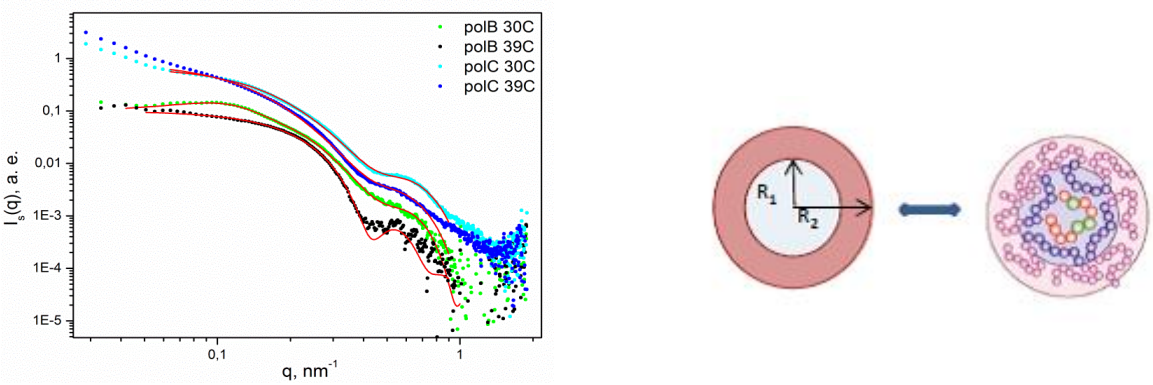

Figure 5.3. (a) SAXS results from the Polymer B/F127 and Polymer C/F127 systems over a range of temperatures. Solid lines are fits to the spherical shell model; *(b)* Schematic representation of hybrid nanoparticles.

The complex polymers with statistical BuOZ-*co*-PiPrOZ central block and hydrophilic terminated PMeOZ blocks show better stability than diblock copolymers and form micelles with temperature increase (Figure 5.4).

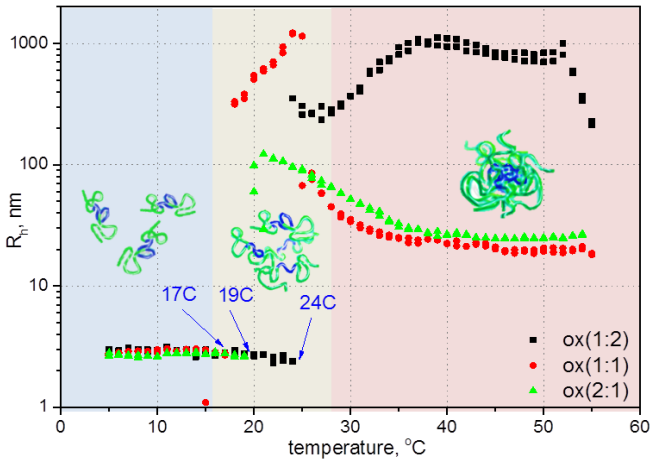

Figure 5.4. DLS data from pure 3c-triblock poly(2-alkyl-2-oxazoline)s, *C* = 14 mg/mL.

Thus, there is no need to use a polymeric surfactant to stabilize the system. Therefore, low molecular weight surfactants (CTAB, SDS) were taken to analyze the polymer/surfactant interactions. The purpose of that part of research was to assess how the mechanism of polymer/surfactant interactions changes in conditions of temperature elevation; and what is different in that process of interactions if we use the thermo-responsive polymer of complex architecture in contrast to homopolymer (Figure 5.5 a, b). Experiments show that the behavior in the mixed system is sensitive to the chemical structure of polymers as well as to the surrounding temperature. Both parameters affect the compactness of polymeric micelles. And then, the compactness of micelles defines the mechanism of polymer/surfactant interactions.

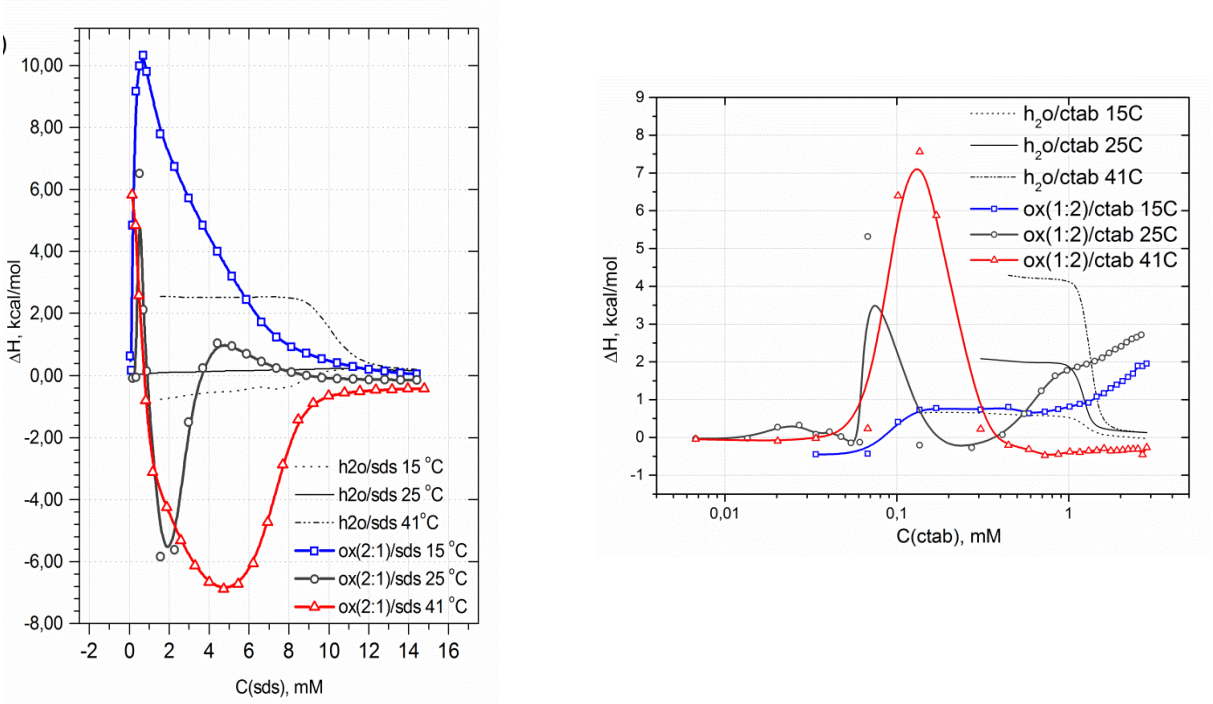

Figure 5.5. ITC curves for (a) SDS titration of polymer ox(2:1) and (b) CTAB titration of polymer ox(1:2) at different temperatures.

In general the mechanism can be presented as follows (Figure 5.6). At the temperature above *cpt*, the polymer exists in the form of swollen Gaussian coil and forms aggregates before the addition of surfactant. The addition of surfactant induces two simultaneous processes. The first one results in an increase in the volume of single Gaussian chain in the polymer aggregates, and the second one promotes the breaking down of large mixed aggregates and the formation of small ones. Furthermore, the first process starts at the lowest concentration and proceeds more intensively. As soon as a sufficient amount of surfactant was added the aggregates disappear from the solution, and polymer/surfactant complexes become visible. These complexes can be characterized by a model of sphere with an attached Gaussian coil. One can assume the micelles of surfactant with the hydrophobic central block of polymer inside of them form spheres, whereas the MeOZ blocks are expanded to the aqueous solution. If the addition of surfactant to polymer is performed at temperature below *cpt*, then any copolymer can be referred to as homopolymer. The mechanism of interactions can be described in two stages: a simple act of interaction and the release of bonding water from the surrounding shell.

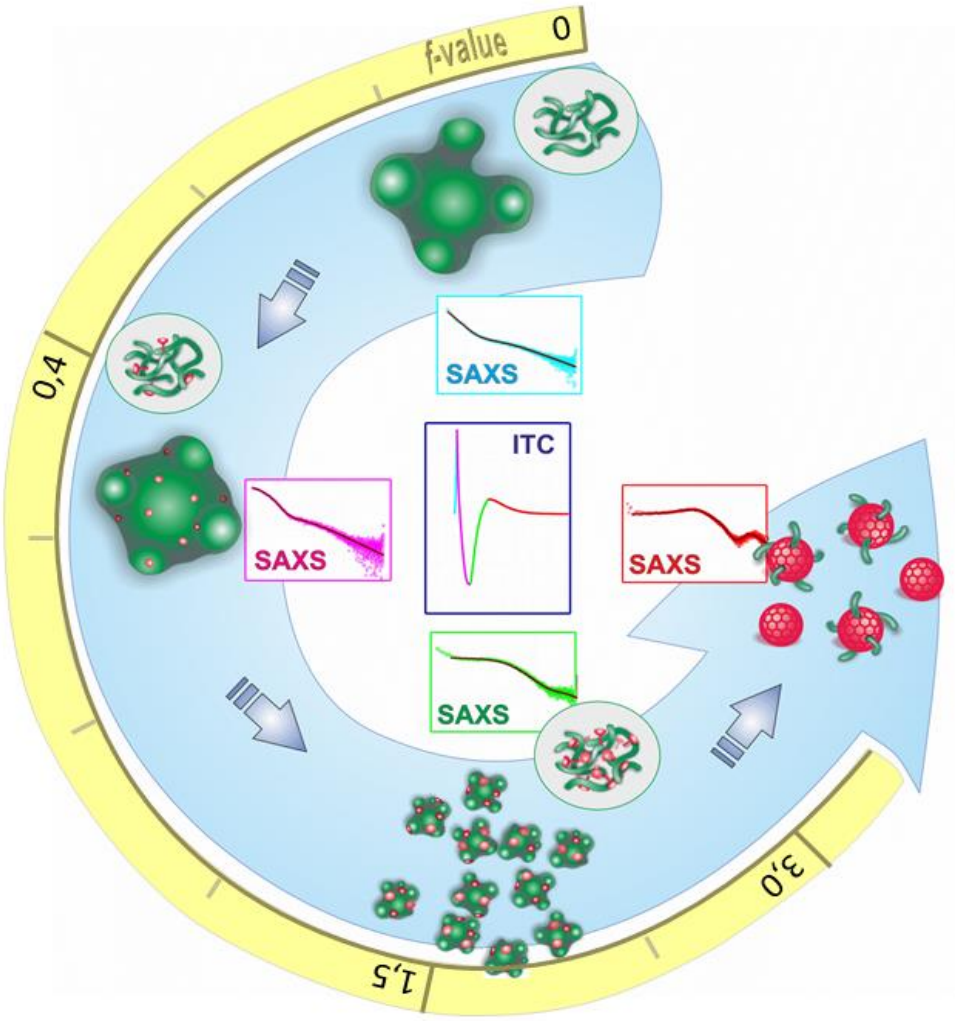

Figure 5.6. Structure sequence of the complexation process of triblock poly(2-alkyl-2-oxazolines) with increasing the concentration of surfactants.

Analysis of ITC thermograms shows no difference in the mechanism of interactions between tri-block copolymer and either anionic SDS or cationic CTAB. The only point is that the cationic CTAB is more sensitive to the conformation of the polymer (Table 5.2).

Table 5.2. Parameters of the interaction between the polymers and surfactant.

surfactant	*cmc**, mM	*cac*** (molecular state), mM	*cac* (micellar state), mM	C_2, mM
SDS	8.4	0.15	0.35	12-14
CTAB	1.25	0.7	0.07	>20

* - *cmc* is taken from the blank titration of surfactant to water and does not show a significant variation with temperature; ** - *cac* is an average value across all polymers; the molecular state and the micellar state correspond to the conformation of the polymer at 15 and 25 (or 41) ºC, respectively.

5.2. pH-Responsive Polymer Systems

Weak polyacids are usually described as polyelectrolytes. They undergo to micro- and sometimes macro-phase separation at low pHs. In our work we used modification of polymethacrylic acid with some amino acids on the side chain of polymer (Sheme 5.2). The polymers were synthesized by H. Mackova and M. Hruby from Department of Supramolecular Polymer Systems in Institute of Macromolecular Chemistry.

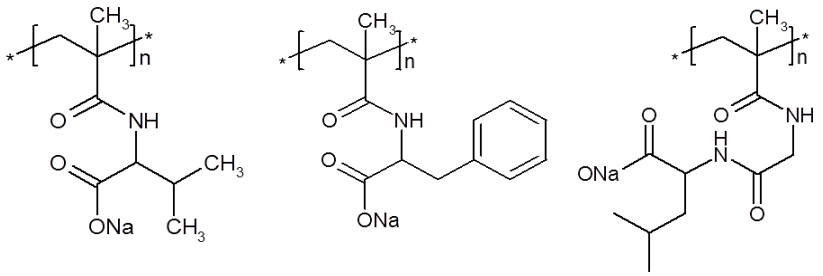

Scheme 5.2. Chemical structure of poly(*N*-methacryloyl-*L*-valine) (P1), poly(*N*-methacryloyl-*L*-phenylalanine) (P2) and poly(*N*-methacryloyl glycyl-*L*-leucine) (P3) (sodium salt forms).

The introduction of amino acid allows us to adjust the hydrophobicity of the whole macromolecule and to regulate eventually the tendency of the polymer to the phase separation. The addition of surfactants is a typical way to prevent the self-association in polymer solutions. Even more, the reaction between polyelectrolytes and oppositely charged surfactants is reviewed very well. Surprisingly, our polymers showed a good solubility in the solution of nonionic surfactant Brij98. Because of only little information about charged polymer – nonionic surfactant interactions, we decided to analyze that type of interactions thoroughly. We found that the type of amino acid regulates the predominant way of interactions in the mixed system that can be driven either by hydrophobic forces or through hydrogen bonding (Figure 5.7 a, b, c). At the same time, while the hydrogen bonding between polyacids and etoxylated surfactants has been described recently, the existence of hydrophobic interactions in such system has not yet been mentioned. The type of interactions has a strong effect on the structure of the final complexes. Complexes which have been formed through the hydrophobic interactions are characterized by a pearl-necklace model. Oppositely, the core-shell structure with the polymer placed on the micellar surface is a result of predominant hydrogen bonding (Figure 5.8).

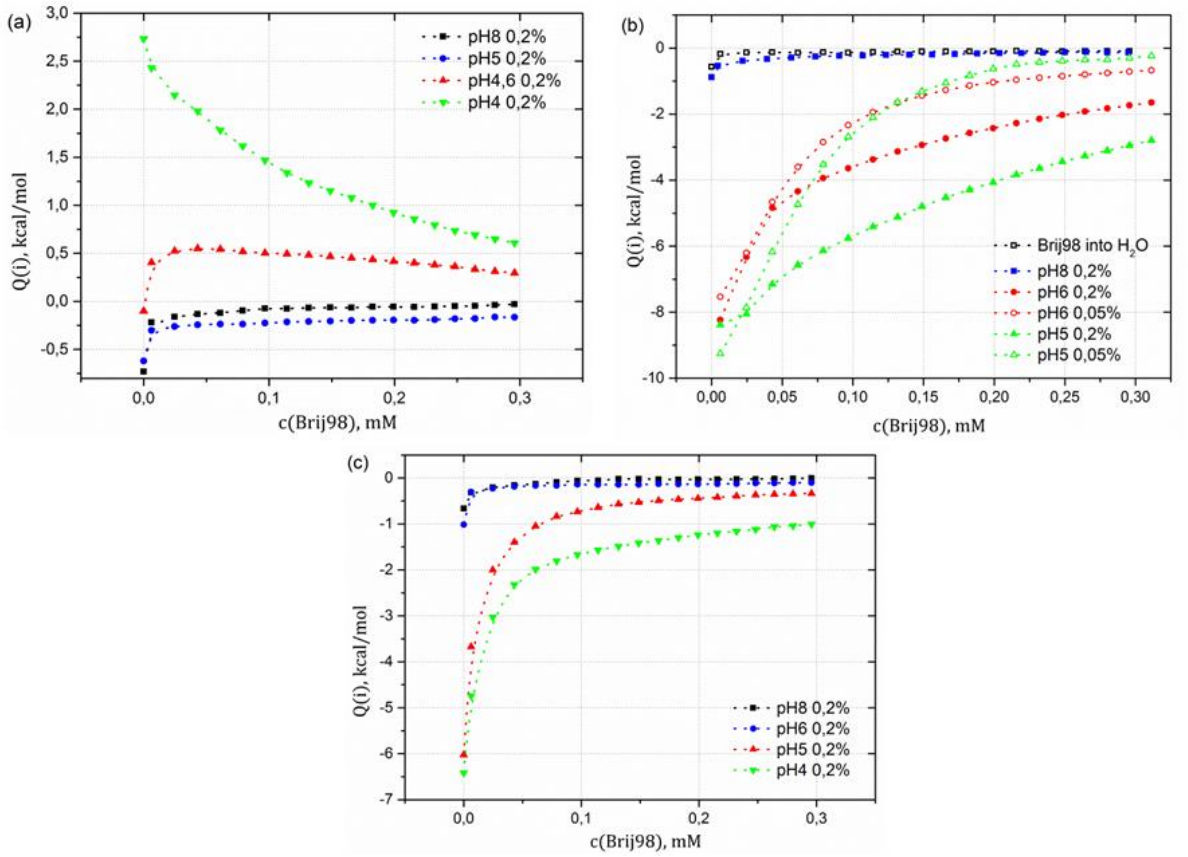

Figure 5.7. ITC curve for the titration of the polymers (a) P1 solution, (b) P2 solution, (c) P3 solution with surfactant Brij98 at different concentrations and pH values (T=25ºC).

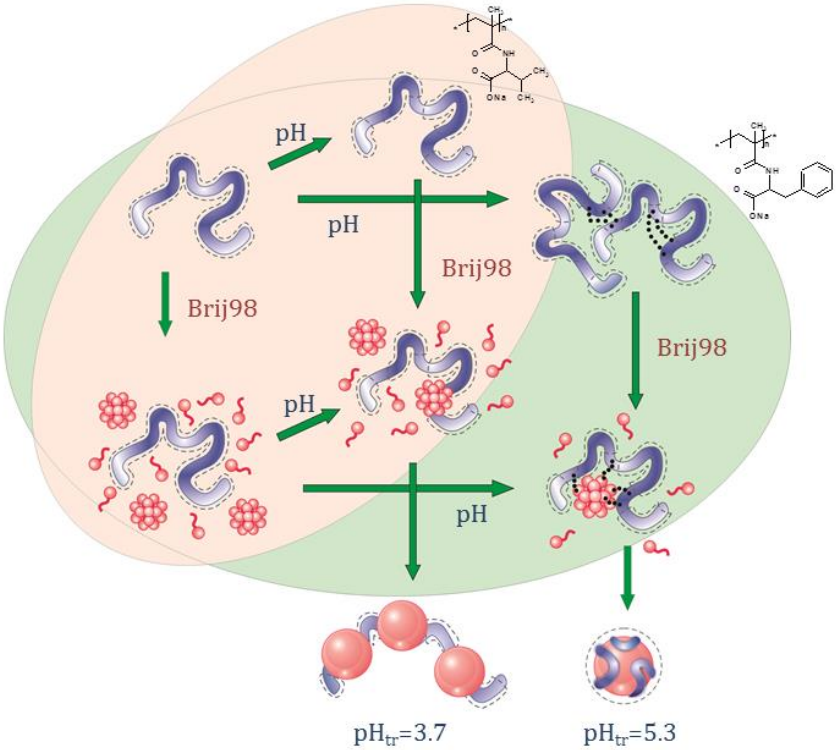

Figure 5.8. Structure sequence of the complexation process in amino-acid-based polymers with increasing the concentration of surfactants and decreasing the pH of solution.

The important aspect of the current work was the interpretation of ITC data. And here, we also have to mention these results. We were able to compare the results obtained from SAXS experiment at certain polymer/surfactant concentration ratios with the results of ITC experiment. In other words, we have tried to analyze the thermodynamic processes in the system and the conformation changes that are responsible for a particular heat effect. Such procedure of investigation is extremely important if we are dealing with a complex process, where a number of stages can be assumed. Assuredly, single measurement of complex structure cannot be used for interpretation of the whole process but a number of consecutive measurements makes the process of transformation in such systems more understandable. Moreover, if the reaction between polymer and surfactant is one act of interaction or several acts but each act can be distinguished, it is also possible to provide a quantitative analysis of interactions. Typically, the models of binding sites are used for ITC experiments. That model supposes a noncooperative binding in the system and fails in case of polymer/surfactant interactions. It is well known that the reason for surface activity lies in cooperation of surfactant molecules. The regular solution theory is more appropriate for that situation. The theory is based on the assumption that the enthalpy of interaction is a combination of heat effects (heat of reaction, heat of dilution, heat of transfer from one solvent to another, heat of aggregation and etc.). We have shown a good applicability of the regular solution theory to the analysis of interactions in polyelectrolyte – nonionic surfactant systems and believe in the perspective of using it for other polymer/surfactant systems.

6. CONCLUSION

1. The idea of controlled phase separation related to the system of thermoresponsive polymers and surfactants has been exploited. Hybrid nanoparticles were obtained by combination of the statistical PBuOZ-*co*-PiPrOZ copolymer and polymeric nonionic surfactant F127. Four polymers with different ratios of hydrophobic (BuOZ) and thermoresponsive (iPrOZ) blocks were analyzed. It was shown that the polymeric structure of surfactant effectively stabilizes the nanoparticles and protects them from further aggregation. The size of hybrid nanoparticles was found to be equal to 10-12 nm in radius, which is very similar to the size of micelle obtained for pure F127 (10 nm). The addition of surfactant affects the value of critical transition temperature. While the *cpt* for pure polymers was 28.5 ºC (Polymers A and C) and 21.5 ºC (Polymer B), the presence of surfactant results in a shift of the *cpt* value down to 26.0, 24.5 and 25.5 ºC for polymers A, B, C, correspondingly. There is a certain relationship between hydrophobicity of the polymer and their critical temperature. Moreover, the preliminary data show that the process of nanoparticle formation proceeds through the stage when the critical temperature is still not reached, but the association between polymer and surfactant has been observed.

   Further analysis of the systems confirms the existence of premicellar complexes with radius of 20 nm followed by rearrangement to the 13 nm dense nanoparticles. It has been shown that there is a dependence between hydrophobicity of the polymer and a presence of aggregates in the solution. Aggregates can be found in the initial step of nanoparticles formation and they disappear with raising temperature. The structure of hybrid nanoparticles can be characterized by a spherical shell model. The core consists of a polymer and the PPO group of F127, whereas the shell composed by the PEO group of surfactant.

   The analysis of the statistical PBuOZ-*co*-PiPrOZ copolymers has been continued by considering the solution behavior of the triblock copolymer PMeOZ-*stat*-(PBuOZ-*co*-PiPrOZ)-MeOZ. The modification of statistical copolymers by introduction of hydrophilic terminal group improves the stability of polymers. The triblock copolymers were able to form micelle-like structure. The important result of our comprehensive analysis is the following; whereas the position of *cpt* is defined predominantly by the ratio of thermoresponsive (iPrOZ) and hydrophilic (MeOZ) blocks, the hydrophobicity of polymers is determined by the difference in the number of thermoresponsive and hydrophobic (BuOZ) blocks. A smaller difference would lead to less thermoresponsive and more hydrophobic

character of polymer. Additionally, the behavior of complex triblock poly(2-alkyl-2-oxazoline)s in combination with ionic surfactants (SDS, CTAB) revealed a dissociation of the initially formed polymeric micelles and formation of the mixed ones. The process of polymer/surfactant interaction is strongly dependent on the polymer state and, basically, on the surrounding temperature. The more compact is the structure of polymer the more complex would be a process of interaction. We were able to monitor the mechanism of polymer/surfactant association on each particular stage. One has to note that while CTAB typically displays weak interactions with uncharged polymers, the binding of CTAB is more selective in respect to the conformation of polymer molecule.

2. The behavior in a system of pH-responsive polymer and nonionic surfactant was investigated. Polymers were obtained from methacrylic acid modified in an initial step by three different amino acids. Thus, three homopolymers with one particular amino acid on the side chain were analyzed. It was observed that the addition of nonionic surfactant to the polymer has an important impact on the polymer conformation and charge distribution on the surface of resulting complexes, but only slightly affects the pH_{tr}. The type of amino acid is a crucial point in the process of complex formation between polymer and nonionic Brij98. Competition of hydrophobic and hydrogen bonds regulates the mechanism of interaction in the current systems. The ability of polymer to hydrogen bonding results in the situation, when the polymer wraps round the surfactant micelle and intermolecular hydrogen bonds between the polymer and the surfactant stabilize this structure. Interestingly it was observed that nonionic surfactant can also interact with a partially protonated polymer via hydrophobic forces. In the latter case, the pearl-necklace structure was found. Molecules of nonionic Brij not only adsorb on the polymer surface but block polymer charge as well.

3. We were able to interpret the ITC curves for uncharged polymer-ionic surfactant interactions at any state of polymer molecule. Regular solution theory was successfully applied to fit results obtained from ITC experiments. The effect of hydrogen bonds on ITC signal was figured out.

7. REFERENCES

1. Gil, E. S., Hudson, S. M., *Prog. Polym. Sci.*, **2004**, 29, 1173-1222.

2. Aseyev, V., Tenhu, H., Winnik, F., *Adv. Polym. Sci.*, Springer Berlin / Heidelberg, **2011**, vol. 242, pp. 29-89.

3. Liu, R., Fraylich M., Saunders, B., *Colloid. Polym. Sci.*, **2009**, 287, 627-643.

4. Aoshima, S., Kanaoka, S., *Adv. Polym. Sci.*, Springer Berlin / Heidelberg, **2008**, vol. 210, 169-208.

5. Dimitrov, I., Trzebicka, B., Müller, A. H. E., Dworak, A.,Tsvetanov, C. B., *Prog. Polym. Sci.*, **2007**, 32, 1275-1343.

6. Schmaljohann, D., *Adv. Drug Delivery Rev*. **2006**, 58, 1655–1670.

7. Schattling, P., Jochum, F. D., Theato, P., *Polym. Chem.*, **2014**, 5, 25-36.

8. Hocine, S., Li, M.-H., Soft Matter, **2013**, 9, 5839-5861.

9. Hoffman, A. S., *J. Controlled Release*, **2008**, 132, 153.

10. I. Goldmints, J. F. Holzwarth, K. A. Smith, T. A. Hatton, *Langmuir*, **1997**, 13, 6130.

11. Stile, R.A., Healy, K.E., *Biomacromolecules*, **2001**, *2*, 185-194.

12. Alarcon, C. D. H., Pennadam, S., Camerou, A., *Chem. Soc. Rev.*, **2005**, 34, 276-285.

13. Twaites, B.R., Alarcon, C.D.H., Lavigne, M., Saulnier, A., Pennadam, S.S., Cunliffe, D.,Gorecki, D.C., Alexander, C. , *J. Control. Release*, **2005**, *108*, 472-483.

14. Adams, N., Schubert, U. S., *Adv. Drug Delivery Rev*., **2007**, 59, 1504.

15. Hoogenboom, R., *Angew. Chem., Int. Ed*,. **2009**, 48, 7978.

16. Roy, D., Brooks, W. L. A., Sumerlin, B. S., *Chemical Society Reviews*, **2013**.

17. Weber, C., Hoogenboom, R., Schubert, U. S., *Progress in Polym. Sci.*, **2012**, 37, 686-714.

18. Park, I.-K., Snigha, K., Arote, R. B., Choi, Y.-J., Kim, W. J., Cho, C.-S., *Macromol. Rapid Comm..*, **2010**, 31, 1122-1133.

19. Morawetz, H., J. Polym. Sci. Part B, *Polym. Phys.*, **2002**, 40, 1080-1086.

20. Dobrynin, A. V., Rubinstein, M., *Prog. Polym. Sci.*, **2005**, 30, 1049-1118.

21. Rijcken, C. J. F., Soga, O., Hennink, W. E., van Nostum, C. F., *J. Control. Release*, **2007**, 120, 131-148.

22. Laguecir, A., Ulrich, S., Labille, J., Fatin-Pouge, N., Stoll, S., Buffle, J., *Eur. Polym. J.*, **2006**, 42, 1135-1144.

23. Li, Y., Gao, G. H., Lee, D. S., *Adv. Healthcare Mater,*. **2013**, 2, 388–417.

24. Mano, J. F., Advanced Engineering Materials, 2008, 10, 515-527.

25. Onaca, O., Enea, R., Hughes, D. W., Meier, W., *Macromo. Biosci.*, **2009**, 9, 129-139.

26. Bawa, P., (Placeholder1) (Placeholder1)Pillay, V., Choonara, Y. E., Toit, L. C., *Biomed. Mater.*, **2009**, 4, 1-15.

27. Hoffman, A. S., *Adv. Drug Delivery Reviews*, **2013**, 65, 10-16.

28. Felber, A. E., Dufresne, M.-H., Leroux, J.-C., *Adv. Drug Deliv. Rev.*, **2012**, 64, 979-992.

29. Tanaka, N., Kitano, H., Ise, N., *Macromolecules*, **1991**, 24, 3017-3019.

30. Dong, J., Ozaki, Y., Nakashima, K., *Macromolecules*, **1997**, 30, 1111-1117.

31. Dormidontova, E., Brinke, G., *Macromolecules*, **1998**, 31, 2649-2660.

32. Anghel, D. F., Winnik, F. M., Galatanu, N., *Colloid Surf. A Physicochem. Eng. Aspects*, **1999**, 149, 339-345.

33. Robb, I. D., Stevenson, P., *Langmuir*, **2000**, 16, 7168-7172.

34. Frtier-McGill, B., Toader, V., Reven, L., *Macromolecules*, **2014**, 47, 4298-4307.

35. Vasilescu, M., Anghel, D. F., Almgren, M., Hansson, P., Saito, S., *Langmuir*, **1997**, 13, 6951-6955.

36. Akinc, A., Thomas, M., Klibanov, AM., Langer, R., *J. Gene Med.*, **2005**, 7, 657-663.

37. Dai, S., Ravi, P., Tam, K. C., *Soft Matter*, **2008**, 4, 435-449.

38. Han, X., Zhang, X., Zhu, H., Yin, Q., Liu, H., Hu, Y., *Langmuir*, **2013**, 29, 1024-1034.

39. Roy, D., Cambre, J. N., Sumerlin, B. S., *Progress in Polymer Science, 2010*, 35, 278-301.

40. Ganta, S., Devalapally, H., Shahiwala, A., Amiji, M., *J. Controlled Release*, *2008*, 126, 187-204.

41. Shim, M.S., Kwon, Y. J., *Advanc. Drug Deliv. Reviews*, **2012**, 64, 1046-1059.

42. Diab, C., Akiyama, Y., Kataoka, K., Winnik, F.M., *Macromolecules*, **2004**, 37, 2556.

43. Xu, L., Zhu, Z., Borisov, O. V., Zhulina, E. B., Sukhishvili, S. A., *Physic. Review Letters*, **2009**, 103.

44. Chen, G., Hoffman, A. S., *Nature*, **1995**, 373, 49-52.

45. Nagarajan, R., Ruckenstein, E., *Langmuir*, **1991**, 7, 2934-2969.

46. Patist, A., Kanicky, J. R., Shukla, P. K., Shah, D. O., *J. Colloid. Interface Sci.*, **2002**, 245, 1-15.

47. Wennerstrom, H., Lindman, B., *Physics Reports*, **1979**, 52, 1-86.

48. Grieser, F., Drummond, C. J., *J. Phys. Chem.*, **1988**, 92, 5580-5593.

49. Holmberg, K., *Curr. Opin. Colloid Interface Sci.*, **2001**, 6, 148-159.

50. Morelli, J. J., Gerald, S., Analysis of Surfactants: Part I, J. Surfactants and Detergents, **2000**, 3, 539-552.

51. Morelli, J. J., Gerald, S., Analysis of Surfactants: Part II, J. Surfactants and Detergents, **2001**, 4, 75-83.

52. Sohrabi, B., Gharibi, H., Tajik, B., Javadian, S., Hashemianzadeh, M., *J. Phys. Chem. B.*, **2008**, 112, 14869-14876.

53. Bergh, M., *Acta Derm. Venereol.*, **1999**.

54. Cullum, D. C., Introduction to Surfactant Analysis, **1994**, Springer Science.

55. Surfactants in Cosmetics. – 2nd ed., edit: Rieger, M. M., Rhein, L. D., **1997**, Marcel Dekker, Inc.

56. Wennerstrom, H., Lindman, B., *Physics Reports*, **1979**, 52, 1-86.

57. Israelachvili, J. N., Mitchell, D. J., Ninham, B. W., *J. Chem. Soc., Faraday Trans. 2*, **1976**,72, 1525-1568.

58. Rosen, M. J., Surfactants and Interfacial Phenomena, 3d edition, **2004**, Wiley.

59. Tadros, T. F., Applied Surfactants: Principles and Applications, **2005**, Wiley.

60. Tian, M., Quin, A., Ramireddy, C., Webber, S. E., Munk, P., Tuzar, Z., Prochazka, K., *Langmuir*, **1993**, 9, 1741.

61. Stepanek, M., Podhajecka, K., Tesarova, E., Prochazka, K., Tuzar, Z., Brown, W., Langmuir, **2001**, 17, 4240-4244.

62. Bednar, B., Edwards, K., Almgren, M., Tormod, S., Tuzar, Z., Macromo. *Chem., Rapid. Commun.*, **1988**, 9, 785-590.

63. Lianos, P., Zana, R., *J. Colloid Interface Sci.*, **1981**, 84, 100-107.

64. Hoffmann, H., *Adv. Mater.*, **1994**, 6, 116-129.

65. Mesa, C. L., *J. Colloid Interface Sci.*, **2005**, 286, 148-157.

66. Interactions of Surfactants with Polymers and Proteins, edit. Goddard, E. D., Ananthapadmanabhan, **1993**, K. P., CRC Press.

67. Nagarajan, R., *Chem. Phys. Letters*, **1980**, 76, 282-286.

68. Gilanyi, t., Wolfram, E., *Collid Surfaces*, **1981**, 3, 181.

69. Goddard, E. D., *J. Colloid. Interface. Sci.*, **2002**, 2356, 228-235.

70. Wang, G., Olofsson, G., *J. Phys. Chem. B*, **1998**, 102, 9276-9283.

71. Cooke, D. J., Blondel, J. A. K., Lu, J., Thomas, R. K., Wang, Y., Han, B., Yan, H., Penfold, J., *Langmuir*, **1998**, 14, 1990-1995.

72. Brackman, J., Engberts, J. B. F. N., *J. Colloid Interface Sci.*, **1989**, 132, 250.

73. Yan, P., Xiao, J.-X., *Colloid Surfaces A: Physicochem. Eng. Aspects*, **2004**, 244, 39-44.

74. Zanette, D., Soldi, V., Romani, A. P. Gehlen, M. H., *J. Colloid Interface Sci.*, **2002**, 246, 387-392.

75. Mia, K. Y., Jamieson, A. M., Sirivat, A., *Langmuir*, **2000**, 16, 6131-6135.

76. Naskar, B., Ghosh, S., Moulik, S. P., *J. Colloid Interface Sci.*, **2014**, 414, 82-89.

77. Wang, R., Wang, Y., *Acta Chimica Sinica*, **2014**, 72, 41-50.

78. Parmar, A., Chavda, S., Bahadur, P.,*Colloid Surface A: Physicochem. Eng. Aspects*, **2014**, 441, 389-397.

79. Wang, Z., *J. Surfactants Deterg.*, **2010**, 13, 97-102.

80. Li, Y., Bao, M., Wang, Z., Zhang, H., Xu, G., *J. Molecular Structure*, **2011**, 985, 391-396.

81. Nambam, J. S., Philip, J., *J. Phys. Chem. B.*, **2012**, 116, 1499-1507.

82. Sharma, R. Murali, R., Murthy, C. N., *Tenside Surfactants Detergents*, **2012**, 49, 136-144.

83. Inanova, R., Alexandridis, P., Lindman, B., *Colloid Surface A: Physicochem. Eng.Aspects*, **2001**, 183, 41-53.

84. Hecht, E., Hoffmann, H., *Langmuir*, **1994**, 10, 86-91.

85. Li, Y., Xu, R., Couderc, S., Bloor, D. M., Holzwarth, J. F., Wyn-Jones, E., *Langmuir*, **2001**, 17, 5742-5747.

86. Niemiec, A., Loh, W., *J. Phys. Chem. B*, **2008**, 112, 727-733.

87. Li, X., Wettig, S. D., Verrall, R. E., *J. Colloid Interface Sci.*, **2005**, 282, 466-477.

88. Lof, D., Niemiec, A., Schillen, K., Loh, W., Olofsson, G., *J. Phys. Chem. B*, **2007**, 111, 5911-5920.

89. Sommer, C., Pedersen, J. S., Garamus, V. M., *Langmuir*, **2005**, 21, 2137-2149.

90. Sastry, N. V., Hoffmann, H., *Colloid Surface A: Physicochem. Eng. Aspects*, **2004**, 250, 247-261.

91. Yosida, K., Sokhakian, S., Dubin, P. L., *J. Colloid. Interface Sci.*, **1998**, 205, 257-264.

92. Li, Y., Dubin, P. L., Havel, H. A., Edwards, S. L., Dautzenberg, H., *Macromolecules*, **1995**, 28, 3098-3102.

93. Herslof, A., Sundelof, L-O., Edsman, K., *J. Phys. Chem.*, **1992**, 96, 2345-2348.

94. Tam, K. C., Wyn-Jones, E., *Chem. Soc. Rev.*, **2006**, 35, 693-709.

95. Fundin, J., Brown, W., *Macromolecules*, **1994**, 27, 5024-5031.

96. Groot, R. D., *J. Chem. Phys.*, **2003**, 118, 11265-11277.

97. Almgren, M., Hansson, P., Mukhtar, E., Stam, J., *Langmuir*, 1992, 8, 2405-2412.

98. Sequaris, J-M., *Langmuir*, **1997**, 13, 653-658.

99. Guillemet, F., Piculell, L., *J. Phys. Chem.*, **1995**, 99, 9201-9209.

100. Svensson, A., Piculell, L., Cabane, B., Ilekti, P., *J. Phys. Chem. B*, **2002**, 106, 1013-1018.

101. Yoshida, K., Sokhakean, S., Dubin, P. L., *J. Colloid Interface Sci.*, **1998**, 205, 257-264.

102. Wang, C., Tam, K. C., *J. Phys. Chem. B*, **2004**, 108, 8976-8982.

103. Wang, C., Tam, K. C., *J. Phys. Chem. B*, **2005**, 109, 5156-5161.

104. Zhou, B., Chu, B., *Advanced Materials*, **2000**, 12, 545-556.

105. Sivadasan, K., somasundaran, P., *Colloid. Surface.*, **1990**, 49, 229-239.

106. Winnik, F. M., Ringsdorf, H., Venzmer, J., *Langmuir*, **1991**, 7, 905-911.

107. Iliopoulos, I., Wang, T. K., Audevert, R., *Langmuir*, 1991, 7, 617-619.

108. Magny, B., Iliopoulos, I., Zana, R., Audebert, R., *Langmuir*, **1994**, 10, 3180-3187.

109. Biggs, S., Selb, J., Candau, F., *Langmuir*, **1992**, 8, 838-847.

110. Stepanek, M., Matejicek, P., Prochazka, K., Filippov, S., Angelov, B., Slouf, M., Mountrichas, G., Pespas, S., *Langmuir*, **2011**, 27, 5275-5281.

111. Stepanek, M., Skvarla, J., Uchman, M., Prochazka, K., Angelov, B., Kovacik, L., Garamus, V. M., Mantzaridis, C., Pispas, S., *Soft Matter*, **2012**, 36, 9412-9417.

112. Uchman, M., Gradzielski, M., Angelov, B., Zosner, Z., Oh, J., Chang, T., Stepanek, M., Prochazka, K., *Macromolecules*, **2013**, 6, 2172-2181.

113. Robb, I. D., Stevenson, P., *Langmuir*, **2000**, 16, 7168-7172.

114. Anghel, D., Winnik, F. M., Galatanu, N., *Colloid. Surface A*, **1999**, 339-345.

115. Bandyapadhyay, P., Ghosh, A. K., Bandyapadhyay, S., *Chem. Phys. Lett.*, **2009**, 476, 244-248.

116. Vasilescu, M., Anghel, D. F., Almgren, M., Hansson, P., Saito, S., *Langmuir*, **1997**, 13, 6951-6955.

117. Light Scattering. Principles and Development, edit. Brown, W., **1996**, Clarendon Press, Oxford.

118. Small-Angle Scattering of X-rays, Guinier, A., Foutnet, G. (Walker C. B., Yudowitch, K. L.), **1955**, John Wiley & Sons.

119. Porod, G., *Kolloid-Z.*, **1951**, 124, 83-114.

120. Biocalorimetry 2, edit.: Ladbury, J. E., Doyle, M. L., **2004**, John Wiley & Sons, Ltd.

121. Schwarz, F. P., Reinisch, T., Hinz, H-J., Surolia, A., *Pure Appl. Chem.*, **2008**, 80, 2025-2040.

122. Tsamaloukas, A. D., Keller, S., Heerklotz, H., *Nature Protocols*, **2007**, 2, 695-704.

123. Macrocalorimetry of Macromolecules. The Physical Basis of Biological Structures, Privalov, P. L., **2012**, John Wiley & Sons, Ltd.

124. ITC Data Analysis, Tutorial Guide, MicroCal.

125. Heerklotz, H. H., Binder, H., Schmiedel, H., *J. Phys. Chem. B*, **1998**, 102, 5363-5368.

126. Diab, C., Winnik, F. M., Tribet, C., *Langmuir*, **2007**, 23, 3025-3035.

127. Couderc, S., Li, Y., Bloor, D. M., Holzwarth, J. F., Wyn-Jones, E., *Langmuir*, **2001**, 17, 4818-4824.